



室蘭工業大学

学術資源アーカイブ

Muroran Institute of Technology Academic Resources Archive



ハノイ市における埋戻し材としての繊維材混合流動化処理土の利用促進に関する研究

| | |
|-------|---|
| メタデータ | 言語: eng 出版者: 公開日: 2019-06-25 キーワード (Ja): キーワード (En): 作成者: ドウ, トウアン アン メールアドレス: 所属: |
| URL | https://doi.org/10.15118/00009906 |

**Study on Promoting Use of Liquefied Stabilized Soil mixed
Fiber Material as Backfilling Material in Hanoi City**

By

DO TUAN ANH

**A DISSERTATION SUBMITTED TO THE FACULTY OF THE
MURORAN INSTITUTE OF TECHNOLOGY
IN PARTIAL FULFILLMENT OF THE REQUIREMENTS FOR THE DEGREE OF
DOCTOR OF ENGINEERING**



**Division of Civil and Environmental Engineering
MURORAN INSTITUTE OF TECHNOLOGY
March 2019**

Acknowledgments

Firstly, I would like to express my sincere gratitude to my advisor Professor. Yukihiro Kahata for the continuous support of my Ph.D study and related research, for his patience, motivation, and immense knowledge. His guidance helped me in all the time of research and writing of this thesis. I could not have imagined having a better advisor and mentor for my Ph.D study.

Besides my advisor, I would like to thank the rest of my thesis committee: Associate Professor Dr. Shima Kawamura and Associate Professor Dr. Noriyuki Sugata, for their insightful comments and encouragement, but also for the hard question which incited me to widen my research from various perspectives.

Special I am grateful to Dr. Duong Quang Hung for his introduction and recommendation to Muroran Institute of Technology and Professor Kohata before I applied for study here.

My sincere thanks are due to Mr. Funamizu Naoyuki and all the staffs of the Centre for International Relations, Muroran IT, Mr. Jinro Endo, Ms. Baek Sangyub, and Ms. Hatsuki Noda for making my life in Hokkaido really comfortable and enjoyable. They always extended instant help whenever I needed. Especially thanks to Associate Professor Naoko Yamaji' teaching, my Japanese has been improved much.

I thank my fellow labmates in for the stimulating discussions, for the sleepless nights we were working together before deadlines, and for all the fun we have had in the last three years. In particular, I am grateful to Dr. Nguyen Cong Giang for enlightening me the first glance of research.

I am indeed indebted to my friends who assisted in life during three years of my doctor course, Mr. Mona Yuttana, Mr. Khongma Saysrath, Mr. Teerawat Kumrai and International friends, and Japanese friends. Thanks to everyone.

Further, I also sincerely thank Associate Professor Dr. Vuong Ngoc Luu of the Hanoi Architectural University (HAU) for offering me recommendation letters to apply for the doctor course.

Last but not the least, I would like to thank my family: my wife, Ms. Nguyen Thi Lan Anh, my son, Do Cong Gia Phuc, and my daughter, Do Ngoc Minh Chau for supporting me spiritually throughout writing this thesis and my life in general.

Abstract

In this study, the applicability of Liquefied Stabilized Soil (LSS) mixed with the fibered material as the backfill materials at Hanoi city in Vietnam has been investigated. Research works including experiment and analysis have been conducted simultaneously aiming to promote the application of LSS in Hanoi city in the coming time. This study is summarized as follows.

(1) The influence of slurry density on strength and deformation characteristics of LSS mixed with fibered material was evaluated. A series of Consolidated–Undrained triaxial compression tests with measured pore water (CUB tests) under the condition on an axial strain rate of 0.054%/min have been carried out for LSS mixed with fibered material amount of 0 and 10 kg/m³ at curing time of 28 and 56 days, respectively. Based on the test results, it was found that when the slurry density is slightly decreased from the appropriate slurry density, it is considered that the maximum deviator stress (q_{\max}) decreased remarkably. In addition, it was found that the local damage caused by shearing even in the LSS mixed with fiber material prepared on the low slurry density is reduced by the effect of reinforcement on the fiber material.

(2) The difference in triaxial shear property of LSS mixed with fiber material cured in laboratory and at field was investigated to be carried out a series of CUB tests for both specimens of LSS mixed with fiber material amount of 0 and 10 kg/m³ prepared by trimming LSS retrieved from a model ground by block sampling and cured in laboratory at curing time of 28 and 56 days, respectively. Based on the test results, it was found that the q_{\max} in $q\sim\varepsilon_a$ relations of LSS mixed with fiber material cured at field tend to be larger than that cured in laboratory.

(3) A procedure for prediction of vehicle-induced vibration from a road surface has been established as a case study for a general road in Hanoi city in conformity with Vietnamese Standard. The vibration propagation from a road surface was analyzed by the 2-D FEM. The numerical results in terms of vibration velocity allow estimating the vibration velocity level, and then it is applicable to the prediction of vehicle-induced vibration. The calculated vibration velocity level on backfilling sandy soil indicated to be higher than the allowable threshold, therefore appropriate measures should be taken to decrease these vibrations.

(4) According to the numerical analysis results on a mitigation of vehicle-induced vibration in case using LSS as backfill material by the established analysis method, it is found that the application of LSS can reduce the ground vibration. This will be a new advantage. Then, it is considered that the application to backfilling ground of LSS become one of effective measure for reduction of vehicle-induced vibration. Therefore, it is considered that the application of the LSS mixed with fibered material as backfilling material will be more promoted in Hanoi city.

Table of Contents

| | |
|--|-----------|
| Acknowledgments..... | i |
| Abstract..... | ii |
| List of Tables..... | vi |
| List of Figures..... | vii |
| Chapter 1 INTRODUCTION..... | 1 |
| 1.1. GENERAL BACKGROUND..... | 1 |
| 1.2. MOTIVAION FOR RESEARCH..... | 3 |
| 1.3. OBJECTIVE OF RESEARCH..... | 3 |
| 1.4. ORGANIZATION OF THESIS..... | 7 |
| Chapter 2 OVERVIEW OF LIQUEFIED STABILIZED SOIL..... | 10 |
| 2.1. INTRODUCTION..... | 10 |
| 2.2. COMPONENT OF LIQUEFIED STABILIZED SOIL..... | 11 |
| 2.2.1 Soil..... | 11 |
| 2.2.2 Cementitious materials..... | 11 |
| 2.3. HISTORICAL DEVELOPMENT..... | 14 |
| 2.4. APPLICATIONS..... | 19 |
| 2.5. SITUATION OF BACKFILLING PROCESS IN VIETNAM..... | 22 |
| 2.5.1 Problem of backfilling method in Vietnam..... | 22 |
| 2.5.2 Inappropriate disposal of excavated soils..... | 23 |
| 2.5.3 Mining of new material from natural resources..... | 24 |
| 2.6. UTILIZATION OF LSS IN VIETNAM..... | 22 |
| 2.7. SUMMARY..... | 26 |
| Chapter 3 INFLUENCE OF SLURRY DENSITY ON PROPERTIES OF LSS..... | 29 |
| 3.1. INTRODUCTION..... | 29 |
| 3.2. TEST PROCEDURE..... | 31 |
| 3.2.1 Test material..... | 31 |
| 3.2.2 Mixing method..... | 31 |
| 3.2.3 Specimen preparation..... | 33 |

| | | |
|------------------|--|-----------|
| 3.2.4 | Test method..... | 34 |
| 3.3. | TEST RESULTS AND DISCUSSION..... | 35 |
| 3.3.1 | Relationship between deviator stress and axial strain..... | 35 |
| 3.3.2 | Deformation property..... | 39 |
| 3.4. | CONCLUSIONS..... | 44 |
| Chapter 4 | METHODS FOR DETERMINING DYNAMIC PARAMETERS OF SOIL..... | 46 |
| 4.1. | INTRODUCTION..... | 46 |
| 4.2. | UTILITY OF MEASURED PARAMETER..... | 46 |
| 1) | Shear wave velocity (V_s)..... | 46 |
| 2) | Shear modulus (G)..... | 47 |
| 3) | Maximum Shear Modulus (G_{max})..... | 47 |
| 4) | Damping Ratio (h)..... | 47 |
| 5) | Poisson's Ratio (n)..... | 48 |
| 4.3. | GEOTECHNICAL APPROACHES TO DETERMINE DYNAMIC SOILS PROPERTIES..... | 48 |
| 1) | Seismic Refraction..... | 48 |
| 2) | Cross-Hole Technique..... | 50 |
| 3) | Down-Hole Techniques..... | 51 |
| 4) | Up-Hole Techniques..... | 53 |
| 5) | Steady-State Surface Wave Technique..... | 54 |
| 6) | Spectral Analysis of Surface Waves (SASW)..... | 55 |
| 7) | Seismic Cone Penetration Test (SCPT)..... | 56 |
| 8) | Suspension PS logging..... | 57 |
| 4.4. | ESTIMATION OF DYNAMIC SOIL PROPERTIES..... | 59 |
| 4.5. | SUMMARY..... | 65 |
| Chapter 5 | STUDY ON VEHICLE-INDUCED VIBRATION..... | 67 |
| 5.1. | INTRODUCTION..... | 67 |
| 5.2. | DEFINITION OF VIBRATION LEVEL..... | 68 |
| 5.3. | ANALYTICAL AND NUMERICAL APPROACHES..... | 69 |
| 5.3.1 | Vehicle motion..... | 69 |
| 5.3.2 | Road Spectrum..... | 69 |
| 5.3.3 | Vehicle loads on pavement..... | 70 |

| | | |
|------------------|---|-----------|
| 5.3.4 | Cyclic vehicle loading spectrum | 70 |
| 5.3.5 | Generation of a time history of cyclic vehicle loading..... | 71 |
| 5.3.6 | Verification..... | 71 |
| 5.4. | ANALYSIS PROCEDURE | 72 |
| 5.4.1 | Selection of material model..... | 73 |
| 5.5. | NUMERICAL MODEL AND CONSIDERED PARAMETERS..... | 76 |
| 5.5.1 | Road and ground conditions..... | 76 |
| 5.5.2 | Finite element model..... | 77 |
| 5.6. | SUMMARY..... | 77 |
| Chapter 6 | REDUCTION OF VEHICLE-INDUCED VIBRATION USING LIQUEFIED STABILIZED SOIL | 80 |
| 6.1. | INTRODUCTION..... | 80 |
| 6.2. | ANALYSIS PROCEDURE..... | 81 |
| 6.2.1 | Simulation of cyclic vehicle load | 81 |
| 6.2.2 | Numerical model and considered parameters | 81 |
| | 1- Building, road and ground conditions | 81 |
| | 2- Characteristics of backfilling materials..... | 83 |
| | 3- Finite element model..... | 85 |
| | 4- Numerical model in Plaxis..... | 85 |
| 6.3. | RESULTS AND DISCUSSION..... | 86 |
| 6.3.1 | Vibration acceleration in Case 1 and Case 2..... | 87 |
| 6.3.2 | Relationship between distance maximum vibration velocity and level..... | 87 |
| 6.4. | CONCLUSIONS..... | 88 |
| Chapter 7 | CONCLUSIONS AND RECOMMENDATIONS..... | 91 |
| 7.1. | SUMMARY OF INVESTIGATIONS..... | 91 |
| 7.2. | SUMMARY OF FINDINGS AND CONCLUSIONS..... | 92 |
| 7.3. | RECOMMENDATIONS FOR FUTURE RESEARCH..... | 93 |

List of Tables

| | |
|---|----|
| Table 1.1 Test conditions of axial strain rate..... | 5 |
| Table 1.2 The comparison between the previous study and this study..... | 6 |
| Table 3.1 Physical Properties of NSF-CLAY..... | 31 |
| Table 3.2 Result of density test..... | 32 |
| Table 4.1 SPT (N*60) – Shear Wave Velocity, vs, Equation for Sand (Andrus et al., 2003)..... | 60 |
| Table 4.2 Recommended Age Scaling Factors (ASF) for SPT (Andrus et al., 2003)..... | 60 |
| Table 4.3 CPT (qc) – Shear Wave Velocity, vs, Equations for Soils (Andrus et al., 2003)..... | 61 |
| Table 4.4 Recommended Age Scaling Factors (ASF) for CPT (Andrus et al., 2003)..... | 62 |
| Table 5.1 Material properties of road..... | 76 |
| Table 5.2 Geotechnical properties of soil layers..... | 76 |
| Table 6.1 Parameters of building..... | 82 |
| Table 6.2 Geotechnical properties of soil layers..... | 82 |
| Table 6.3 Material properties of road..... | 84 |
| Table 6.4 Physical properties of backfilling materials..... | 85 |

List of Figures

| | |
|--|----|
| Figure 1.1 Motorbikes and scooters on the streets of Hanoi city | 1 |
| Figure 1.2. Smoke created by burning waste in a street in Hanoi city | 2 |
| Figure 1.3 Metro rout map of Hanoi city up to 2030..... | 2 |
| Figure 1.4 $q \sim \varepsilon_a$ relation of Vinh Phuc-Clay LSS..... | 5 |
| Figure 1.5 $q \sim \varepsilon_a$ relation of NSF -Clay LSS..... | 5 |
| Figure 1.6 Flow chart of this dissertation..... | 7 |
| Figure 2.1 Flow of Liquefied soil stabilized method (Tomoharu et al., 2005)..... | 17 |
| Figure 2.2 Cement treated soil using as slope protection (Tang et al., 2001)..... | 17 |
| Figure 2.3 Production system for foam mixed lightweight soil..... | 18 |
| Figure 2.4 Placement of cement treated soil along slope (Tang et al., 2001)..... | 18 |
| Figure 2.5 Placement of cement treated soil along slope (Tang et al., 2001)..... | 18 |
| Figure 2.6 Use of LSS for filling cavity under road surface..... | 18 |
| Figure 2.7 LSS used for backfill at upper part of cut and cover tunnel..... | 19 |
| Figure 2.8 LSS used for invert material of shield tunnel..... | 20 |
| Figure 2.9 Using LSS for various backfilling works in Japan..... | 21 |
| Figure 2.10 Cave-in and road collapses in Hanoi city..... | 22 |
| Figure 2.11 inappropriate disposal of excavated soils from construction sites in Hanoi..... | 23 |
| Figure 2.12 Bank erosion due to depletion of sand in streambed..... | 24 |
| Figure 3.1 Available range of slurry density | 32 |
| Figure 3.2 Schematic drawing of pits | 34 |
| Figure 3.3 Schematic figure of test apparatus | 34 |
| Figure 3.4 $q \sim \varepsilon_a$ relations up to 3 % | 37 |
| Figure 3.5 $q \sim \varepsilon_a$ relations up to 0.5 % | 38 |
| Figure 3.6(a) $q_{max} \sim$ curing days relations for Field LSS | 38 |
| Figure 3.6(b) $q_{max} \sim$ curing days relations for Laboratory LSS | 39 |
| Figure 3.7. Definition of various Young's moduli | 39 |
| Figure 3.8(a) $E_0 \sim$ curing days relations for Field LSS..... | 41 |

| | |
|---|----|
| Figure 3.8(b) $E_0 \sim$ curing days relations for Laboratory LSS..... | 41 |
| Figure 3.9 $E_{tan}/E_0 \sim q/q_{max}$ relations..... | 42 |
| Figure 3.10 $E_{eq}/E_0 \sim q/q_{max}$ relations..... | 44 |
| Figure 4.1 Field and laboratory methods for determining dynamic parameters..... | 49 |
| Figure 4.2 Cross-hole method..... | 52 |
| Figure 4.3 Down-hole method..... | 53 |
| Figure 4.4 Up-hole method..... | 54 |
| Figure 4.5 Steady-State Surface Wave Test..... | 55 |
| Figure 4.6 Seismic Cone Penetration Test..... | 57 |
| Figure 4.7 - Suspension PS Logging test..... | 58 |
| Figure 4.8 $h \sim \gamma$ relation of sandy soils (PI = 0 %)..... | 64 |
| Figure 4.9 $h \sim \gamma$ relation of sandy soils (PI = 35 %)..... | 65 |
| Figure 5.1 Relationship between maximum cyclic vehicle load and the grade of surfaces on roads of various classes..... | 72 |
| Figure 5.2 Schematic diagram of prediction procedure for train-induced vibration from road..... | 73 |
| Figure 5.3 Cam-Clay model parameters in Plaxis..... | 75 |
| Figure 5.4 Mohr-Coulomb model parameters in Plaxis..... | 75 |
| Figure 5.5 Finite element model in Plaxis..... | 77 |
| Figure 6.1 Numerical model of the considered soil structure system..... | 82 |
| Figure 6.2 Ground profile..... | 83 |
| Figure 6.3 Typical cross section of Giai Phong road..... | 83 |
| Figure 6.4 Finite element model in Plaxis..... | 84 |
| Figure 6.5 Vertical acceleration at point E for load amplitude =400 kN/m, $f = 10$ Hz..... | 86 |
| Figure 6.6 Horizontal acceleration at point E for load amplitude =400 kN/m, $f = 10$ Hz..... | 86 |
| Figure 6.7 Vertical acceleration at point H for load amplitude =400 kN/m, $f = 10$ Hz ... | 86 |
| Figure 6.8 Horizontal acceleration at point H for load amplitude =400 kN/m, $f = 10$ Hz..... | 86 |
| Figure 6.9 Distance and maximum velocity..... | 86 |
| Figure 6.10 Distance and maximum vibration level..... | 86 |

Chapter 1

INTRODUCTION

1.1. GENERAL BACKGROUND

Viet Nam is experiencing rapid urbanization and motorization owing to economic development after the introduction of “Doi Moi” policy. Urban transportation problems such as traffic congestion and air pollution are becoming important challenges for the nation’s two major cities of Hanoi and Ho Chi Minh. This study outlines the current status and issues of motorcycle-dominated urban transportation in both cities, reviews the present regulatory framework regarding the bus transportation, and recommends the regulatory improvements for the promotion of public transportation.

At present, Hanoi city of Vietnam, a city with more motorbike than households, has to contend with heavy congestion, air pollution and frequent traffic accidents. In recent years, Hanoi city has been ranked one of the worse cities in Asia for air pollution. In May 2017, US embassy’s quality monitor in Hanoi city had registered a hazardous spike in particular mater, reaching a level seven times according to recommendation of the World Health Organization. In addition, Hanoi’s population jumped from about 2.7 million in 2000 to about 3.2 million in 2006 (and is expected to reach 4.5 million in 2020), resulting



Figure 1.1 Motorbikes and scooters on the streets of Hanoi city



Figure 1.2 Smoke created by burning waste in a street in Hanoi city

in a dramatic increase in traffic volume on city roads and severe traffic congestion.

The current situation need to be solved as soon as possible. The solutions were given including expanding the transport capacity of existing public transportation and road networks, a new urban mass rapid transit system. Therefore, plan of Railway Construction was formed in 2002 to aim modernization of rail transport. Hanoi’s Transport Plan aims to increase the share of public transport from the current low figure of 9% of trips, to above 60% by 2030, by which time Hanoi is slated to have six new metro lines and three Bus Rapid Transit (BRT) lines as shown in Figure 1.3. Vietnamese government hopes the metro can tackle both traffic and environmental issues.

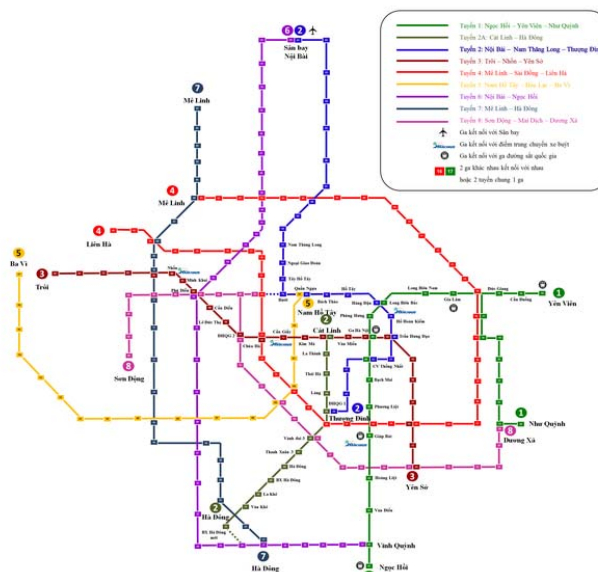


Figure 1.3 Metro route map of Hanoi city up to 2030

However, it is predicted that a huge quantity of excavated soil will be discharged from the underground construction projects in the city over the next decade. In addition, at present, excavated soils from construction sites are disposing inappropriate due to the shortage of landfill sites in the cities. Whereas, most backfilling material for construction works is being extracted from natural sources such as sand mining from river and gravel from mountain, which cause significantly negative impact on environment. On the other hand, during operating the metro systems, ground-born vibration is caused by train-track structure exciting the tunnel, adjacent soil layers. Created waves propagate to the foundations of nearby building and annoying to nearby resident. In Vietnam, standards or literatures have been not found to predict ground-born vibration until now. Therefore, environmental impact assessment and the dynamic parameters of soil have been not estimated clearly.

1.2. MOTIVAION FOR RESEARCH

In order to handle excavated soil from the construction projects, developed countries have applied recycling methods for excavated soil and Japan has always been at the forefront of the development of science and technology. One of recycling methods been used popularly for excavated soil is Liquefied Stabilized Soil (LSS), which the soil is mixed with water (or muddy water) and cement stabilizer and reused as backfilling material (Kuno, 1997; JGS, 2005). LSS will be effective methods to solve the problems of soil generated from construction sites and shortage of backfilling material in Vietnam.

LSS will be useful not only for construction of transport infrastructure Projects, but also design of geotechnical engineering and also for new direction of development of science and technology during development of geotechnical projects in Vietnam.

1.3. OBJECTIVE OF RESEARCH

In Muroran institute of technology, Prof. KOHATA Yukihiro and researchers at Geotechnical engineering Laboratory of Muroran Institute of Technology have continued to study and develop LSS. Although utilities of LSS during recycling excavated soil have been shown, LSS indicates a brittle characteristic with an increasing of strength and a decreasing of aseismatic performance similar to cement stabilized soil. Therefore, the improvement of this property of LSS is very important task. In order to improve ductile performance of LSS, Professor KOHATA et al have carried out the method to be mixing LSS with crushed newspaper fibered material. From the test results, it was shown that a

brittle property after the peak was improved by mixing with crushed newspaper.

The previous research in 2010 performed with both LSS using NSF-clay which is fine powder clay bought in Japanese market and Vinh Phuc-Clay which spread in Hanoi area as an original material, it concluded that the strength and deformation behaviors of both LSS tend to be similar (Giang, 2010). Figure 4 and Figure 5 show the relationship between deviator stress q ($=\sigma_1 - \sigma_3$) and axial strain ε_a from Consolidated–Undrained triaxial compression tests under confining pressure $\sigma'_c = 98$ kPa of Vinh Phuc-Clay LSS and NSF-Clay mixed by fibered material content of 0, 10, 20 kg/m³ at 56 days, respectively. The tests were performed under axial strain rate of 0.054 %/min. Thus, the behaviors of both LSS is the same. Also, the other results of the research indicated that the physical behaviors of both LSS tend to be similar.

The previous research in 2015 investigated the time-dependency on shear deformation characteristics of LSS using NSF-clay mixed by fiber material contents of 0, 20 kg/m³. On the other hand, the target density of slurry of 1.280 g/cm³ was selected. A series of Undrained triaxial compression tests under confining pressure $\sigma'_c = 98$ kPa had been performed with four different conditions of axial strain rate shown in Table 1. (Hung, 2015). The specimens had been cured under conditions of indoor and outdoor, respectively. The results of the research indicated that (1) the maximum deviator stress, q_{max} in $q \sim \varepsilon_a$ curve of LSS mixed with fibered material indicates similar value independently of curing days. However, in case of LSS without fibered material, there is a tendency to increase the initial stiffness as increasing of curing days; (2) the range of indicating E_{tan}/E_0 value of 1.0 tends to be larger on LSS mixed with fibered material. This is due to the reinforcing effect of the fibered material in LSS; (3) the rigidity during loading before the peak in $q \sim \varepsilon_a$ relationship increases temporarily in a large strain level after a creep stage and a change of strain rate independently of curing days. In addition, a procedure for prediction of train-induced vibration from railway tunnels in conformity with condition of Vietnam has been established as an example for Hanoi metro line. The vibration propagation from tunnel into the ground surface was analyzed by two dimensional element method (2-D FEM). And then, the established procedure was used to evaluate train-induced vibration as using LSS for backfilling ground of cut and cover tunnel. The results has shown that the LSS could reduce train-induced vibration from tunnel.

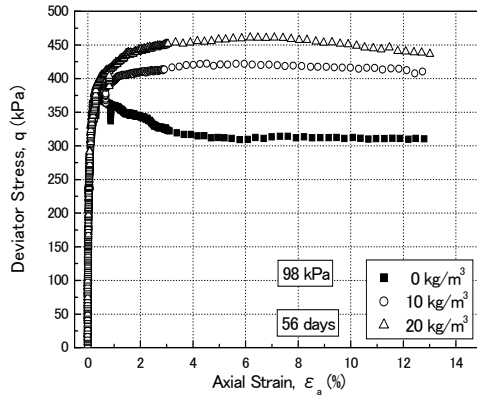


Figure 1.5 $q \sim \epsilon_a$ relation of Vinh Phuc-Clay LSS

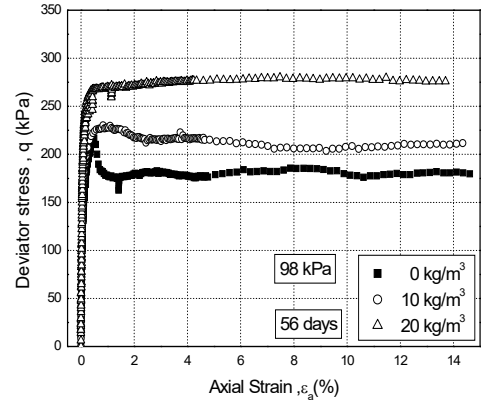


Figure 1.5 $q \sim \epsilon_a$ relation of NSF -Clay LSS

Table 1.1 Test conditions of axial strain rate

| | |
|--------|--|
| Case 1 | $0.054 \% \text{ min } (\dot{\epsilon}_0)$ |
| Case 2 | $0.54 \% \text{ min } (10\dot{\epsilon}_0)$ |
| Case 3 | $\dot{\epsilon}_0 \rightarrow 10\dot{\epsilon}_0 \rightarrow \dot{\epsilon}_0$ |
| Case 4 | $\dot{\epsilon}_0 \rightarrow C \rightarrow \dot{\epsilon}_0 \rightarrow C \rightarrow 10\dot{\epsilon}_0 \rightarrow C \rightarrow \dot{\epsilon}_0$ ※Creep applied before rate change |

In this study, in order to investigate influence of slurry density on strength and deformation properties of LSS reinforced with fiber material, NSF-clay was used as a presentative of LSS using excavated soil. In addition, to evaluate reduction of train-induced building vibrations by using LSS for back filling. The objective of this study is to promote using LSS mixed fiber material as backfilling material in Ha Noi city, Vietnam.

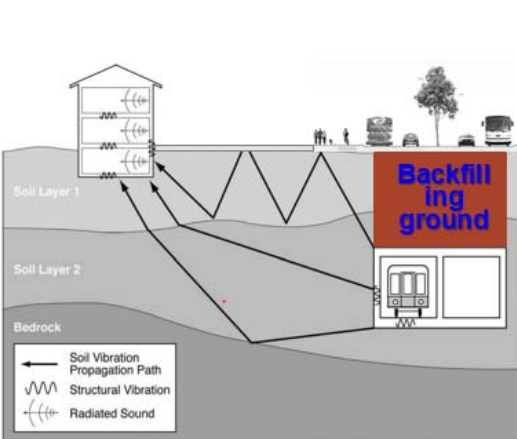
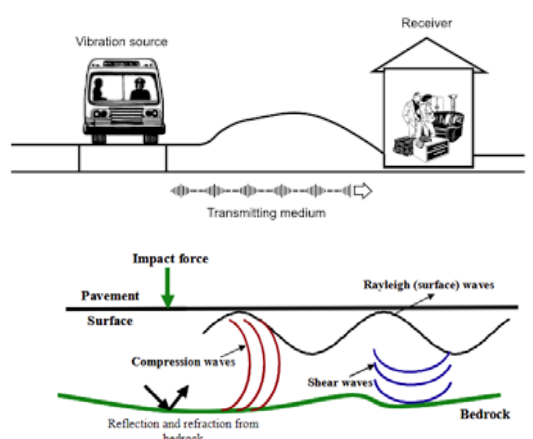
The first of all, the effect of slurry density on strength and deformation property of LSS reinforced with small strain level of different densities of specimens prepared laboratory was discussed. The influence of density on strength and deformation characteristics of LSS mixed with paper was investigated. On the other hand, in order to analyze effect of the slurry density when LSS mixed with fiber material worked on condition of field reality, four test pits were built and were filled up by LSS mixed with fibered material at test field in Muroran-IT campus. Their length is 50 centimeters, their width is 40 centimeters and their deep is 30 centimeters. These test pits were constructed with different densities of LSS mixed fiber material. These pits were cured under natural

condition. And then, the in-situ compressive stiffness of the LSS was evaluated and the non-uniformity of back fill ground by LSS mixed with fibered material was discussed by comparing the results between laboratory tests and field tests.

Secondly, methods for estimation of soil dynamic parameters in conformity with current condition of Vietnam was suggested by selectively adopting the methods of previous researches in the world. Then, a procedure for prediction of vehicle-induced vibration from road in Vietnam was fully established. The road in Hanoi city currently near the building was selected to analysis in this study. Vehicles-induced dynamic loading to building was simulated by means of vehicles-road-ground interaction model. Results of the simulation in term of force time history was input data for vehicles-soil interaction problem. The vibration propagation from vehicles on the road was analyzed by the 2-dimensional finite element method (FEM). Numerical results from the model in term of vibration velocity allow estimating the vibration velocity level, and then it is applicable to the prediction of vehicles-induced vibration propagated from road.

Finally, reduction of vehicles-induced vibration as using LSS for backfilling ground was evaluated by using established procedure. This study analyzed 2 cases including LSS and backfilling soil as backfilling material for area near building.

Table 1.2 The comparison between the previous study and this study

| Previous study | | This study | |
|--|---|---|---|
| Density of slurry (g/cm ³) | Content of fiber material (kg/m ³) | Density of slurry (g/cm ³) | Content of fiber material (kg/m ³) |
| 1.280 | 0 and 20 | 1.280 and 1.216 | 0 and 10 |
|  <p>The diagram shows a building on the left and a receiver on the right. A red box labeled 'Backfilling ground' is between them. The ground is divided into 'Soil Layer 1', 'Soil Layer 2', and 'Bedrock'. Arrows indicate the 'Soil Vibration Propagation Path' from the building through the soil layers and bedrock to the receiver. A legend identifies symbols for 'Soil Vibration Propagation Path', 'Structural Vibration', and 'Radiated Sound'.</p> | |  <p>The diagram shows a 'Vibration source' (a bus) on 'Pavement' and a 'Receiver' (a building) on the right. An 'Impact force' is applied to the pavement, creating 'Compression waves' (red) and 'Shear waves' (blue) that travel through the 'Surface' and 'Bedrock'. 'Rayleigh (surface) waves' are also shown. A 'Transmitting medium' is indicated between the bus and the receiver. A legend identifies 'Reflection and refraction from bedrock'.</p> | |

1.4. ORGANIZATION OF THESIS

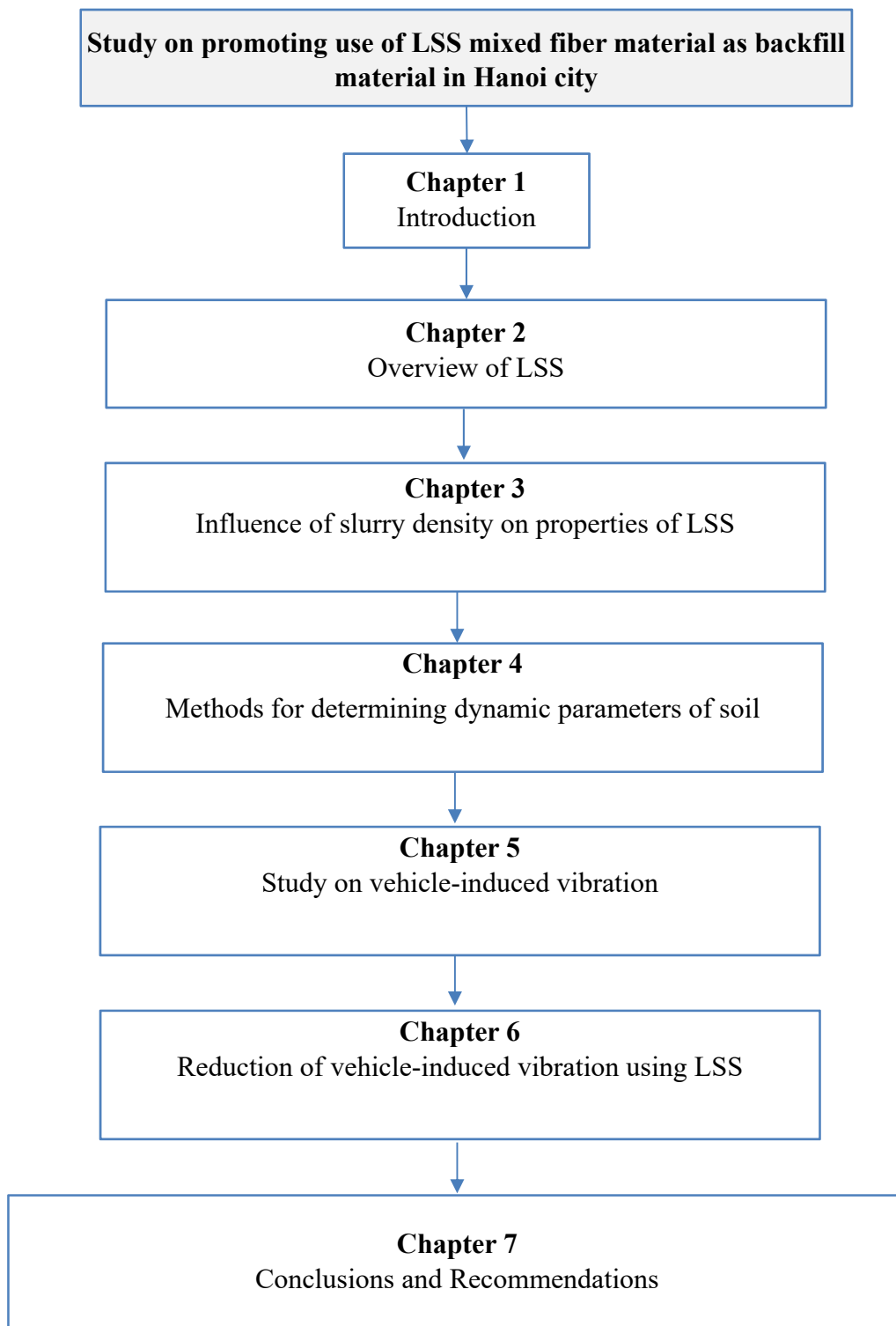


Figure 1.6 Flow chart of this dissertation

As seen in Figure 1.6, this dissertation contains seven chapters. The introduction (Chapter 1) describes the general background, objectives and scopes of research and organization of the dissertation.

Chapter 2 presents an overview of LSS as an effective method for utilization of excavated soil. The problems regarding excavating works in Vietnam was pointed out and then feasibility for utilization of LSS in Vietnam has been highlighted in this chapter.

Chapter 3 is to investigate influence of slurry density on deformation and strength characteristics of LSS by triaxial compression tests. Two slurry densities were prepared and then they were cured in laboratory and at field, respectively.

Chapter 4 present methods for determining dynamic parameters of soil. Methods for estimation of soil dynamic parameters in conformity with current condition in Vietnam is suggested in the chapter. Use of the methods in order to estimate soil dynamic parameters for backfilling site in Hanoi bring reliable results.

Chapter 5 establishes fully a procedure for prediction of vehicle-induced vibration in backfilling ground in Ha Noi city, Vietnam.

Using the established procedure, chapter 6 evaluates the reduction of vehicle-induced vibration as using LSS for backfill ground of building in Hanoi city.

Finally, the conclusions drawn from this study and recommendations for future works were given in chapter 7.

REFERENCES

Luu, D. H. (2010): Metro-a mode of indispensable public transportation in big cities, *Journal of Vietnam federation of civil engineering association* (in Vietnamese).

Kuno, G., eds (1997): Liquefied stabilized soil method-Recycling technology of construction-generated soil and mud, *Gihodo publication* (in Japanese).

Japanese Geotechnical Society (2005): Committee Report Chapter 2, 2.1, 2.2 on test methods and physical properties of cement-modified soil, *Proc. of symposium*, pp.2-22, on survey, design, construction and properties evaluation methods of solidifying stabilized soil using cement and cement-treated soil (in Japanese).

Kohata, Y. (2006): Mechanical property of liquefied stabilized soil and future issues, *Doboku Gakkai Ronbunshuu, F*, Vol.62, No.4, 618-627 (in Japanese).

Kohata, Y., Fujikawa, T., Ichihara, D., Kanda, M., and Murata, O. (2002): Strength and deformation properties of fibered material mixed in liquefied stabilized soil obtained from uniaxial compression test, *Proc. of the 36th Japan National Conf. on Geotech. Eng.*, pp.635-636 (in Japanese).

Kohata, Y., and Tsushima, H. (2004): Effect of fibered material mixing in liquefied stabilized soil on the triaxial shear characteristics, *Proc. of the 39th Japan National Conf. on Geotech. Eng.*, 721-722 (in Japanese).

Kohata, Y., Ichikawa, M., Nguyen, C. Giang., and Kato, Y. (2007): Study of damage characteristics of liquefied stabilized soil mixed with fibered material due to triaxial shearing, *Geosynthetics Engineering Journal*, Vol.22, 55-62 (in Japanese).

Ito, K., Kohata, Y., and Koyama, Y. (2011): Influence of additive amount of cement solidification agent on mechanical characteristics of Liquefied Stabilized Soil mixed with fibered material, *Japanese Geotechnical Society Hokkaido Branch Technical Report Papers*, Vol.51, 131-136 (in Japanese).

Giang, N. C. (2010): Study on advanced effective utilization of excavated soil in Hanoi city – Vietnam, *a thesis, division of civil and environmental engineering; graduate school of Muroran Institute of technology*.

Chapter 2

OVERVIEW OF LIQUEFIED STABILIZED SOIL

2.1. INTRODUCTION

The soil stabilization is process improving if geotechnical properties to stratify engineering requirements. Until now, numerous kinds of stabilizers including cement, lime and fly ash etc. were used as soil additives to improve its properties. The LSS manufacturing process utilizes soil which has been excavated in construction projects and which would otherwise be discharged to natural environment as soil waste. LSS can be used for confined spaces or excavation areas and it can be easily placed without vibration and compaction. The characteristics, benefits, advantages and applications of LSS has been shown such as:

Characteristics:

- Impermeability

Benefit:

- Reduce cost of construction projects
- Reduce manpower
- Protect environment

Advantage:

- Excavated out easily
- Quick setting time
- Convenient compared to normal backfilling
- Faster than normal backfilling
- No soil stockpile needed

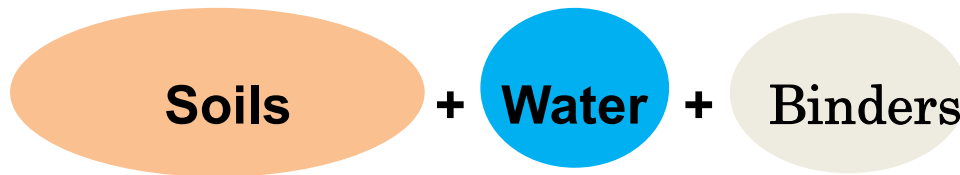
Application:

- Backfill sing concrete pump

- Cavities and excavated trenches can be backfilled easily

2.2. COMPONENT OF LIQUEFIED STABILIZATION SOIL

Liquefied stabilized soil involves the use of binder materials in soils to improve its geotechnical properties such as compressibility, strength, permeability, flexibility and durability. The components of liquefied stabilized soil include soils, binders (cementitious materials).



2.2.1. Soil

Most soils in liquefied stabilized soil method are soft soils. The stabilization has been performed to achieve desirable engineering properties. The main purpose of liquefied stabilized method is to recycle excavated soil for backfilling processes for construction projects. Therefore, almost types of excavated soils can be used for this method. However, fine-grained granular materials are the easiest to stabilize due to a large surface area in their contact diameter. The excavated soils can be modified to perform mainly with the purpose of improving their usability in construction. At present, excavated soils are stabilized by binders which are selected in relation to the type of soil. The stabilization has improved the strength of the soils and their resistance to softening.

2.2.2. Cementitious materials

In stabilizing a soil, these are hydraulic (primary binders) or non-hydraulic (secondary binders) materials that when in contact with water or in the presence of pozzolanic minerals reacts with water to form cementitious composite materials. The commonly used binders are: cement, lime or fly ash. In order to decide which binder should be used, the analysis have be performed based on test results and in fact condition of projects.

1. Cement

Cement had been known as the binding agent since the invention of soil stabilization technology in the 1960's. It may be considered as primary stabilizing agent or hydraulic binder because it can be used alone to bring about the stabilizing action required. Cement reaction is not dependent on soil minerals, and the key role is its reaction with water that may be available in any soil. This can be the reason why cement is used to stabilize a

wide range of soils. Numerous types of cement are available in the market; these are ordinary Portland cement, blast furnace cement, sulfate resistant cement and high alumina cement. Usually the choice of cement depends on type of soil to be treated and desired final strength. Hydration process is a process under which cement reaction takes place. The process starts when cement is mixed with water and other components for a desired application resulting into hardening phenomena. The hardening (setting) of cement will enclose soil as glue, but it will not change the structure of soil. The hydration reaction is slow proceeding from the surface of the cement grains and the Centre of the grains may remain unhydrated. Cement hydration is a complex process with a complex series of unknown chemical reactions. However, this process can be affected by presence of foreign matters or impurities, water-cement ratio, curing temperature, the presence of additives, and specific surface of the mixture.

2. Lime

Lime is the oldest traditional stabilizer used for soil stabilization. Lime-treated soil was studied extensively in the literature. Numerous field and laboratory studies were conducted to evaluate the improvement of geotechnical properties by lime. Several types of soils, lime contents and curing conditions and methodologies were used for this purpose. The mechanism of treatment comprised hydration, cation exchange, flocculation-sagglomeration of soil particles and pozzolanic reaction to form Calcium Silicate Hydrate (C-S-H) and Calcium Aluminate Hydrate (C-A-H) as cementitious materials. The factors affecting lime treated soil are lime content, curing time, curing temperature and soil mineralogy. Soil-lime mixtures have advantages and disadvantages. Its advantages comprise significantly increase soil strength, reduce plasticity (increase workability) and increases soil durability. In addition, a considerable reduction in consolidation settlement and improve compressibility characteristics were observed. Unclear behavior was noted for the permeability of soil-lime mixture when compared with the original soil. Carbonation, sulfate attack and environment impact are a number of the disadvantages of lime-treated soil. Some studies were conducted to provide some guidelines to reduce the deleterious effects of these cons. Magnesium oxide and hydroxide can be proposed as alternative for lime since they possess chemical characteristics make them eligible to overcome the mentioned cons. Moreover, the result of few conducted studies used magnesium based additives to stabilize the soil was significant improvement achieved in soil strength, workability and durability. Therefore,

it is need to conduct extensive studies to determine the efficiency of this material in soil stabilization.

3. Fly ash

Fly ash has been used successfully in many projects to improve the strength characteristics of soils. Fly ash can be used to stabilize bases or subgrades, to stabilize backfill to reduce lateral earth pressures and to stabilize embankments to improve slope stability. Typical stabilized soil depths are 15 to 46 centimeters. The primary reason fly ash is used in soil stabilization applications is to improve the compressive and shearing strength of soils. The compressive strength of fly ash treated soils is dependent on:

- To enhance strength properties
- Stabilize embankments
- To control shrink swell properties of expansive soils
- Drying agent to reduce soil moisture contents to permit compaction

Class C fly ash can be used as a stand-alone material because of its self-cementitious properties. Class F fly ash can be used in soil stabilization applications with the addition of a cementitious agent (lime, lime kiln dust, CKD, and cement). The self-cementitious behavior of fly ashes is determined by ASTM D 5239. This test provides a standard method for determining the compressive strength of cubes made with fly ash and water (water/fly ash weight ratio is 0.35), tested at seven days with standard moist curing. The self-cementitious characteristics are ranked as shown below:

- Very self-cementing > 500 psi (3,400 kPa)
- Moderately self-cementing 100 - 500 psi (700 - 3,400 kPa)
- Non self-cementing < 100 psi (700 kPa)

It should be noted that the results obtained from ASTM D 5239 only characterizes the cementitious characteristics of the fly ash-water blends and does not alone provide a basis to evaluate the potential interactions between the fly ash and soil or aggregate.

The use of fly ash in soil stabilization and soil modification may be subject to local environmental requirements pertaining to leaching and potential interaction with ground water and adjacent water courses.

Soil Stabilization to Improve Soil Strength

Fly ash has been used successfully in many projects to improve the strength characteristics of soils. Fly ash can be used to stabilize bases or subgrades, to stabilize backfill to reduce lateral earth pressures and to stabilize embankments to improve slope stability. Typical stabilized soil depths are 15 to 46 centimeters (6 to 18 inches). The primary reason fly ash is used in soil stabilization applications is to improve the compressive and shearing strength of soils. The compressive strength of fly ash treated soils is dependent on:

- In-place soil properties
- Delay time
- Moisture content at time of compaction
- Fly ash addition ratio

2.3. HISTORICAL DEVELOPMENT

The original concept comes from the United States, soil mixing was first developed by Intrusion-Prepakt, Inc. of Cleveland Ohio (Liver et al. 1954) as “Intrusion Grout Mixed-in-Place Piles”.

In 1961, the mixed in place already used under license for more than 300 000 lineal meters of piles in Japan for excavated support and groundwater control. Continued until early 1970’s by Seiko Kogyo Company, to be suggested by diaphragm walls and deep mixing method (Soil-Mix Wall). In addition, Herrin and Mitchen (1961) suggested that there is no one of optimum lime content with which maximum strength of lime stabilized soils can be expected under all condition. That is, for a specific condition of curing time and soil type an optimum lime content which caused a maximum strength exists.

The development and research on deep mixing started from laboratory model tests in 1967 by the Port and Harbour Research Institute of Japanese Ministry of Transportation. Research was continued by Okumura, Terashi et al. through 1970’s including 1- investigation of lime-marine reaction, and 2- develop appropriate mixing equipment. Unconfined compressive strength (UCS) of 0.1 to 1 MPa achieved. Early equipment (Mark I-IV) used the first marine trial near Hamada Airport (10 m below water surface). In addition, Swedish Lime column method for treating soft clays under embankment using unslaked lime was researched (Kjeld Paus, Linden- Alimak AB, in cooperation with Swedish Geotechnical Institute, Euroc AB, and BPA Byggproduktion AB). And then, this follows observations by Paus on fluid lime column installation in the United State.

In the late 1960's, China reported to be considering implementing Depp lime mixing concept from Japan.

Development of Soil Mixed wall method for retaining walls, using overlap multiple augers was started in Japan by Seiko Kogyo Co. of Osaka in 1972 to improve lateral treatment continuity and homogeneity/quality of treated soil.

The first Japanese full-scale Deep Mixing project was conducted in 1974. First applications in reclaimed soft clay at Chiba (June) with and Applications elsewhere in Southeast Asia follow the same year. In addition, intensive trials conducted with Lime Columns at Ska Edeby Airport, Sweden: basic tests and assessment of drainage action (columns 15 m long and 0.5 m in diameter). In 1974, first detailed description of Lime Column method by Arrason et al. (Linden Alimaik AB). And the first similar trial embankment using Swedish Lime Column method in soft clay in Finland (6 m high, 8 m long; using 500-mm-diameter lime cement columns, in soft clay) in 1974.

In 1975, deep mixing's first appearance in an international forum in Bangalore, India, a Swedish paper on Lime Colum by Broms and Boman. In addition, a Japanese paper on Deep Lime Mixing (DLM) by Okumura and Terashi were presented to the Swedish paper on lime columns (Broms and Boman), and Japanese paper on DLM (Okumura and Terashi) presented at same conference in Bangalore, India. Both countries had proceeded independently to this point. Limited technical exchanges occur thereafter. Following their research from 1973 to 1974, PHRI develops the forerunner of the Cement Deep Mixing (CDM) method using fluid cement grout and employing it for the first time in large-scale projects in soft marine soils offshore. (Originally similar methods include DCM, CMC (still in use from 1974), closely followed by DCCM, DECOM, DEMIC, etc., over the next five years). In addition, First commercial use of Lime Column method in Sweden for support of excavation, embankment stabilization, and shallow foundations near Stockholm (by Linden Alimak AB, as contractor and SGI as consultant/researcher) in 1975.

Public Works Institute Ministry of Construction, Japan, in conjunction with Japanese Construction Machine Research Institute began research on the Dry Jet Mixing (DJM) method using dry powdered cement (or less commonly, quick-lime) in 1976. It was also the same year that Soil Mixed Wall (SMW) method used commercially for first time in Japan by Seiko Kogyo Co.

In 1977, Cement Deep Mixing (CDM) method had been marked development. CMD method Association established in Japan to coordinate technological development via a collaboration of industrial and research institutes and the first practical use of CMD (marine and land uses). First design handbook on lime columns (Broms and Boman) published by Swedish Geotechnical Institute. China commences research into CDM, with first field application in Shanghai using its own land-based equipment in 1978.

The first commercial using in Japan of Dry Jet Mixing was marked in 1980, and then it quickly superseded Deep Lime Mixing (DLM) with land-use only. In addition, DJM Association established in Japan. After that, in 1983, Eggestad publishes state-of-the-art report in Helsinki dealing with new stabilizing agents for Lime Column method.

In 1984, SWING method developed in Japan, followed by various related jet-assisted (W-R-J) methods in 1986, 1988, and 1991.

The Tenox Company reported more than 1000 projects completed with SCC method in Japan (1989), prior to major growth thereafter (9000 projects to end of 1997, with a \$100 to 200 million/year revenue in Japan and elsewhere in Southeast Asia). And then, in 1990, Dr. Terashi, involved in development of DLM, CDM, and DJM since 1970 at Port and Harbor Research Institute, Japan, gives November lectures in Finland. Introduces more than 30 binders commercially available in Japan, some of which contain slag and gypsum as well as cement. Possibly leads to development of “secret reagents” in Nordic Countries thereafter.

Low Displacement Jet Column Method (LDis) developed in Japan in 1991. In the same year, Bulgarian Academy of Sciences reports results of local soil-cement research and Geotechnical Department of City of Helsinki, Finland, and contractor YIT introduce block stabilization of very soft clays to depths of 5 m using a variety of different binders.

In early 1990s, First marine application of CDM at Tiajin Port, China: designed by Japanese consultants (OCDI) and constructed by Japanese contractor with his own equipment (Takenaka Doboku).

In 1991, Chinese Government (First Navigational Engineering Bureau of Ministry of Communications) builds first offshore CDM equipment “fleet”, using Japanese technology used for first time (1993) at Yantai Port. (Reportedly the first wholly Chinese Design-Build DMM project.). And Jet and Churning System Management (JACSMAN) developed by Fudo Company and Chemical Grout Company in Japan.

DJM Association Research Institute publishes updated Design and Construction Manuals (in Japanese) in 1993. In the same year, CDM Association claims 23.6 million m³ of soil treated since 1977. And SMW claims 4000 projects completed worldwide since 1976, comprising 12.5 million m² (7 million m³). According to report in Japan, from 1977 to 1995, more than 26 million m³ of CDM treatment reported and about 15 million m³ of DJM treatment.

In 1997, SMW method used for massive ground treatment project at Fort Point Channel, Boston, MA (largest DMM project to date in North America), and other adjacent projects. Input at design stage to U.S. consultants by Dr. Terashi (Japan).

From 1998 to around the year 2000, a variety of numerical modeling work has been performed on the interaction of soil cement columns in soft clays, for example Kerin and Karstunen (2009), Chai et al. (2010) and Abushara et al. (2009). These studies have focused on settlement reduction from “T” shaped columns, “cross” shaped columns and “multi columns” supported embankment loading.

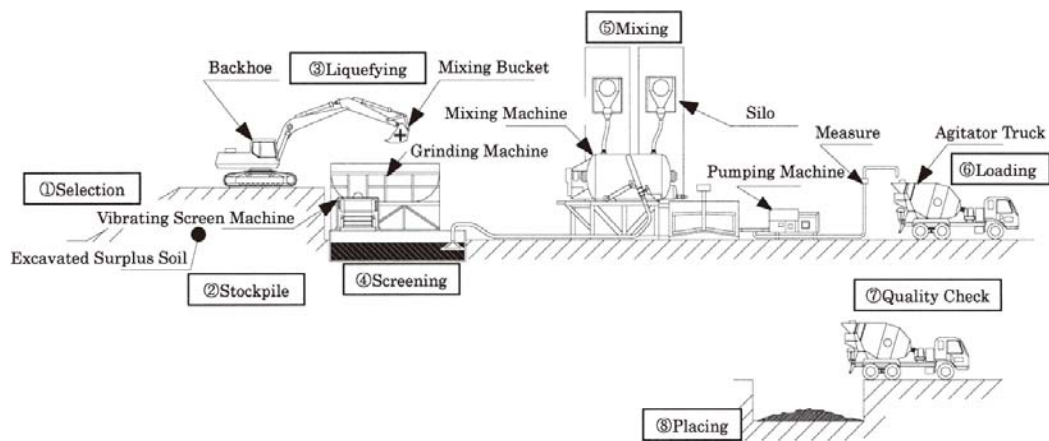


Figure 2.1 Flow of Liquefied soil stabilized method (Tomoharu et al., 2005)

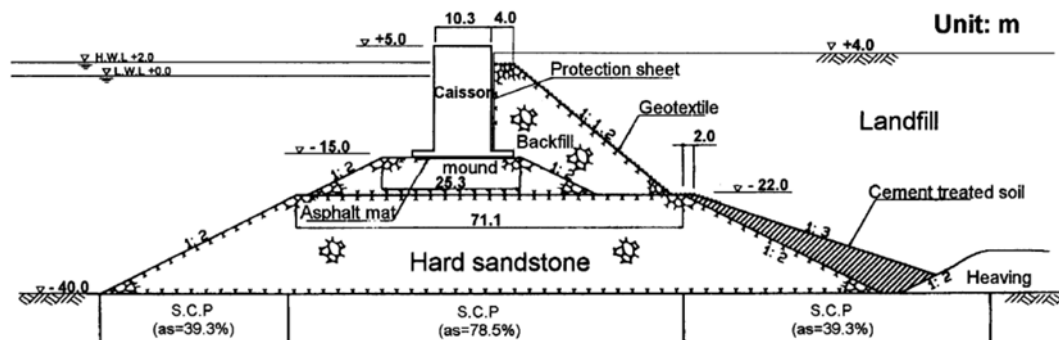


Figure 2.2 Cement treated soil using as slope protection (Tang et al., 2001)

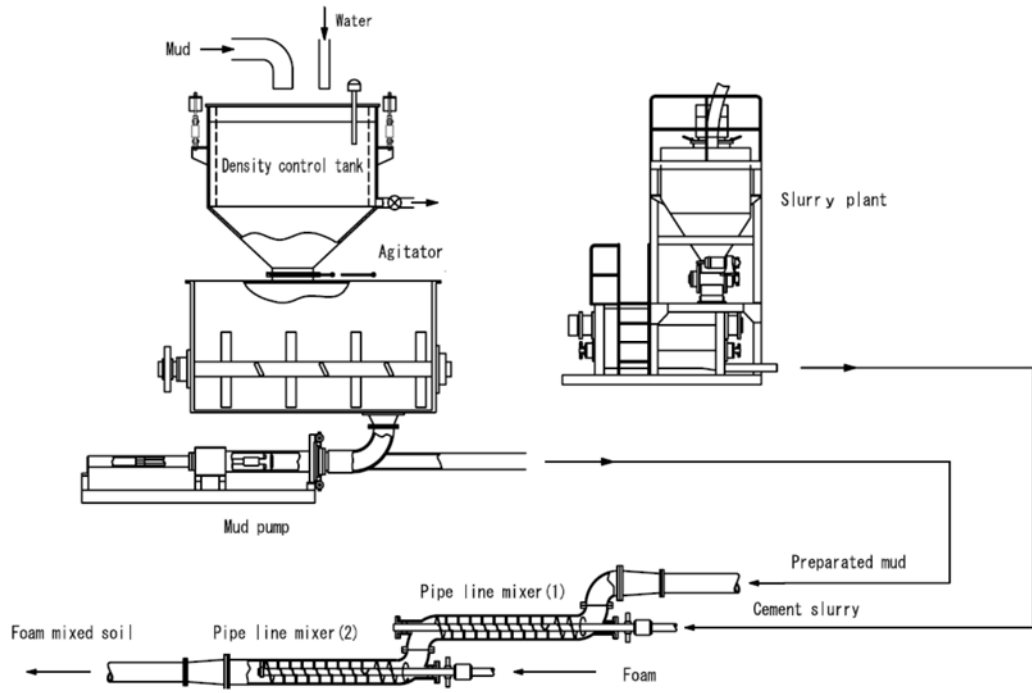


Figure 2.3 Production system for foam mixed lightweight soil

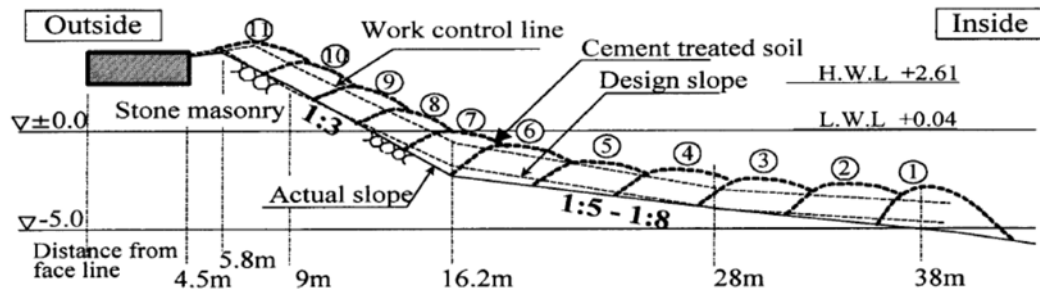


Figure 2.4 Placement of cement treated soil along slope (Tang et al., 2001)



Figure 2.5 Placement of cement treated soil along slope (Tang et al., 2001)

2.4. APPLICATIONS

In 1997, Kuno et al. presented one of several applications of LSS method; filling a cavity under pavement of urban road (Figure 2.8). The cavity is inferred mainly in the way that the submerged backfilled sand in the ground is washed out little by little to a nearby open space, for example sewage pipes, and thus, a cavity is created and grown. This application is thought to be possible of decreasing time and cost comparing to a conventional method. Thus two kinds of filed performance tests were conducted in order to verify capability and applicability of the method and acquire necessary field data for future maintenance works. The first field performance test used an on-site plant and a stabilized soil of low strength and relatively high flow condition while the second test use remote plant and stabilized soils of high strength and low flow condition. The tests were evaluated in term of adequate mix proportion, working system, working time, filling outcome, occupation of road, result of quality control test, and so on. Through two sequential field performance tests, it is confirmed that the method possesses good capability of filling cavities under the pavement and make it possible to decrease time and cost.

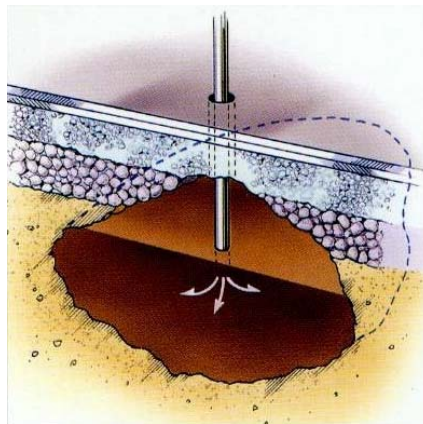


Figure 2.6 Use of LSS for filling cavity under road surface

Murata (2011) reported that LSS consists of slurry made of on-site soil, water, cement and sand of clay as appropriate LSS is used for backfill at upper part of a cut and cover tunnel and as an invert material of a shield tunnel (Figure 2.9). Pit sand is usually used for backfill, but LSS is much better than the sand, because it is easy to use with on-site soil and LSS can be buried without compaction into a narrow space. The lower part of shield tunnel is usually buried by low-strength concrete (unconfined compressive strength: about 10 MN/m^2). From the environmental point of view, however, LSS, which can reuse on-site soil, is now often use. Mixture of LSS was designed from the results of

unconfined compressive tests and repeated loading tests. Then, it was designed the unconfined compressive strength of liquefied soil should be 6 MN/m^2 for safety purpose. To hold this strength level for some on-site soil, a very large amount of cement is needed ($300 \sim 400 \text{ kg/m}^3$ of LSS). So, a method to mix wasted fiber materials into LSS has been studied in order to increase the strength and ductility and decrease the total material cost. Studied have been promoted on what types of wasted fiber material are available and what rigidity level of wasted fiber material is needed.

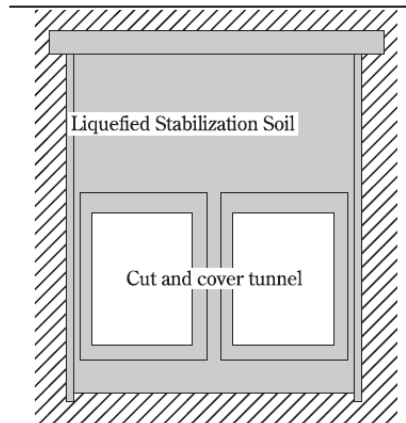


Figure 2.7 LSS used for backfill at upper part of cut and cover tunnel

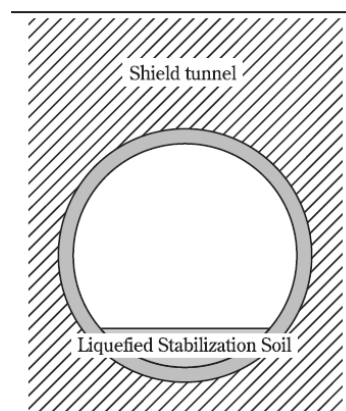


Figure 2.8 LSS used for invert material of shield tunnel

The design of strength and quality control method of LSS used as building foundation is proposed by Tomoharu et al. (2005). The results of the research pointed out that it is feasible for LSS to apply for the building foundation in future perspective. Another application of LSS is for constructing fences or retaining walls. Yoshihiro et al. (2006) reported that concrete block construction, which is common for these structures, tends to collapse under strong earthquakes, thus causing a threat to traffic, whereas liquefied stabilized soil block construction is capable of avoiding such damage due to the greater toughness of the material. Also, soil blocks are advantageous over concrete blocks in term

of appearance. In their research, they have examined the effects of adding PVA fiber to LSS blocks under atmospheric condition. Tests were carried out on the drying shrinkage properties, resistance to atmospheric exposure, and uniaxial compressive strength. It found that PVA fiber reduces the drying shrinkage, crack propagation, and compressive strength of LSS block. The following Figure 2.10 is more examples of using LSS for various backfilling works in Japan.

Recently, most underground pipelines have been backfilled by LSS (Figure 2.10e). Figure 2.11 shows a construction site of the pipelines using LSS. Kawabata et al. (2008) conducted full scale field test for buried pipe using steel pipe of 3500 mm-diameter and 26 mm-thickness. Five cases of backfilling methods were applied. From the test results,

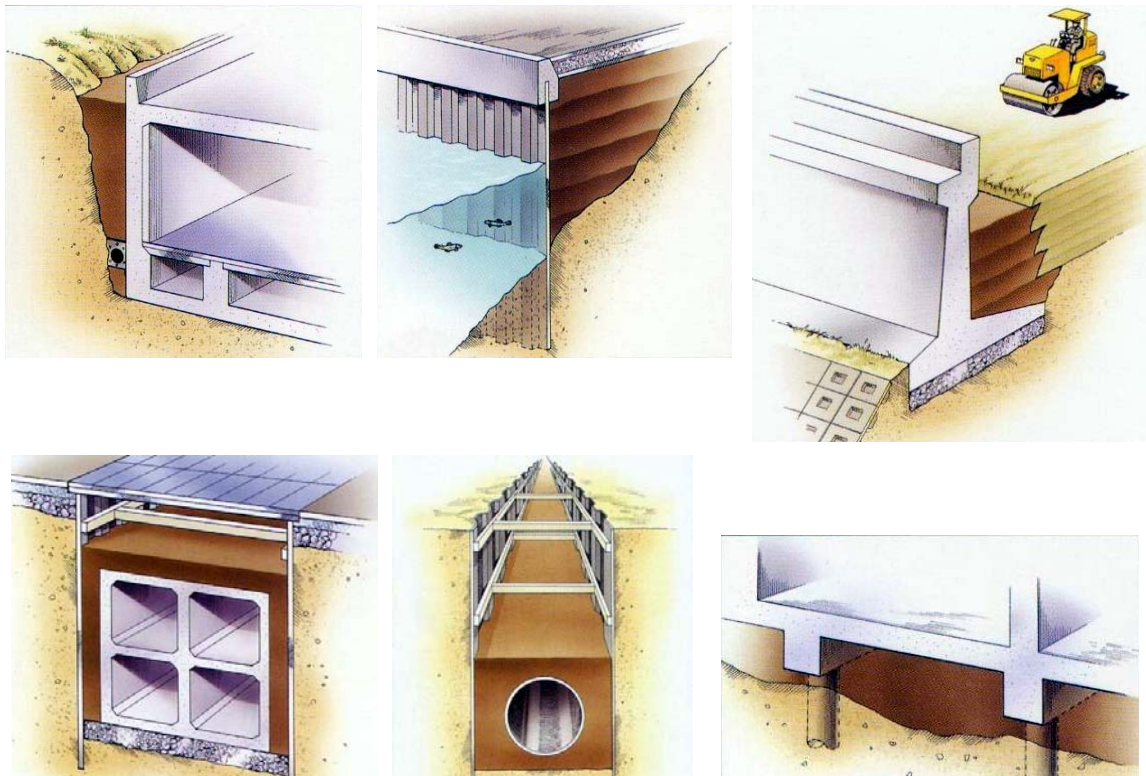


Figure 2.9 Using LSS for various backfilling works in Japan

it was found that the behavior of buried pipe was strongly influenced by the stiffness of backfilling method. In particular, the pipe which is backfilled with LSS showed stable behavior. Moreover, Kashiwaghi et al. (2009) and Kawabata et al. (2010) have proposed a method for thrust restraint using LSS. Mode I pit experiments using a model pipe having a diameter of 260 mm were carried out in order to examine the effectiveness of the LSS for the thrust restraint of buried bend. LSS was applied to the passive area of the model pipe and dry silica sand was used as backfill material. The model pipe was laterally loaded at a speed of 1 mm/min after backfilling to simulate the thrust force. The lateral resistance

and horizontal displacement of the model pipe were both measured. The earth pressure distributions of the passive ground were observed. The results showed that the lateral resistance of the bend in using LSS was increased. It is verified that LSS is an effective backfill material for thrust restraint. Also, other experimental research results showed that the bending stiffness in case using LSS with geosynthetics was increased (Kawabata et al., 2009). In addition, the passive resistance was considerably increased in case using LSS with geogrid (Kawabata et al., 2008).

In 2006, Kohata has proposed a reinforcement method for LSS by mixing crushed newspaper as a fibered material into LSS, and carried out a series of unconfined compression tests and triaxial tests. The results indicated that by reinforcement effect, brittle property of LSS mixed with fibered material after the peak was improved.

2.5. SITUATION OF BACKFILLING PROCESS IN VIETNAM

2.5.1. Problem of backfilling method in Vietnam



Figure 2.10 Cave-in and road collapses in Hanoi city

According to report of Ministry of Construction of Vietnam, more and more cave-ins and local subsidence have been appeared at urban areas in Hanoi city because sewer pipes and water supply pipes were damaged. Main reason of the problems is to soil loosened during underground infrastructure construction and water leaked from ruptured underground pipelines. The earth under cities' roads is crisscrossed with public utility networks supplying electricity, telecommunications services, heating and for drainage. Large underground projects such as subways, shops and tunnels are also intensifying. The

roads are often dug open to install or repair various utility networks, which are managed by different utility providers. Sometimes, the same section of a road is repeatedly dug up and repaved by different departments. If backfilled soil has not been sufficiently compacted, loosened soil under the road will be easily washed away by heavy rain, which is resulting in cavities and road collapses, according to the report. Road cave-ins used to occur only on automotive lanes, whereas in the last two years they also affected bicycle lanes and pedestrian walks. Sewage pipes and rainwater drainage pipes usually run underneath bicycle lanes and pedestrian walks, which are more likely to cave in after heavy rainfall. The report suggested that if there is no other underground construction project, usually, the road depression will not be very deep.

Therefore, the cavity under the pavement is inferred mainly in the way that the submerged poor backfilled material in the ground is washed out little by little to a nearby open space, for example sewage pipe or base-floor of high-rise building under construction, and then, cavity is creative and grown. On the other hand, the poor backfilled material which is insufficiently compacted causes the instability of water supply pipe. Moreover an over compaction in the construction stage can bad impact on the pipe structure. These are two of reasons make the main water supply pipe line of Hanoi city easier to break (Ministry of Construction, 2014). The line was broken ten times since operated in 2012 until 2014.

2.5.2. Inappropriate disposal of excavated soils

Nowadays, excavated soils from construction sites are becoming a serious problem in Vietnam. It becomes more and more difficult to find reclamation sites for excavated soil to dump around big city. Because of shortage of reclamation sites and part of soil is disposed inappropriate, it causes the environmental pollution.



Figure 2.11 inappropriate disposal of excavated soils from construction sites in Hanoi

According to a new study released today by Ministry of Natural Resources and Environment of the Socialist Republic of Vietnam, about 1,000,000 m³ of excavated soil will have to be trucked from construction projects to disposal sites in Hanoi city over the next decade or two. The construction of the first phase of the metro line project alone, for example, will generate some 1,500,000 m³ of excavated soil. The study estimates that it could cost 100 million dollars or more to transport and dispose of these soils depending on the future availability of sites. Another project, the City of Hanoi's own water and sewer capital program, will produce more than 800,000 m³ between now and the end of the decade. The question of where to put this extracted soil, according to the Ministry, some area surrounding Hanoi city are now restricting or banning the importation of soils.

2.5.3. Mining of new material from natural resources

In Vietnam, most backfilling material for construction is being extracted from natural sources. Mining of the materials such as sand from river and gravel from mountain has a significant impact on the natural environment. The demand for sand and gravel continues to increase day by day. Excessive instream sand-and-gravel mining causes the degradation of rivers. Instream mining lowers the stream bottom, which lead to bank erosion (see Figure 2.17). Depletion of sand in the streambed and along coastal areas causes the deepening of rivers and estuaries, and the enlargement of river mouths and coastal inlets. It may also lead to saline-water intrusion from the nearby sea. The effect of mining is compounded by the effect of sea level rise. Any volume of sand exported from streambeds and coastal areas is a loss to the system.

Excessive instream sand mining is a threat to bridges, river banks and nearby structures. Sand mining also affects the adjoining groundwater system and the uses that local people make of the river.

Instream sand mining results in the destruction of aquatic and riparian habitat through large changes in the channel morphology. Impacts include bed degradation, bed



Figure 2.12 Bank erosion due to depletion of sand in streambed

coarsening, lowered water tables near the streambed, and channel instability. These physical impacts cause degradation of riparian and aquatic biota and may lead to the undermining of bridges and other structures. Continued extraction may also cause the entire streambed to degrade to the depth of excavation. Sand mining generates extra vehicle traffic, which negatively impairs the environment. Where access roads cross riparian areas, the local environment is being impacted.

2.6. UTILIZATION OF LSS IN VIETNAM

From the above discussion about many advantages as using of LSS for construction works in Japan and current situation of excavating works in Vietnam, it can be said that if LSS will be applied in Vietnam, the aforementioned serious problems can be solved. Thus, a feasible research whether LSS can be applied in Vietnam has been carried out by Nguyen et al., 2010. In the research, a series of physical tests for Hanoi clay (Vinh Phuc-Clay) which was obtained from areas around the planned sites of subway at Hanoi and consolidated-undrained triaxial compression tests (CUB tests) were performed to investigate strength and deformation properties of LSS using Vinh Phuc-clay as a base material (Vinh Phuc-clay LSS). The test results were compared with that of LSS using base material of NSF-clay which is common clay for LSS in Japan. The effects of crushed waste newspaper as a fiber material into these LSS were also investigated. In addition, the vibration characteristic of ground in the case using Vinh Phuc-clay LSS for backfilling of cut and cover tunnel was examined by two-dimensional FEM in his research. The results of the study indicated that Vinh Phuc-clay could provide conditions satisfying LSS' terms determined in Japanese clay, and confirmed that the LSS method is applicable in Vietnam. Moreover, the strength and deformation properties of Vinh Phuc-clay LSS mixed with fibered material has been improved. Also, the LSS shows excess consolidation behavior caused by cementation effect, and remarkable reinforcement effect by adding fibered material in comparison with Japanese NSF-clay LSS. In addition, the result confirmed that the LSS has effect on reduction of ground vibration caused by traffic load.

2.7. SUMMARY

An overview of Liquefied Stabilizes Soil (LSS) has been presented in this chapter. In Japan, the utilization of LSS in construction fields brings double advantages from the environment point of view. Thus, two big problems which are shortage of backfilling material usually extracted from natural sources and excavated soil generated from

construction sites have been effectively solved together. On the other hand, at present, Vietnam is facing serious problems concerning the excavating works which excavated soil is inappropriately disposed to surrounding environment due to the shortage of reclamation sites and the negative impacts on living environment and society as mining sand and gravel from river and mountain to be backfilling material for construction works and so on. In 2010, A feasible research on applicability of LSS in Vietnam has pointed out that LSS using Vinh Phuc-clay that spread in Hanoi city of Vietnam can be manufactured conforming to standards designated for Japanese LSS. From these, it should be expected that LSS can be applied in Vietnam as soon as possible.

Based on the above, the aim of this dissertation is to investigate the deformation and strength characteristics of LSS and LSS mixed with crushed waste newspaper as a fiber material which was proposed by Kohata, 2006 and then to promote the use of LSS in Vietnam in near future.

REFERENCES

Okumura, T. and Terashi, M. (1975): Deep lime-mixing method of stabilization for marine clays. *In: Proceeding of the 5th Asian Region Conference on Soil Mechanics and Foundation Engineering*, Bangalore, Vol.1, pp. 69-75.

Terashi, M., Tanaka, H. and Okumura, T. (1979): Engineering properties of lime treated marine soils and DMM. *In: Proceedings of 6th Asian Regional Conference on Soil Mechanics and Foundation Engineering*, Vol.1, pp.191-194.

Terashi, M. (1983): Practice and problems of the deep mixing method of soil stabilization, *Soils and Foundations*, Vol. 31-8, pp.75-83.

Kawasaki, T., Niina, A., Saitoh, S., Suzuki, Y. and Honjo, Y. (1981): Deep mixing method using cement hardening agent. *In: Proceedings of 10th International Conference on Soil Mechanics and Foundation Engineering*, Stockholm, pp.721-724.

Suzuki, Y. (198): Deep chemical mixing methods using cement as hardening agent. *In: Symposium of Soil and Rock Improvement Technology Including Geotextile, Reinforced Earth and Modern Piling Methods Asian Institute of Technology*, Bangkok, pp.B-1-1-B-1-24.

Bergado, D. T., Manivannan, R., Balasubramaniam, A.S., (1996): Proposed criteria for discharge capacity of prefabricated vertical drains, *Geotextiles and Geomembranes*, Vol.14, pp.481–505.

Tatsuoka, F., Kohata, Y., Uchida, K. and Imai, K. (1996): Deformation and strength characteristics of cement treated soils in Trans-Tokyo Bay Highway project, *In: Proceedings of the 2nd International Conference on Ground Improvement Geosystems*, Vol.1, pp.453-459.

Uddin, K., Balasubramaniam, A.S and Bergado, D.T. (1997): Engineering behavior

of cement treated Bangkok soft clay, *Geotechnical Engineering Journal*, Vol.28, pp.89-119.

Horpibulsuk, S., Rachan, R., Chinkulkijniwat, A., Raksachon, Y., Suddeepong, A. (2010): Analysis of strength development in cement-stabilized silty clay from microstructural considerations, *Construction and Building Materials*, Vol.24, pp.2011-2021.

Chai, J.C. and Miura, N. (2005): Cement/lime mixing ground improvement for road construction on soft ground, *Ground Improvement - Case Histories, Ed. B*, Indraratna, and J.Chu, Elsevier, pp. 279-304.

Kuno, G., Okamoto, S. and Shibata, Y. (1998): Recycling excavated soil to back-filling material with liquefied stabilized soil method, *Proc. CIB world building congress*, Gaevle, Sweden, 7-12 June 1998.

Kuno, G., eds (1997): Liquefied stabilized soil method-Recycling technology of construction-generated soil and mud, *Gihodo publication* (in Japanese).

Ministry of Environment (2012): Installation of industrial waste treatment facilities, situation on the authorization of the industrial waste treatment industry (achievements of 2009), *press release material* (March 27th, 2012) (in Japanese).

Japanese Geotechnical Society (2005): Committee Report Chapter 2, 2.1, 2.2 on test methods and physical properties of cement-modified soil, *Proc. of symposium*, pp.2-22, on survey, design, construction and properties evaluation methods of solidifying stabilized soil using cement and cement-treated soil (in Japanese).

Kohata, Y. (2006): Mechanical property of liquefied stabilized soil and future issues, *Doboku Gakkai Ronbunshuu, F*, Vol.62, No.4, pp.618-627 (in Japanese).

Kuno, G., Miki, H., Mori, N. and Iwabuchi, J. (1995); Study on back filling method with liquefied stabilized soil as to recycling excavated soils, *Individual papers 20th world road congress*, Montreal, Canada.

Kuno, G., Miki, H., Mori, N. and Iwabuchi, J. (1996); Application of the liquefied stabilized soil method as a soil recycling system, *Proc. the second international congress on environmental geotechnic*, Osaka, Japan.

Miki, H., Iwabuchi, J. and Chida, S. (2005): New soil treatment methods in Japan.

Tang, Y. X. Miyazaki, Y. and Tsuchida, T. (2001): Practices of reused dredging by cement treatment, *Soils and Foundations*, Vol. 41(5), pp.129-143.

Hino, T., Taguchi, T., Chai, J. C., and Shen, S. L. (2008): The Ariake sea coastal road project in the Saga lowlands: Properties of soft foundations and use of dredged clayey soil as an embankment material, *In: Proceeding of the International Symposium on Lowland Technology*, ISLT, IALT, Busan, Korea, pp.467-472.

Chai, J.C., Hino, T., Igaya, Y. and Yamauchi, Y. (2011): Embankment construction with saturated clayey fill material using geocomposites, *Geotechnical Engineering Journal of the SEAGS & AGSSEA*, Vol.42 (1), pp.35-41.

Kuno, G., Miki, H., Mori, N. and Iwabuchi, J. (1997); Filling a cavity under pavement

of urban road with liquefied stabilized soil, *Road construction rehabilitation and maintenance*, XIII th IRF world meeting, Toronto, Canada .

Tomoharu, O., Mitsuo, N., Hiroki, Y., Mamoru, F. and Hiroyuki, A. (2005): Liquefied stabilized soil method for building foundation, *Japanese Society of Material Science*, Japan, Vol.54, No.11, pp.1129-1134 (in Japanese).

Murata, O. (2001): Recent research and development on soil and foundation engineering at Railway Technical Research Institute (Japan), *QR of RTRS*, Vol.42, No.3, pp.122-124.

Kawabata, T., Sawada, Y., Oguchi, K., Totsugi, A. Hironaka, J. and Uchida, K. (2007): Large scale tests of buried bend with lightweight thrust restraint using geosynthetics, *ISOPE2007*, Lisbon, Portugal.

Kawabata, T., Sawada, Y., Kashiwagi, A., Izumi, A. and Uchida, K. (2008): The effect of liquefied stabilized soil with geosynthetics against thrust force of buried bend, *Proc. of the Eighteenth (2008) International offshore and Polar engineering conference Vancouver*, BC, Canada, July 6-11, 2008, pp.660-664.

Kawabata, T., Takafumi, H., Kashiwagi, A., Izumi, A. and Kada, M. (2009): Bending test for liquefied stabilized soil with steel rebar, *Proc. of the Nineteenth (2009) International offshore and Polar engineering conference*, Osaka, Japan, June 21-26, 2009.

Kashiwagi, A., Kawabata, T., Satoshi, O. and Uchida, K. (2009): Evaluation of lateral resistance for buried conditions around pipe with horizontal loading, *Proc. of the Nineteenth (2009) International offshore and Polar engineering conference*, Osaka, Japan, June 21-26, 2009.

Kawabata, T., Kashiwagi, A., Sawada, Y., Okuno, S., Ling, H., and Mohri, Y. (2010): Lateral Loading Experiment on Buried Pipe Using Liquefied Stabilized Soil as Backfill Material for Thrust Restraint, *ASCE Library, Pipelines 2010*, pp.1244-1254.

Nguyen, C. G. (2010): Study on advanced effective utilization of excavated soil in Hanoi city – Vietnam, *a doctoral thesis*, division of civil and environmental engineering, graduate school of Muroran Institute of technology.

Chapter 3

INFLUENCE OF SLURRY DENSITY ON PROPERTIES OF LSS

3.1 INTRODUCTION

In recent years, infrastructure system and many new urban areas in Hanoi city have been built and modernized. Urban traffic network has been invested, upgraded. Public transportation, especially Bus Rapid Transit (BRT) and urban railway has been invested. Vietnamese government had the plan that Hanoi's transport plan aims to increase the share of public transport. That is, the current low figure of 9 % trips is increased to above 60 % by 2030, by which time Hanoi city is slated to have six metro lines and three Bus Rapid Transit (BRT) lines. However, a huge excavated soil has been generated at construction sites which is away as waste to disposal areas being one of the challenges facing the urbanization industrialization rates in Hanoi city. Specifically, the excavated soil generated at construction projects has been trucked to disposal sites. In addition, sand produced from mountain or river valleys is easy to be compacted to a degree of compaction prescribed a standard according to conventional backfilling methods in Vietnam. On the other hand, disposal sites in the capital city are already overloaded with the large volume of excavated soil generated at present. This situation has caused not only increasing the cost of the projects, but also the environmental pollution and depletion of natural resources.

In order to improve the situation, there is an urgent need to act strategically on recycling excavated soil for use as backfill at the sites. In addition, recycling excavated soil plays an important role of sustainable construction and environmental protection and this is also a sustainable development strategy of Hanoi city authority.

CHAPTER 3 INFLUENCE OF SLURRY DENSITY ON PROPERTIES OF LSS

In Japan, “Liquefied-Stabilized Soil (LSS), which is one of premixing cement treated-soil, has recently been increasing in Japan for backfilling processes owing to its advantages. The excavated soils discharged from construction projects can be recycled to become backfilling material. Therefore, LSS which is one of the effective methods of using the construction-generated soil can solve the problem in Hanoi city at present. The application of LSS to improve ground has successfully achieved in many construction projects. The technology involves adding cement stabilizer to slurried soil and create stability of soil layer without compaction. In addition, the advantages of LSS have been shown various types of excavated soils which is not necessarily good quality material to have the appropriate fluidity by adjusting the density of soft soil with high moisture content can be effectively used. Different LSS can be created from the slurry based premixed stabilized soil using high-quality soil materials. However, the strength, stiffness and brittleness of LSS increase with the increase of cement stabilizer amount.

Fiber material from crushed waste newspaper was proposed as an effective reinforcement to improve the ductility of LSS for possessing a unique combination of fiber material, cement stabilizer and excavated soil. It was found that the brittleness of LSS mixed with fiber material after the peak in $q\sim\varepsilon_a$ curve was improved as compared to LSS without fiber material with proper dispersion of fiber material reinforcement.

Recently, the LSS decreased slurry density is used in order to be reduced vertical earth pressure. However, the study on strength and deformation properties of the LSS decreased a slurry density has not been investigated.

In this study, the triaxial compressive property of LSS decreased slurry density was investigated. The model ground was built with LSS mixed with fiber material amount of 0, 10 kg/m³ (Pc-0, 10), respectively into four pits in campus. In parallel, the specimens of same batch were also molded and cured in the laboratory. The specimens were prepared by trimming LSS retrieved from the model ground (field LSS) and cured laboratory

(laboratory LSS) at the same curing time of 28 and 56 days. A series of CUB tests were carried out under the conditions at constant strain rate of 0.054%/min and the effective confined pressure of 98 kPa. Testing processes had been performed for two time periods in 2016 and 2017, respectively. Based on test results, influence of slurry density on triaxial compressive properties for LSS reinforced with fiber material was discussed.

3.2 TEST PROCEDURE

3.2.1 Test material

In this study, NSF-CLAY was used as a homogenous base material, which was commercially available cohesive soil with very well defined the physical properties clearly. Table 3.1 shows main physical properties of NSF-CLAY. The Geoset 200 provided by Taiheiyo Cement Co. was used as cement stabilizer. This is special cement stabilizer for soft clay and problematic soil. Newspaper crushed like cotton by a food processor was used as fiber material.

| | |
|---|-------|
| Density of particle ρ_s (g/cm ³) | 2.762 |
| Liquid limit W_L (%) | 60.15 |
| Plastic Limit W_p (%) | 35.69 |
| Plasticity Index I_p | 24.46 |

Table 3.1 Physical Properties of NSF-CLAY

3.2.2 Mixing method

There are two LSS mixing methods to be suitable for excavated soil including the slurry type and adjustment slurry type. For the slurry type, water is added suitably to excavated soil to adjust density of slurry, and then cement stabilizer is added and mixed. For adjustment slurry type, water is added to excavated soil, then fine-grained sand or cohesive soil is added in order to adjust density of slurry and after that cement stabilizer is added and mixed. In this study, the LSS of slurry type was selected due to easier procedure.

CHAPTER 3 INFLUENCE OF SLURRY DENSITY ON PROPERTIES OF LSS

In this study, various mixing tests have been carried out by changing slurry density and amount of cement stabilizer while investigating the bleeding rate, flow value and unconfined compressive strength of LSS at 28 curing days.

The values obtained in this way were to present a standard mix proportion for this study.

Figure 3.1 shows relation among slurry density, flow value and unconfined compression strength q_u when the cement stabilizer of 100 kg/m^3 was added in the previous study. The bleeding rate is less than 1%. Based on this figure, the target slurry density $D_{\rho_f} = 100\%$ was determined to be 1.280 g/cm^3 with unconfined compressive strength of 200-500 kPa and flow value of 160-300 mm. Table 3.2 shows the content of fiber material, the density of slurry ρ_f , the density of LSS before mixing fiber material ρ_{LSS} and the wet density of specimens ρ_t at 28 curing days. The slurry density ρ_t was controlled within $\pm 0.001 \text{ g/cm}^3$ with target slurry density.

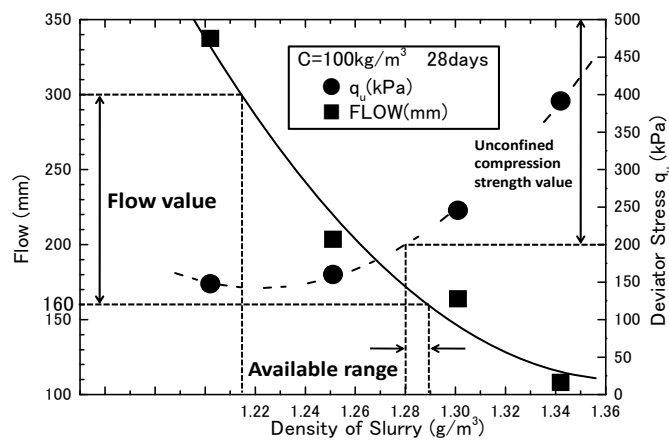


Figure 3.1 Available range of slurry density

| Content of Fiber material | ρ_f (g/cm^3) | ρ_{LSS} (g/cm^3) | ρ_t (g/cm^3) |
|---------------------------|---------------------------------|-------------------------------------|---------------------------------|
| 0 kg/m^3 | 1.281 | 1.350 | 1.362 |
| 10 kg/m^3 | 1.280 | 1.351 | 1.363 |

Table 3.2 Result of density test

3.2.3 Specimen preparation

The purpose of this study is to determine influence of slurry density on strength and deformation properties of liquefied stabilized soil reinforced with fiber material. Therefore, density of slurry decided based on the standard mix proportions.

In previous studies, slurry density of 1.280 g/cm³ was used as original slurry density to create LSS reinforced with fiber material. The ductility of LSS improved by mixing with fiber material was confirmed through test results of a series of CUB tests.

In this study, two densities of slurry were made including 1.280 g/cm³ ($D_{\rho_f} = 100\%$) and 1.216 g/cm³ ($D_{\rho_f} = 95\%$). The content of cement stabilizer used in this study was 80 kg/m³ after densities of slurry reaching 1.280 g/cm³ and 1.216 g/cm³, respectively.

LSS was produced by adding and mixing cement stabilizer into slurry of LSS clay with hand mixer. In the production process, the determination of the density was performed by measuring the mass of slurry filled into a stainless steel mold of 400 cm³ called “AE mortar container”. After achieving the desired density, fiber material with amount of 0, 10 kg/m³ (Pc-0, 10) was added and mixed by hand mixer. In order to determine fluidity of LSS mixed fiber material, the flow test was performed in accordance with JHS A313–Japan Highway Public Corporation Standard. Moreover, the fresh LSS mixed with fiber material is made to be removed the air inside specimen applying vacuum.

In this study, the fresh LSS mixed fiber material was placed into mold of 5 cm in diameter and 10 cm in height. The top surfaces of specimens were covered by a polymer film and were cured under air humidity and temperature of 20 ± 3 °C. In parallel, the fresh LSS was poured into four pits laid nonwoven geotextile filter, which performs the functions of separation and stabilization in marginal conditions of LSS shown in Figure 2. After placing, the surface of LSS was covered with a polymer sheet and cured under outdoor condition. And then, a series of CUB tests had been carried out at 28 and 56 curing days.

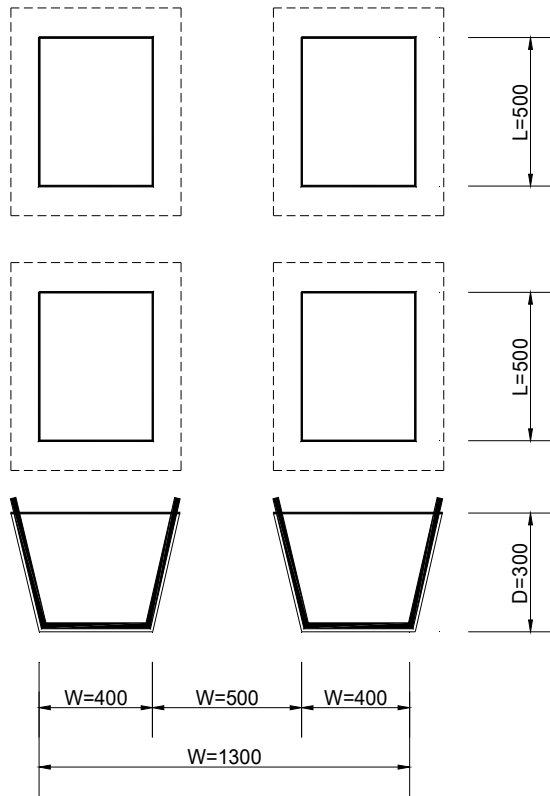


Figure 3.2 Schematic drawing of pits

3.2.4 Test method

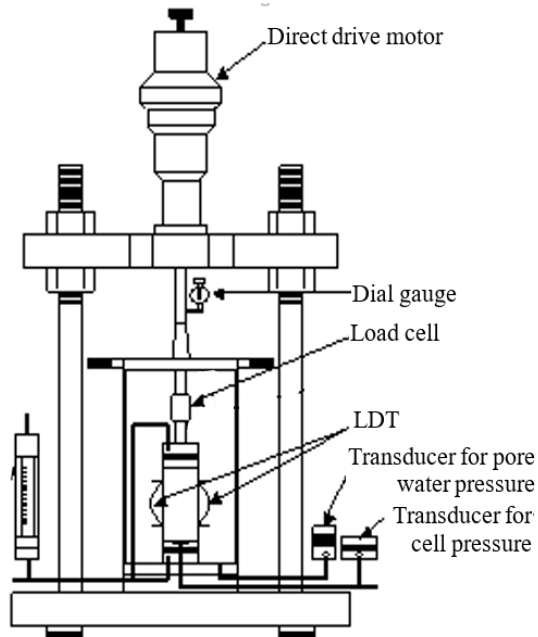


Figure 3.3 Schematic figure of test apparatus

In this study, a couple of Local Deformation Transducer (LDTs), which can measure the axial deformation from small strain level without the bedding error due to the compression of loose layers at the top and bottom ends of specimen or filter paper, were set on the diagonally opposite surface of specimen diameter as shown in Figure 3.3. The top and bottom ends of LDT was set between two pseudo-hinged attachments fixed on the surface of rubber membrane at the points which were glued to the specimen to prevent slipping between the membrane and the surface of specimen. When the value of LDT exceeds a measurable range, the axial displacement was used the value of dial gauge by correcting the bedding error. In this test, a digital servo motor was used for the loading device. This device enables to control the axial displacements with high precision, and can ignore backlash when reversing the loading direction. The whole operation of apparatus during test was automatically controlled by a PC software.

The CUB tests were performed for both $D_{pf} = 95\%$ LSS and $D_{pf} = 100\%$ LSS specimens at curing time of 28 and 56 days. Specimens were saturated by the double suction method which vacuum pressure was applied and the de-aired water was flowed through specimen under a back pressure of 196 kPa.

A series of CUB tests was performed after isotropic consolidation for 12 hours under the effective confined pressure of 98 kPa. In order to unify with previous studies, small unloading/reloading loops during monotonic loading was applied and axial strain rate was 0.054%/min.

3.3 TEST RESULTS AND DISCUSSION

3.3.1 Relationship between deviator stress and axial strain

Figure 3.4(a)~(c) show relationship between the deviator stress $q (= \sigma_1 - \sigma_3)$ and the axial strain ε_a in range of 0~3 % from CUB tests under the confining pressure $\sigma'_c = 98\text{kPa}$ of both $D_{pf} = 100\%$ LSS and 95% LSS mixed with fiber material of 0, 10 kg/m^3 (Pc-0, 10) at 28 curing days obtained from test results in 2016 and 2017, respectively. In

CHAPTER 3 INFLUENCE OF SLURRY DENSITY ON PROPERTIES OF LSS

Figure 3.4(a), although there is not noticeable difference of the maximum deviator stress between Pc-0 and Pc-10 in the case of $D_{\rho_f} = 100\%$ LSS, the deviator stress of Pc-10 is not suddenly decreased after the peak stress state compared with Pc-0. On the other hand, the peak stresses are not clearly in both cases of Pc-0 and Pc-10 of $D_{\rho_f} = 95\%$ LSS. And, the maximum deviator stress, q_{\max} of Pc-10 specimens tend to be larger than that of Pc-0 ones. Therefore, the brittle property observed in case of specimen without fiber material has been improved by the reinforcement effect of added fiber material as similar to the previous results. The figures show that all specimens of laboratory LSS achieve q_{\max} at axial strain $\varepsilon_a = 0.5\%$ and specimens of field LSS achieve q_{\max} at various axial strains. Because the temperature of field LSS during curing time could not be controlled, it may cause effect on increasing strength of specimens. Figure 3.4(b) and (c) show the deviator stress $q (= \sigma_1 - \sigma_3)$ of field LSS specimens to be larger than laboratory LSS specimens. In addition, q_{\max} of LSS specimens reinforced with fiber material substantially tend to be larger than LSS specimens without fiber material and q_{\max} of $D_{\rho_f} = 100\%$ tend to be larger than $D_{\rho_f} = 95\%$ for both laboratory LSS and field LSS. It is considered that liquefied stabilized soil reinforced with fiber material is more advantageous than application of liquefied stabilized soil in order to be constructed aseismic ground. Figure 3.5(a)~(c) show the relationship between the deviator stress $q (= \sigma_1 - \sigma_3)$ and the axial strain ε_a in range of 0~0.5% for the cases of $D_{\rho_f} = 100\%$ and $D_{\rho_f} = 95\%$ mixed with fiber material of 0, 10 kg/m^3 (Pc-0, Pc=10), respectively. From the figure, as comparing $q \sim \varepsilon_a$ relation, although slurry density decreased 5% from $D_{\rho_f} = 100\%$ to $D_{\rho_f} = 95\%$, the reduction of q_{\max} at axial strain $\varepsilon_a = 0.5\%$ was about 30-35%. However, when the $q \sim \varepsilon_a$ relations are compared at same strain, the deviator stress of LSS specimen reinforced with fiber material is larger than that of LSS specimen without it.

Figure 3.6(a) and (b) show relationship between q_{\max} and curing days for field and laboratory LSS mixed with fiber material amount 0, 10 kg/m^3 (Pc-0, Pc-10) at 28 and 56

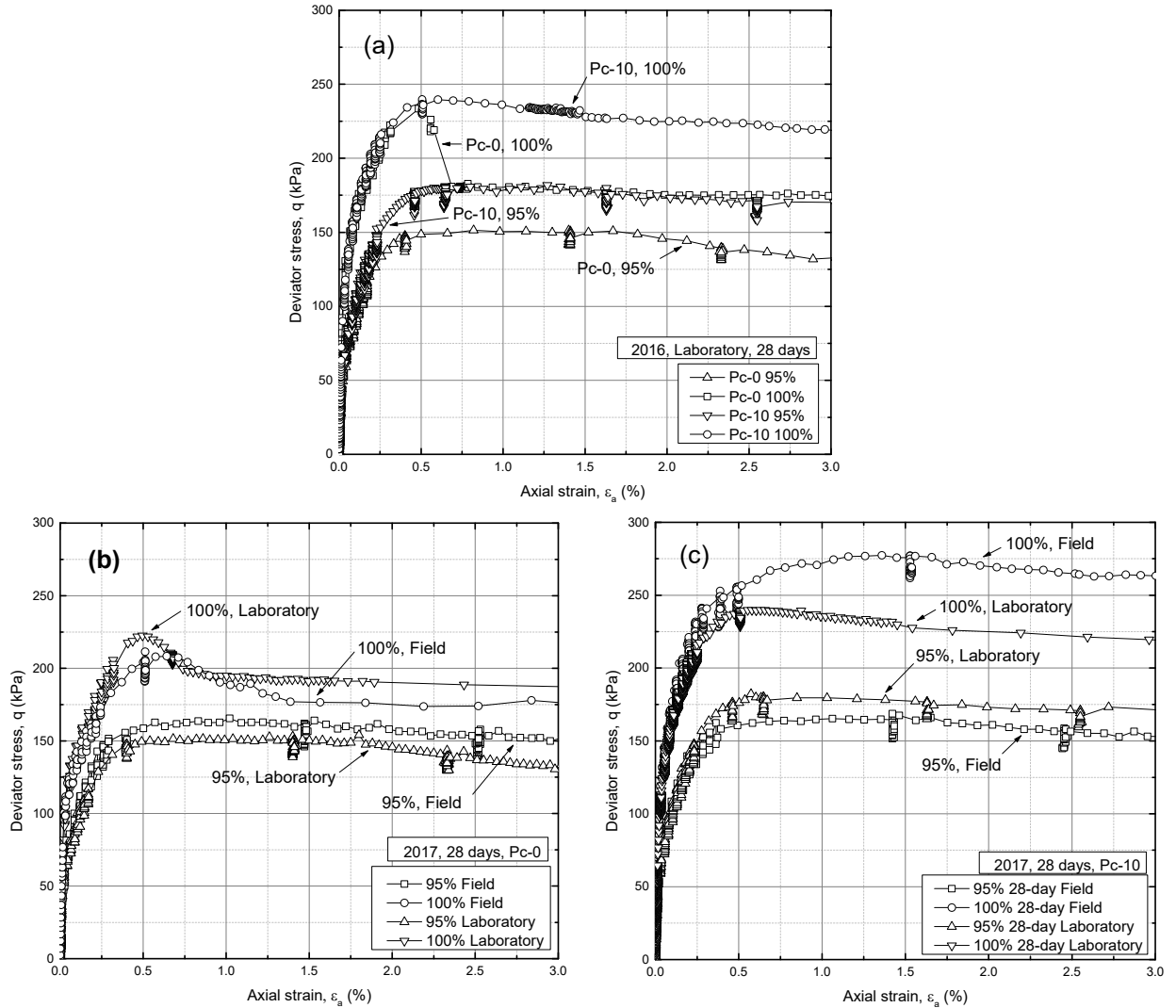


Figure 3.4 $q \sim \epsilon_a$ relations up to 3 %

curing days, respectively. The maximum deviator stress q_{max} has been obtained from relationship between deviator stress $q (= \sigma_1 - \sigma_3)$ and axial strain ϵ_a , which are results of CUB tests under the confining pressure $\sigma'_c = 98$ kPa. Except for the q_{max} of field LSS, Pc-10, $Dp_f = 100\%$, q_{max} of LSS of all other cases tend to increase as increasing of curing days. In general, q_{max} of cement-treated soil tend to increase during curing increases. It is considered that the reduction of q_{max} of field LSS, Pc-10, $Dp_f = 100\%$ was caused by the weather conditions. Because the specimens had been prepared in the beginning of winter in Hokkaido, where the temperatures sometime drop below 0°C . The effects of freezing and thawing processes of water inside the specimens under field curing condition might lead to this issue. For this reason, it is necessary to be considered for further study.

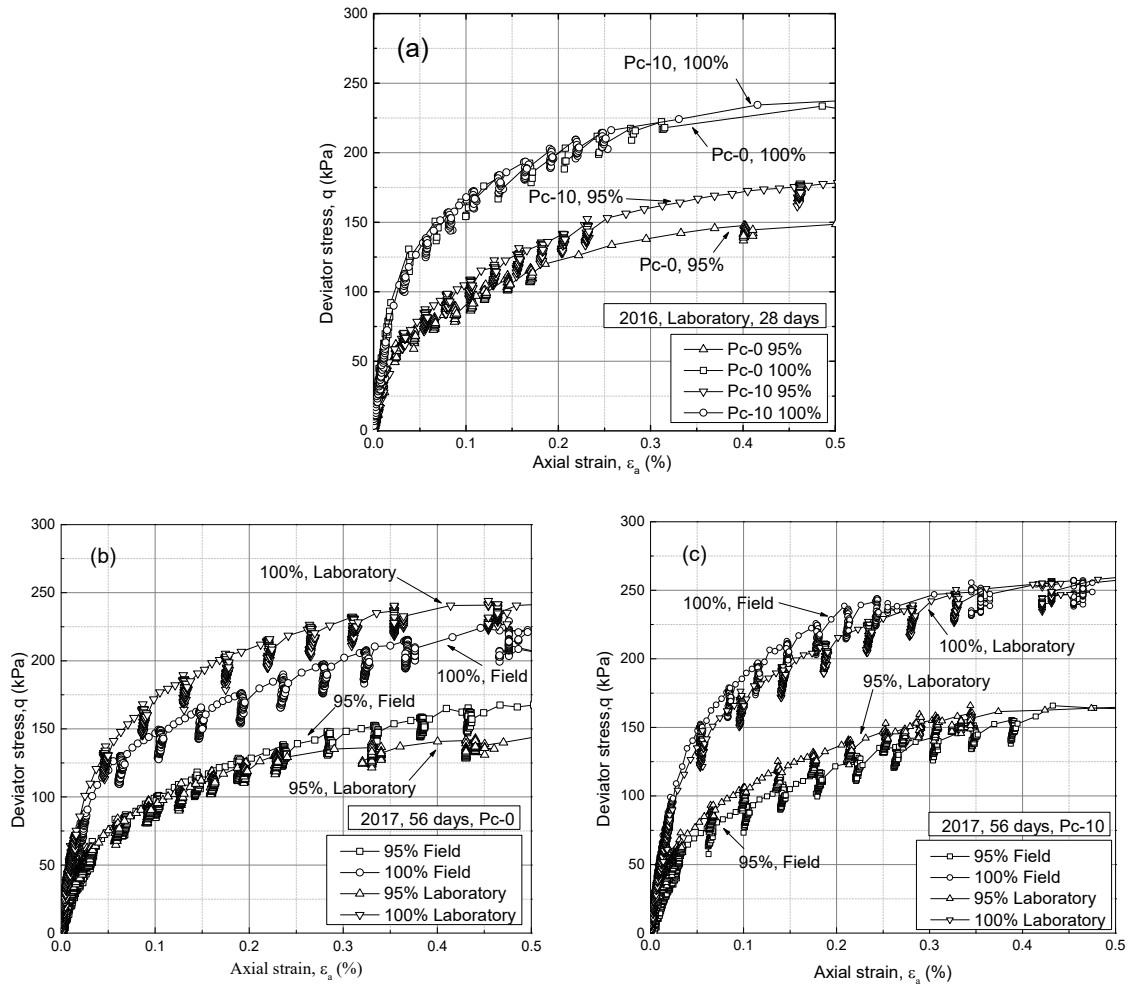


Figure 3.6 $q \sim \epsilon_a$ relation up to 0.5 %

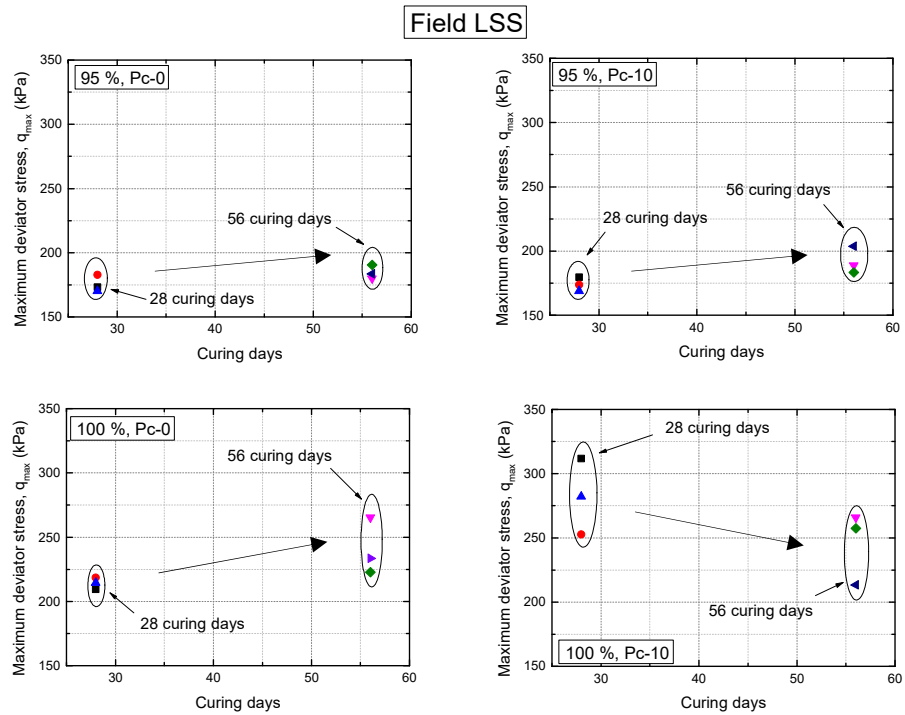


Figure 3.6(a) $q_{max} \sim$ curing days relation for Field LSS

Laboratory LSS

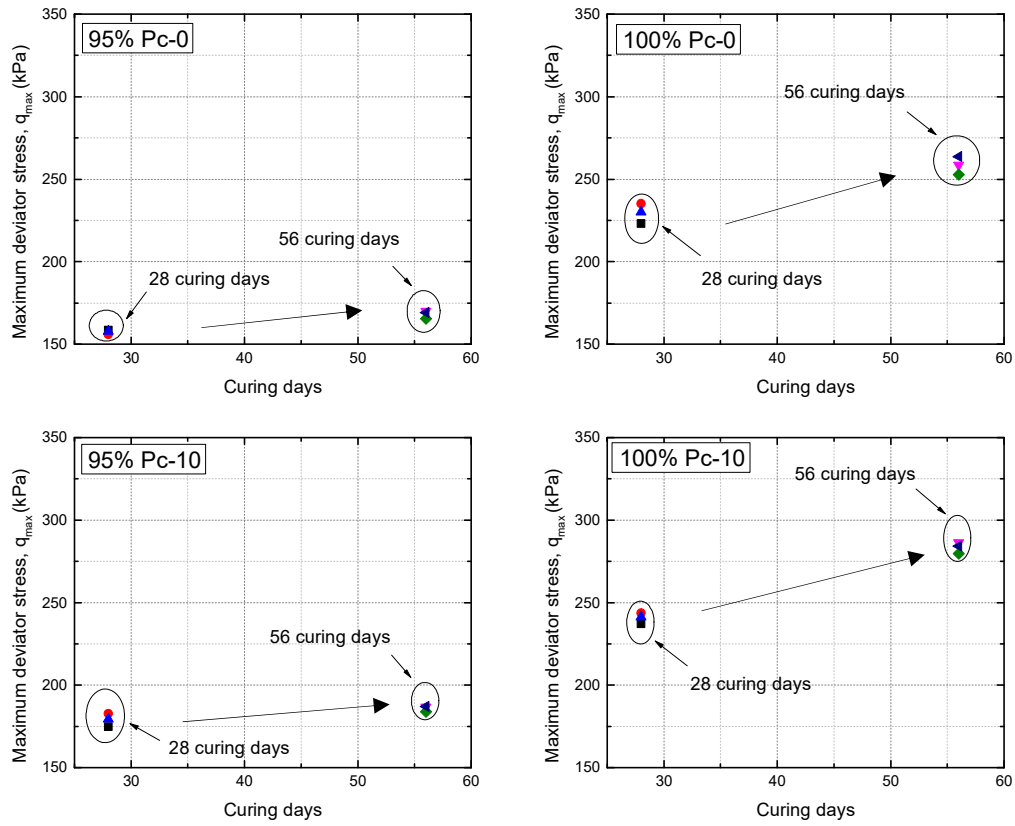


Figure 3.6(b) q_{max} ~curing days relation for Laboratory LSS

3.3.2 Deformation property

a) Definition of Young’s modulus

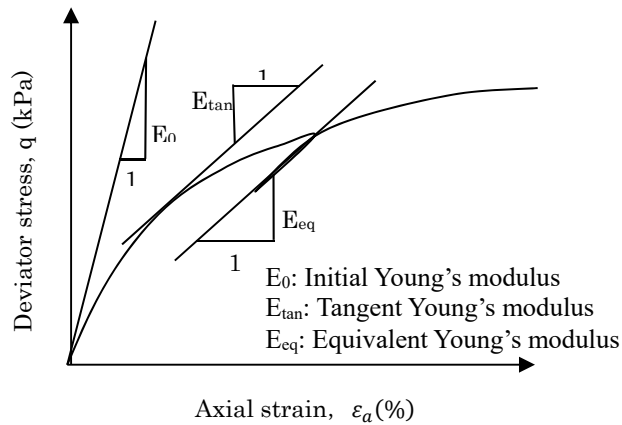


Figure 3.7. Definition of various Young’s moduli

Figure 3.8 shows the definitions of various Young’s moduli. The initial Young’s modulus E_0 is defined as initial stiffness at $\epsilon_a=0.002$ % or less. The tangent Young’s modulus E_{tan} is defined as tangential gradient in $q\sim\epsilon_a$ curve, it indicates the non-linearity

of deformation property in $q \sim \varepsilon_a$ relation. The equivalent Young's modulus E_{eq} is obtained from small unloading/reloading loop during monotonic loading. The E_{eq} indicates a changing degree of damage under the shearing.

b) Tangent Young's modulus E_{tan}

Figure 8(a) and (b) show the influence of curing days on Initial Young's modulus E_0 of $D_{\rho_f} = 100\%$ and $D_{\rho_f} = 95\%$ cured field and laboratory conditions, respectively. It is found from Figure 8(a) and (b) that the values of E_0 increase as the increasing of curing days except for that of E_0 for LSS specimen of Pc-10, $D_{\rho_f} = 100\%$. In case of LSS specimen of Pc-10, $D_{\rho_f} = 100\%$, the value of E_0 decreases at 56 days. It is considered to have become in the beginning of winter. It might cause reduction of E_0 under curing field condition. The effect of curing temperature on E_0 is also consistent with previous study. In present study, the temperature inside the ground during curing in the field has not been measured. Therefore, investigation of effect of temperature on E_0 of LSS need to be considered for further study. Figure 8(b) show that E_0 of Pc-0 LSS are larger than E_0 of Pc-10 LSS and E_0 of $D_{\rho_f} = 100\%$ larger than $D_{\rho_f} = 95\%$.

Figure 9(a)~(e) show relationship between E_{tan}/E_0 and q/q_{max} of Pc-0, Pc-10 for $D_{\rho_f} = 100\%$, $D_{\rho_f} = 95\%$, respectively. The results have been obtained from the analysis of $q \sim \varepsilon_a$ curve of CUB tests under the confining pressure of 98 kPa. The figures show that reduction rate of $D_{\rho_f} = 95\%$ is larger than that of $D_{\rho_f} = 100\%$. Therefore, it seems that the nonlinearity increases as decreasing of slurry density. On the other hand, cement-treated soil has been reported that nonlinearity of stress-strain curve decreases as curing increases. In the results of this study, the nonlinearities of 28 and 56 days tend to be similar. It is considered that the curing days of 56 days were short in order to investigate the effect of curing days on nonlinearity.

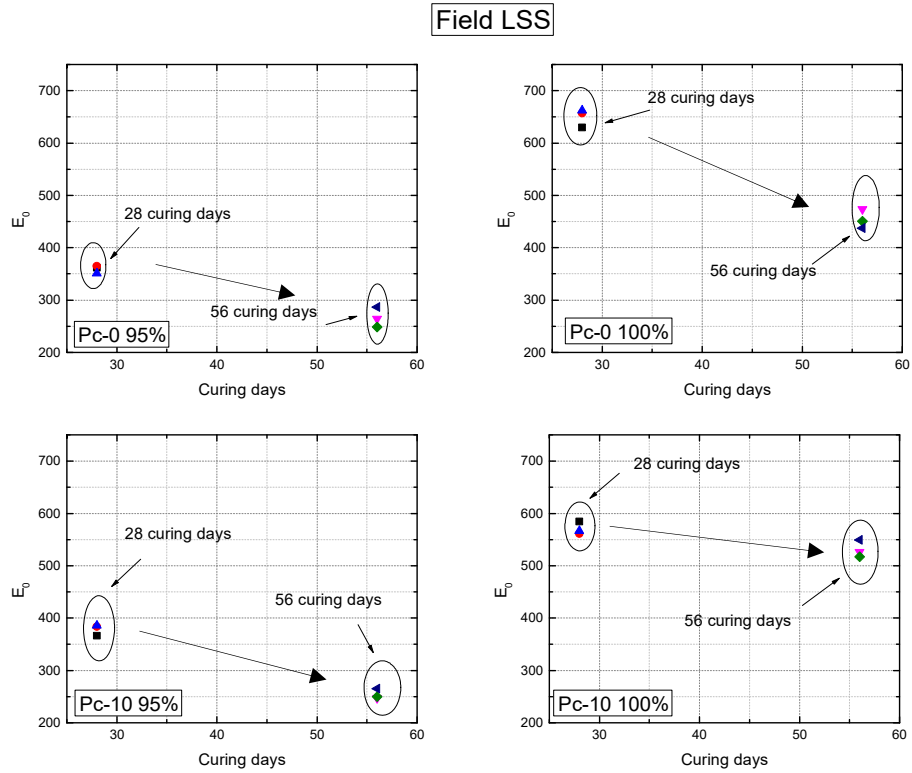


Figure 3.8(a) E_0 -curing days relations for Field LSS

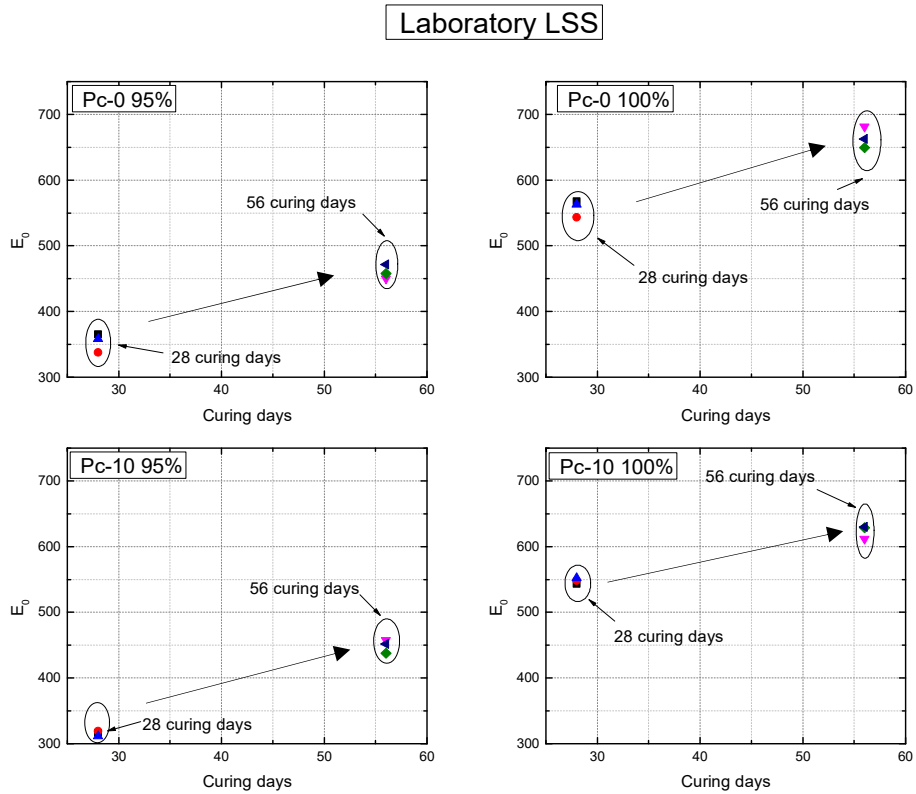


Figure 3.8(a) E_0 -curing days relations for Field LSS

c) Equivalent Young's modulus, E_{eq}

Figure 10(a)~(e) and relationship between E_{eq}/E_0 and q/q_{max} of both Pc-0, Pc-10 for $D_{pF}=100\%$, $D_{pF}=95\%$, respectively. The values of E_{eq} were obtained from the $q\sim\varepsilon_a$ curve of the CUB tests under the confining pressure of 98 kPa at small loading/unloading loop during monotonic loading.

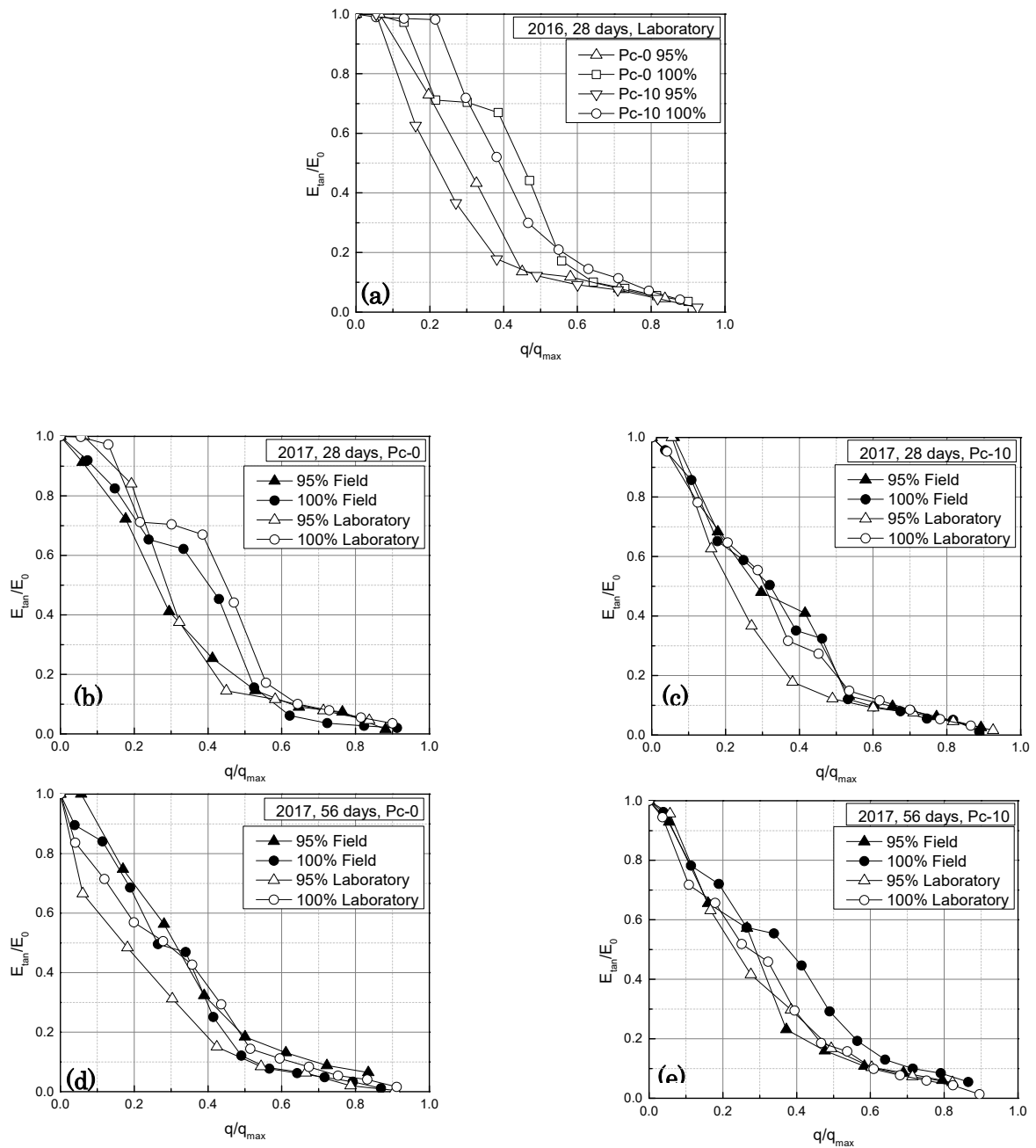


Figure 3.9 $E_{tan}/E_0\sim q/q_{max}$ relations

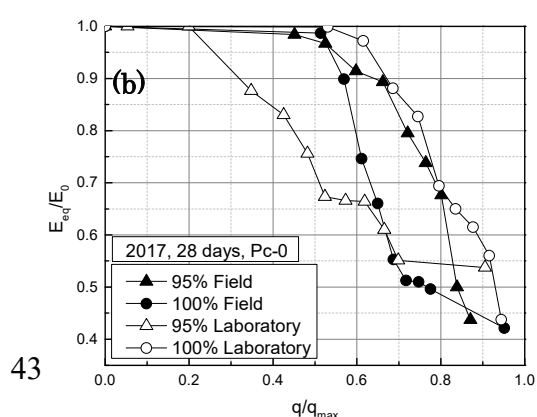
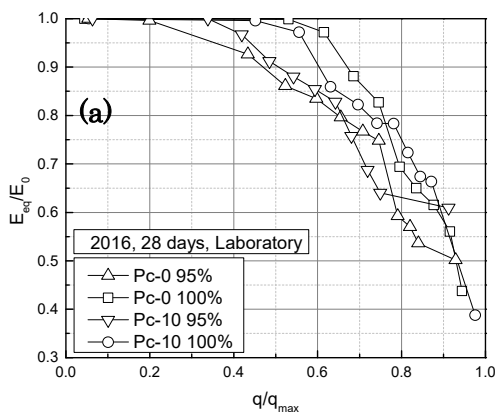
In general, it has been reported that initial Young's modulus E_0 of cement-treated soil at small strain is independent of the confining pressure, thus, the E_{eq}/E_0 is considered to indicate the change degree of damage during shear. At the initial portion of shear, the soil specimen shows local failure, and finally, the soil specimen is collapsed as the shear band is formed. This behavior can be explained considering that cementation is broken therefore soil fabric changes and in consequence elastic properties change.

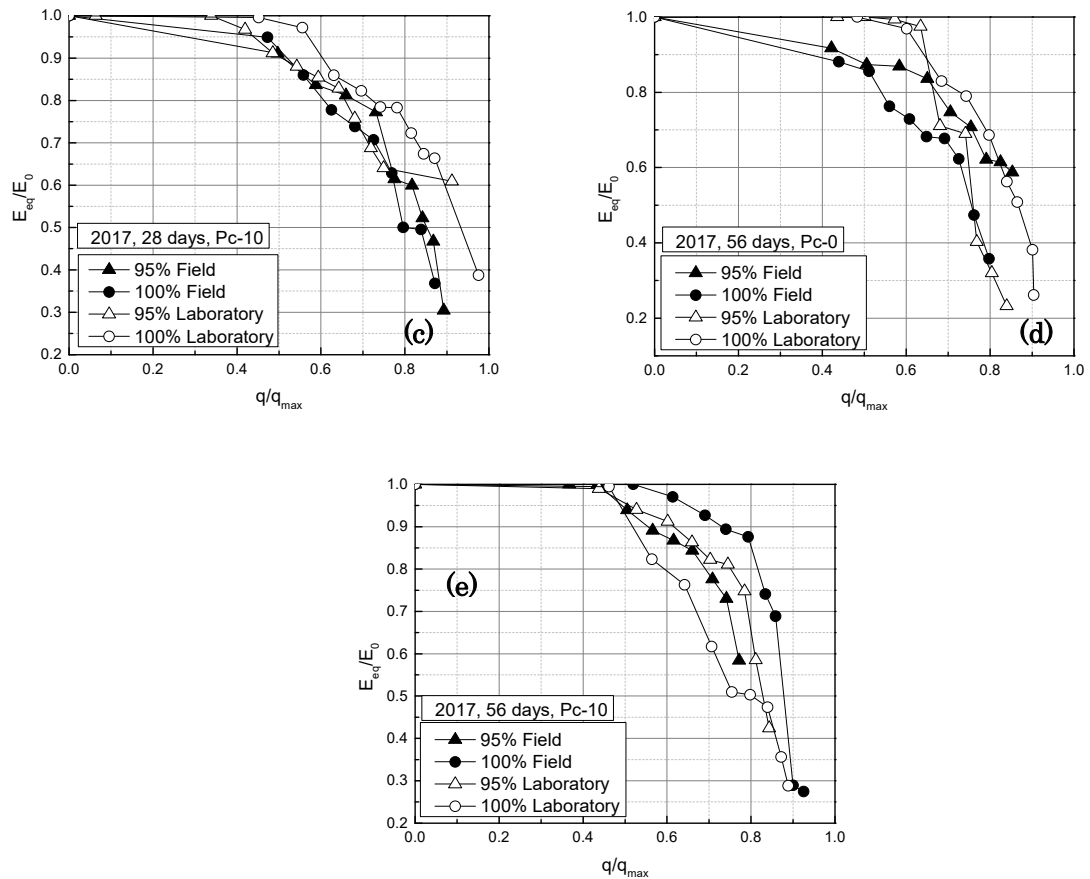
There is no significant difference in reduction rate of E_{eq}/E_0 of Pc-0 and Pc-10 in $D_{\rho f} = 100\%$ and $D_{\rho f} = 95\%$ except Pc-0 at 28 curing days for both field and laboratory. However, it is seen from these figures that the reduction rate of E_{eq}/E_0 of Pc-10, $D_{\rho f} = 100\%$ tends to be slightly smaller than that of Pc-0, $D_{\rho f} = 95\%$. Thus, Pc-10, $D_{\rho f} = 100\%$ will cause the reduction of the local damage during shear.

It is seen from Figure 10 (a) that the reduction rate of E_{eq}/E_0 of $D_{\rho f} = 95\%$ tends to be larger than that of $D_{\rho f} = 100\%$ as comparing reduction rate E_{eq}/E_0 between $D_{\rho f} = 100\%$ and $D_{\rho f} = 95\%$ at 28 curing days cured laboratory. Therefore, the reduction of slurry density is suggested to be increased the local damage during shear.

As shown in Figure 10(a)~(d), the significant tendency is not seen. That is, a scattering of $E_{eq}/E_0 \sim q/q_{max}$ relations are large. It is considered that damage are caused due to a cured condition in field, an influence of disturbance during sampling and during setting a specimen on an apparatus and so on.

Then, in the judging from the overall point of view, it is considered that the specimen prepared on the reduction of slurry density is easily damaged.



Figure 3.10 $E_{eq}/E_0 \sim q/q_{max}$ relations

3.4 CONCLUSIONS

The following conclusions were derived based on test results.

1. When the slurry density is slightly decreased from the appropriate slurry density obtained from the standard mix proportion design figure, it is considered that the q_{max} decreased remarkably. In addition, it is found that the local damage caused by shearing even in the case of low slurry density is reduced by the effect of reinforcement on the fiber material.
2. The $E_{tan}/E_0 \sim q/q_{max}$ relation of both LSS cured in laboratory and at field shows relatively similar tendency. In addition, it seems that the nonlinearity of $q \sim \epsilon_a$ relation increase as decreasing slurry density.
3. The influence of slurry density on the degree of damage caused by shear is large and it seems that the degree of damage tends to be reduced by the addition of fiber material.

REFERENCES

- 1) Kuno, G., eds (1997): Liquefied stabilized soil method-Recycling technology of construction-generated soil and mud, *Gihodo publication* (in Japanese).
- 2) Japanese Geotechnical Society (2005): Committee Report Chapter 2, 2.1, 2.2 on test methods and physical properties of cement-modified soil, Proc. of symposium, pp.2-22, on survey, design, construction and properties evaluation methods of solidifying stabilized soil using cement and cement-treated soil (in Japanese).
- 3) Kohata, Y. (2006): Mechanical property of liquefied stabilized soil and future issues, *Doboku Gakkai Ronbunshuu, F, Vol.62, No.4, pp.618-627* (in Japanese).
- 4) Kohata, Y., Ichikawa, M., Nguyen, C. Giang., and Kato, Y. (2007): Study of damage characteristics of liquefied stabilized soil mixed with fibered material due to triaxial shearing, *Geosynthetics Engineering Journal, Vol.22, pp.55-62* (in Japanese).
- 5) Ito, K., Kohata, Y., and Koyama, Y. (2011): Influence of additive amount of cement solidification agent on mechanical characteristics of Liquefied Stabilized Soil mixed with fibered material, *Japanese Geotechnical Society Hokkaido Branch Technical Report Papers, Vol.51, pp.131-136* (in Japanese).
- 6) Duong, Q. Hung., Kohata, Y., Omura, S., and Ozaki, K. (2014): Strength and deformation characteristics of liquefied stabilized soil reinforced by fiber material prepared at laboratory and field, *Geosynthetics Engineering Journal, Vol.29, pp.33-40*.
- 7) Goto, S., Tatsuoka, F., Shibuya, S., Kim, Y-S., and Sato, T. (1991): A simple gauge for local small strain measurements in the laboratory, *Soils and Foundations, Vol.31, No.1, pp.169-180*.
- 8) Kohata, Y., Tatsuoka, F., Wang, L., Jiang, L. G., Hoque, E., and Kodaka, T. (1997): Modelling the non-linear deformation properties of stiff geomaterials, *Géotechnique, Vol.47, No.3, pp.563-580*.
- 9) Kohata, Y., Jiang, L. G., Murata, O., and Tatsuoka, F. (1999): Elastic-properties-based modelling of non-linear deformation characteristics of gravels, *Proc. of the second Inter. Symposium on Pre-Failure Deformation Characteristics of Geomaterials-IS Torino 99, pp.533-539*.

Chapter 4

METHODS FOR DETERMINING DYNAMIC PARAMETERS OF SOIL

4.1 INTRODUCTION

The response of soil to cyclic loading is controlled mostly by mechanical properties of soil. There are several types of geotechnical engineering problems associated with dynamic loading such as wave propagation, machine vibrations, seismic loading, liquefaction and cyclic transient loading, etc. The mechanical properties associated with dynamic loading are shear wave velocity (V_s), shear modulus (G), damping ratio (D), and Poisson's ratio (ν). The customary name for this type of properties is “dynamic soil properties”, even though they are also used in many non-dynamic type problems. The engineering problems governed by wave propagation effects induce low levels of strain in the soil mass. On the other hand, when soils are subjected to dynamic loading that may cause a stability problem then, large strains are induced.

The selection of the appropriate testing method used for engineering problems needs careful consideration and understanding of the associated level of strain. There are a variety of laboratory and field methods that measure the low- and high-strain soil behavior. This paper addresses the methods that are based on geophysics that for the most part encompass the low-strain properties or wave propagation type problems.

4.2 UTILITY OF MEASURED PARAMETER

1) Shear wave velocity (V_s)

Shear wave velocity (V_s) is the most commonly used measured parameter used in shallow soil geophysics for soil characterization. It is used to calculate the following parameters in the elastic range of soil behavior. The importance in its utility is that the particle of motion travels perpendicular to the direction of wave propagation being able to measure the shear properties of the soil skeleton and not the fluids that cannot take shear.

2) Shear modulus (G)

Shear Modulus (G) is a calculated parameter based on the V_s using the simple elastic relationship $G_{\max} = \rho \times V_s^2$. The mass density is often estimated or measured by a nearby subsurface sampling or using correlations. Advanced correlations to estimate the value of the dynamic shear modulus are available based on the standard penetration test, Atterberg Limits (plasticity index) and grain size distributions (Vucetic and Dobry, 1991, Idriss, et al., 1980). The shear modulus is used to perform more advanced soil modeling, and dynamic response of the soil-structure interactions. Shear modulus at lowstrain levels as measured by geophysical techniques will provide the elastic parameter for machine foundation analysis or earthquake engineering. The important utility of this parameter is that it can be used as a varying parameter with respect to strain making the soil response represent the real modulus degradation in soil behavior. This parameter is used in defining the stiffness matrices for finite element analysis of earth structures and foundation soils.

3) Maximum Shear Modulus (G_{\max})

Maximum Shear Modulus (G_{\max}) is used to normalize the shear modulus (G) vs. shear strain relationships. These normalized relationships allow the engineer to use well-established degradation curves and scale them to the measured in-situ value of G_{\max} . For example, the classic relationships of the shear moduli for cohesionless and cohesive soils are provided in Seed, et al., (1984) and Sun, et al., (1988). In the absence of extensive dynamic soil testing at all ranges of shear strain these curves are used and G_{\max} is used as the scaling parameter.

4) Damping Ratio (h)

Damping Ratio (h) is used in several dynamic analysis procedures to provide a realistic motion attenuation. This ratio is based on the material damping properties. The damping ratio vs. shear strain relationships for cohesionless and cohesive soils are provided in Seed, et al., (1984) and Sun, et al., (1988). Since damping ratio is also shear strain dependent, it is required to have several values with strain. Dynamic analysis results are also influenced by the damping ratio for single and multi-degree modal systems. The effects of soil-structure interaction also influence the damping of the system making it an area where recent research has focused. The utility of this parameter is based on the ability of the system to absorb dynamic energy and how this will affect the duration and modes of vibration.

5) Poisson's Ratio (ν)

Poisson's Ratio (ν) is a fundamental parameter that is difficult to measure and it is usually estimated in engineering calculations. The ratio of horizontal to vertical strain is required to relate moduli and strains in a solid body. A suggested range of values for Poisson's ratio for soils is from 0.2 to 0.5, less common values may be as low as 0.1 for loess deposits. This ratio can be calculated [$\nu = E/(2G-1)$] based on laboratory tests at low strains if G and E are obtained from torsional and longitudinal vibration, respectively.

4.3 GEOTECHNICAL APPROACHES TO DETERMINE DYNAMIC SOILS PROPERTIES

Geophysical methods have been used for many years by engineers in soils and foundation applications. Geophysics not only provides means to probe the properties of soils, sediments and rock outcrops, but are also used to determine dynamic properties of soils, particularly the soil's compression and shear wave velocities, as well as the soil's elastic and shear moduli. These properties are key parameters in predicting the response of soils and soil-structure systems to dynamic loading. The geophysical methods used in determining dynamic properties of soils are mainly field or in-situ tests based on measurement of velocities of waves propagating through the soil. The most common tests used for such purposes are presented subsequently.

1) Seismic Refraction

The seismic refraction method is well suited for general site investigations for soil dynamics and earthquake engineering purposes. This technique provides for the determination of elastic wave velocities of a layered soil profile. Wave velocities and thickness of each layer are determined as long as the wave velocities increase with each successively deeper layer. The test aims to accurately measure the arrival-times of the seismic body waves, which consists of Compression P- and shear S- waves, produced by a near-surface seismic source. The source travels through the soil to a linear array of detectors placed at the ground surface. Compression P-waves arrive at a receiver faster than shear S-waves, thus obscuring the arrival of the latter waves i.e. the S-waves.

The parameters relate to compression wave velocity (v_p) and shear wave velocity (v_s) of soil, G , E , ν , by the following equations (Das, 1995; Kramer, 1996; Verruijt, 1994):

Shear modulus:

$$G = \rho \cdot v_s \tag{4.1}$$

Elastic modulus:

$$E = \frac{\rho \cdot v_p^2 (3v_p^2 - 4v_s^2)}{v_p^2 - v_s^2} \tag{4.2}$$

Poison's ratio:

$$\nu = \frac{v_p^2 - 2v_s^2}{2(v_p^2 - v_s^2)} \tag{4.3}$$

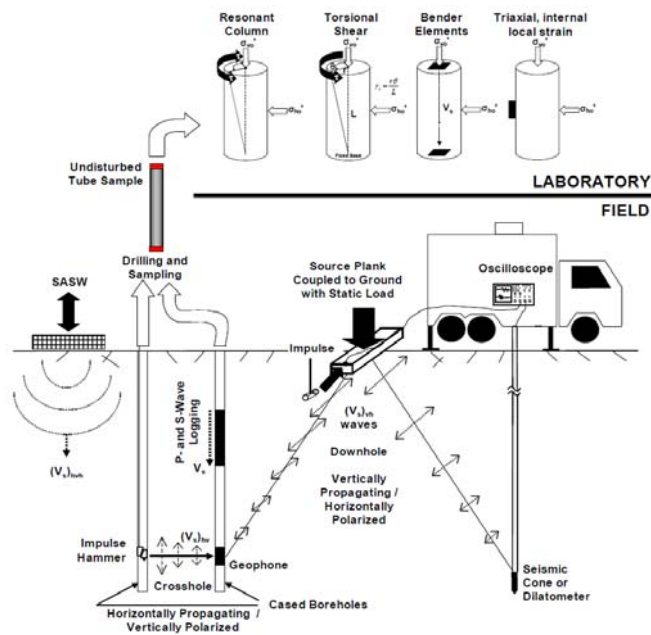


Figure 4.1 Field and laboratory methods for determining dynamic parameters

The parameters can be determined by field and laboratory method presented in available literatures (Das, 1995; Kramer, 1996; Karl, 2005; Schneider et al., 1999). A representation of these test procedures is shown in Figure 4.1.

Advantages and disadvantages

The seismic refraction test is a popular test because of its simplicity and because of the low costs involved. It is a non-invasive test, meaning that no boreholes or cone penetrations are necessary. This is a significant benefit of the test since boreholes are expensive and cone penetration tests may have difficulties penetrating hard layers. However, there are some disadvantages to the seismic refraction test. Firstly, the test assumes that the P-wave velocity increases monotonically with depth. Layers that are softer than the layer above cannot be detected with the seismic refraction test. When the underlying layer is softer, wave paths will become more vertical and therefore no

critically refracted wave can exist. Not only will the soft layer be impossible to detect, it will also make the underlying layers seem deeper than is effectively the case. Secondly, the assumed horizontality of the layers can lead to wrong estimations of the P-wave velocities when the layers are actually inclined, as the assumed wave path is not valid for inclined layers. This problem is overcome by measuring the arrival times in two directions from the source. Finally, one should be aware that “blind spots” can be caused by layers that are too thin or layers that have a too low impedance contrast with the overlying layer. An important advantage of the seismic refraction test is that it can be combined with The Spectral Analysis of Surface Waves test. Both tests use the same test set-up and measurement data. They differ only in the postprocessing of these data. Combining the postprocessing of the two tests has some important synergies.

2) Cross-Hole Technique

The cross-hole method uses two or more boreholes, with an excitation source in one borehole and receivers in the others. Using more than two boreholes makes the method more reliable and makes the method useable for material damping estimations.

Test procedure

The method starts with the drilling of the required number of boreholes. In soft soils, the boreholes typically need a lining, preferably made of plastic tubing. There are two ways of performing the cross-hole method. The first method starts with the drilling of the complete boreholes. After the drilling of the boreholes, the source and receivers are installed at a certain depth and stepwise lowered into the hole. In the second method, the drilling is also done stepwise. After each drilling step, the source and receiver are installed at the bottom of the borehole and the experiment is executed. As for the up-hole method, one can use a falling weight or a rotary source as excitation. For the cross-hole test, the rotary source can be used to create horizontally polarized shear waves and the falling weight can be used to create vertically polarized shear waves. The combination of both can identify an anisotropic soil model, with a different vertical and horizontal shear wave velocity. An explosive source can be used to generate dilatational waves. High frequency signals are preferred, so that near field effects are avoided.

The other boreholes are used for the installation of vibration receivers, for which geophones or accelerometers may be used. The receivers are lowered to the same depth as the excitation source, which means that horizontally traveling waves are measured. To

CHAPTER 4 METHODS FOR DETERMINING DYNAMIC PARAMETERS OF SOIL

ensure a good coupling between soil and receiver, a backfill material may be needed. This is not needed if the drilling is also done stepwise. When all receivers and the excitation source are installed at the same depth, the experiment can start. The excitation source is activated, triggering the data acquisition and the ground motions are recorded in each of the receiving boreholes. This process is repeated until a sufficiently high SNR is obtained by stacking the time signals. The averaged time signals are used for the determination of the arrival time and the motion intensity. The latter is needed for the estimation of the material damping ratio. The source and receiver are then lowered further in the borehole. Typical step lengths are between 0.5 and 1m. When measurements are done to depths over 20m, it might be necessary to measure the inclination of the holes. This inclination has an effect on the distance between boreholes, which becomes significant for large depths. If the inclination is measured, the cross-hole method can be used up to depths of 50 to 80m.

Advantages and disadvantages

Because multiple boreholes are needed, the method is very expensive. However, results for the wave velocities are of good to very good quality. One has to be aware of the risk that refracted waves, traveling through nearby stiffer layers, may arrive before the direct horizontal wave. This risk increases when layers are thin and when the receiving boreholes are further from the transmitting borehole. This makes the spacing between the boreholes a crucial test parameter. The numerical accuracy increases when the boreholes are well separated, but a large distance between the boreholes increases the likelihood that refracted waves arrive before the the direct waves. A disadvantage of the method is the assumption of horizontal layers. When this assumption does not hold, the results will be incorrect. Another disadvantage is the difficulty of estimating the damping properties. To obtain a reasonable accuracy, the receivers need to be clamped to the borehole wall very well.

3) Down-Hole Techniques

Seismic down-hole tests measure the shear and dilatational wave velocities by placing vibration receivers in a borehole and measuring the arrival times of both types of waves.

Test procedure

Figure 4.3 shows a schematic of the test setup. The test starts with the drilling of a borehole and the installation of a vibration source next to it. A vibration receiver is then clamped to the borehole wall at a certain depth z_1 . This receiver may be a geophone or an accelerometer. Next, the excitation source is used to generate dilatational and shear waves, of which the arrival is detected by the receiver in the borehole. Pressure sensors are installed at the source, to serve as a trigger for the start of the measurements. To reduce the uncertainty due to noise, the test is repeated a number of times. The results of all tests are stacked to obtain a higher signal to noise ratios. The receiver is then lowered into the borehole, with steps Δz that are typically between 0.5 and 1 m. The test is repeated for every receiver depth z_i . If enough sensors are available, then an alternative to this stepwise procedure is to install a series of sensors simultaneously in the borehole. This procedure allows for a faster execution of the down-hole test.

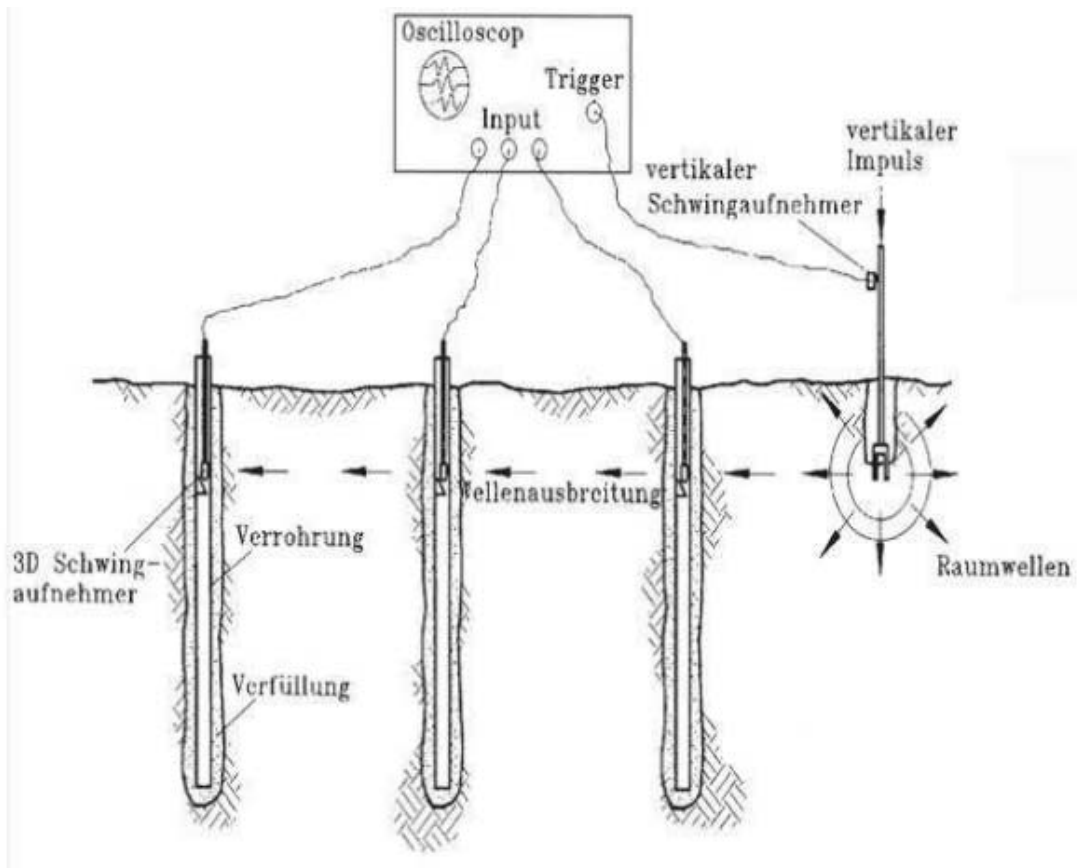


Figure 4.2 Cross-hole method

Advantages and disadvantages

The advantage of the down-hole method is that it provides fairly accurate results, with a high spatial resolution. The disadvantage over the Seismic Cone Penetration Test method is the elevated cost of the method.

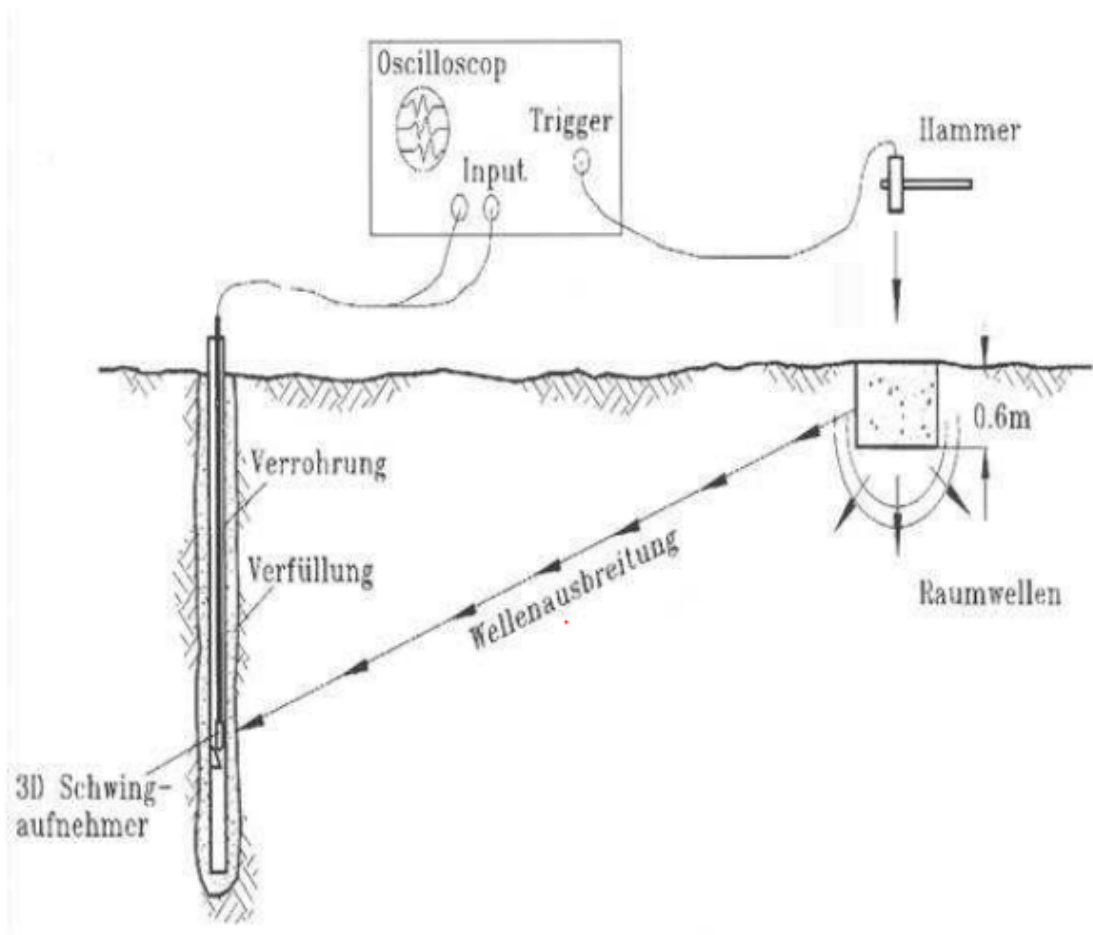


Figure 4.3 Down-hole method

4) Up-Hole Techniques

Seismic up-hole tests measure the shear and dilatational wave velocities by placing an excitation source in a borehole and measuring the arrival times of both types of waves at the surface.

Test procedure

The up-hole test is very similar to the down-hole test. Figure 4.4 shows the test setup. The excitation source is now located in the borehole and the vibrations are recorded at the surface. The test thus starts with the drilling of a borehole and the installation of a vibration receiver, a geophone or an accelerometer, next to it. An excitation source is then lowered into the borehole. The possibilities for the excitation source are limited due to

the fact that it has to be useable in a confined space. To generate P-waves, a vertical source needs to be used, this can for example be a falling weight. To generate S-waves, a rotary source may be used. As for the down-hole method, the test is repeated a number of times for every excitation depth. The different data records are then stacked to obtain a higher signal to noise ratios.

Advantages and disadvantages

The advantage of the up-hole method is that it provides fairly accurate results, with a high spatial resolution. The disadvantage over the SCPT method is the elevated cost of the method.

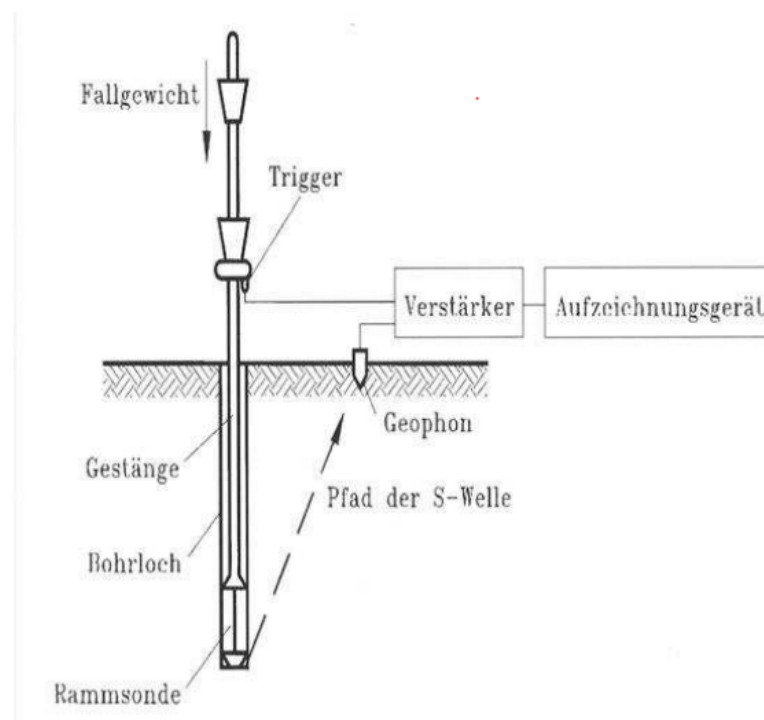


Figure 4.4 Up-hole method

5) Steady-State Surface Wave Technique:

The steady state surface wave technique does not require boreholes and is another in-situ method used to measure the shear modulus (G) of all types of soils. In this test, an electromagnetic oscillator at high frequency (30 to 1000 cycles/second, cps) or a rotating mass type oscillator to produce low frequency vibrations (less than 30 cps) are used. These surface vibrators generate Rayleigh R-waves, which at low strains have nearly the same velocity as the shear waves. The ground surface can be deformed as shown in Figure 4.5. The shear wave velocity is computed from the Rayleigh wave-length measured with receivers placed along the ground surface.

6) Spectral Analysis of Surface Waves (SASW):

The Spectral Analysis of Surface Waves (SASW) test is a non-invasive test method to determine the dynamic shear modulus and the material damping ratio of shallow soil layers. The SASW method has been used to investigate pavement systems, to assess the quality of ground improvement, to determine the thickness of waste deposits, and to identify the dynamic soil properties for the prediction of ground vibrations.

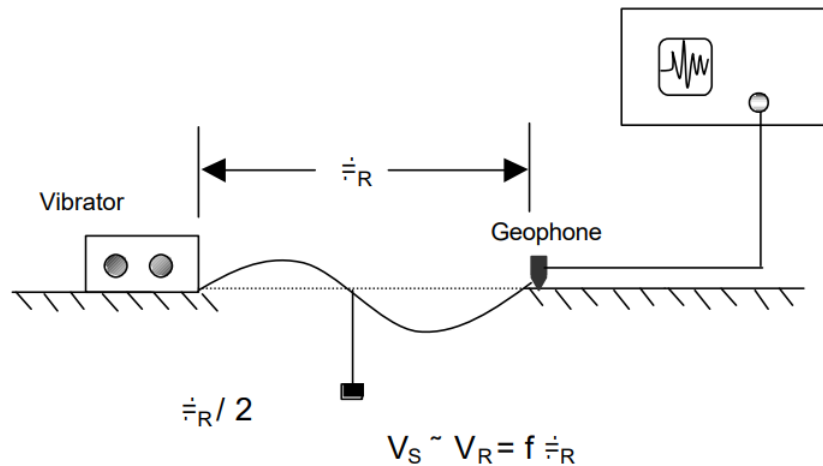


Figure 4.5 Steady-State Surface Wave Test

Physical principle

The method relies on the measurement of surface waves. Surface waves propagate in the horizontal direction and decay exponentially with depth. For low frequencies, the wavelength of the surface waves is large and the surface waves reach deep soil layers. These layers are generally stiff and weakly damped, resulting in a high phase velocity and a low attenuation coefficient. For high frequencies, the wavelength of the surface waves is smaller and the surface waves travel through shallow soil layers. These layers are generally softer and more strongly damped, resulting in a lower phase velocity and a higher attenuation coefficient. As a consequence, the phase velocity and attenuation coefficient of surface waves vary with the frequency and are determined by the variation of the soil properties with depth.

Advantages and disadvantages

As the SASW method is based on a non-invasive test, it is an inexpensive method since it does not require the use of cone penetration or boreholes. The test can also be executed relatively quickly. It is also an advantage that the test can lead to estimations of both the shear wave velocity and the material damping ratio. On the other hand, the resolution of the test is limited in terms of depth and spatial scale: it is difficult to identify

the properties of deep layers (more than 10-15 m) and to detect thin layers. This may not be an issue, as deep and thin layers may also have little impact in ground vibration predictions, depending on the frequency range of interest. Furthermore, the depth problem can be overcome by the use of a passive SASW. The experimental setup of the SASW method is the same as for the seismic refraction test, which means that the data collected from an SASW test allow for the simultaneous determination of the dilatational wave velocity. Combining both inversion analyses into one, gives important synergies. In every iteration step, one soil profile is generated, which is used to compute the theoretical dispersion curve and surface response. The first is compared with the experimental curve from the SASW method and the latter is compared to experimental surface response data. A combined residual is now minimized. In this technique, the layer interfaces for the P- and S-wave velocity will match. Furthermore, one can use information from the S-wave velocity profile to make assumptions about possible inverted P-wave velocity profiles. This would increase the reliability of the P-wave velocity estimations.

7) Seismic Cone Penetration Test (SCPT)

The SCPT has been more recently developed (Campanella and Robertson 1984). The test combines the seismic downhole technique with the standard Cone Penetration test. A seismic pick-up or receiver is added to the cone, then the similar procedure as the one followed with the seismic downhole test is used. At the surface, a shear force is induced while the penetration is paused momentarily. In order to compare the intensity of signals arriving at the receiver at various depths, a source that is capable of generating repeatable signals is used. This is insured by the use of a single hammer weight and height of fall (Campanella and Davies, 1994). Typical test set up of the SCPT is presented as Figure 6. The shear wave velocity, V_S , is calculated by dividing the difference in travel path between two depths by the time difference between the two signals recorded. Advantages of the SCPT in comparison with other conventional seismic in-situ tests, reside in its speed, the fact that it also provides static soil properties such as point bearing (q_c) and sleeve frictional resistance (f_s) as well as ground profiling and stratigraphy of the site. The strain induced immediately around the probe during penetration is a very large strain and thus, both large and small strain parameters can be obtained. In addition the SCPT can be considerably less expensive than other conventional seismic techniques.

Advantages and disadvantages

This technique has the advantage that a high resolution can be obtained. Another advantage is that it does not require a borehole, nor the difficulties associated with placing sensors in a borehole. However, being an invasive method, the cone might be unable to penetrate hard layers, placing a potentially unacceptable limit on the measurement depth.

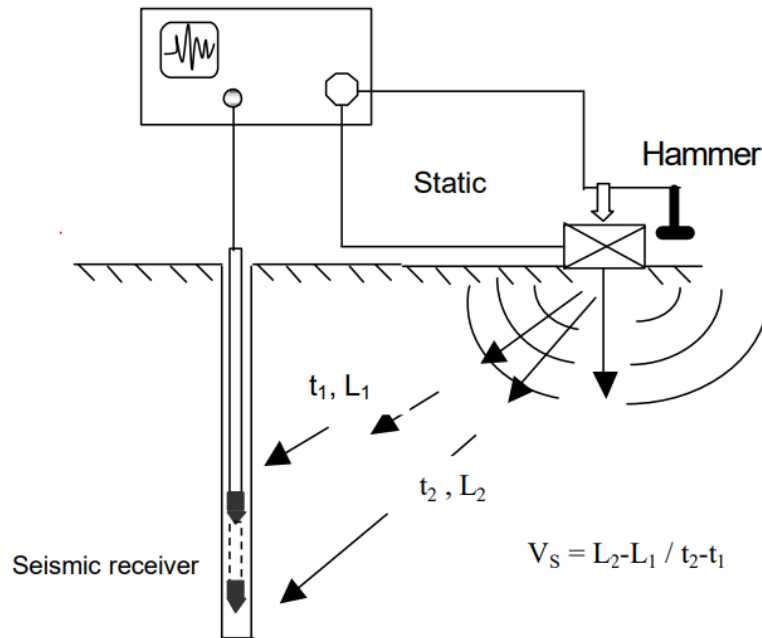


Figure 4.6 Seismic Cone Penetration Test

8) Suspension PS logging

The suspension PS logging is a recently developed tool for measurement of seismic wave velocity profiles. A seismic source and two receivers are built in a single borehole probe. Compression (P) and shear (S) waves are generated by a seismic source that involves the use of a solenoid hammer. The solenoid hammer produces a pressure wave in the borehole fluid. This pressure wave converts into seismic body waves (P and S) at the borehole wall. The waves travel in a radial direction from the borehole wall. Receivers contain two-component geophones, one vertical to record P-waves, and one horizontal for recording of S-waves. The body waves are converted back to pressure waves in the borehole fluid and detected by the geophones. The source and the two receivers are connected with rubber-filter tubes to isolate vibration between them. The Spacing between two receivers is usually one (1) meter (Nigbor and Imai, 1994). Figure 8 shows a schematic of the test field setup.

Advantages and disadvantages

The major advantage of the method is the depth to which it can be used, maximum depths up to 700 m have been reported. The test duration depends on the desired spatial resolution. The conventional test is executed by lowering the probe one meter at a time. In this case, there is no overlapping of the soil intervals for which average velocities are measured and one can approximately measure 100 soil intervals in 2.5 hours. If the resolution is increased, by using a step of half a meter, the test time is almost doubled. In some tests, and for certain depth intervals, intervals of 0.2 m have been used. In both

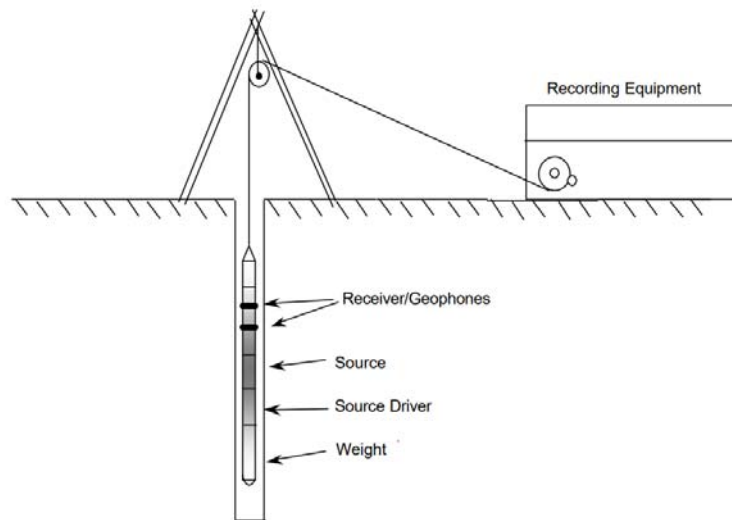


Figure 4.7 - Suspension PS Logging test

cases a SIRT (Simultaneous Iterative Reconstruction Technique) analysis routine can be used to perform a least-squares inversion of the overlapping average velocities at each one meter depth interval.

From the analysis of methods determining the ground dynamic parameters, the procedures should be met the following requirements:

- Requirements of equipment and facilities for the tests
- Requirement of professional skill of engineer
- Requirement of experience of engineer

From the current situation of Vietnam, it is realized that:

- Due to the financial difficulties, almost project consider only in static problem without using the dynamic parameters

CHAPTER 4 METHODS FOR DETERMINING DYNAMIC PARAMETERS OF SOIL

- From the point of view of commercial efficiency, expenses for investment of the dynamic tests is very expensive, so hardly laboratory can equip if they have no financial support from non-profit organization. For example, University of Transport Technology, Hanoi, Vietnam has been supported the finance of 6.5 million dollars by Japan International co-operation Agency (JICA) to invest the equipment for their laboratory but it has no apparatus for determining the dynamic parameters of soil specimen.
- In Vietnam, The standard of geotechnical investigation is for calculation and design of the static problems. Moreover the testing standards for the dynamic problems with fully legal corridor have not been promulgated to promote this field unless the special projects or works must refer to other standards from foreign country.

Therefore, it is necessary to select a suitable method for estimating the ground dynamic parameters in Vietnam. The objective of this chapter is to establish a procedure based on the methods of previous researches in the world for estimating the ground dynamic parameters which is suitable for current condition of Vietnam.

Recently, Andrus et al. (2003) have developed the procedures for estimating dynamic properties of soils in South Carolina of America. When site-specific shear wave velocity, v_s , are not available or need to be supplemented, an estimation of the shear wave velocity, v_s , can be made by the use of correlations with in-situ testing such as the Standard Penetration Test (SPT) or the Core Penetration Test (CPT). The procedures for correlating SPT and CPT results with shear wave velocity, v_s , have been summarized in design standard, Geotechnical Earthquake Engineering, South Carolina Department of Transportation (2008).

The unified formulas which express the dynamic shear moduli and the damping ratios in terms of maximum dynamic shear modulus, cyclic shear strain amplitude, mean effective confining pressure and soil's plasticity index have been proposed by Ishibashi, Zhang (1993). The formulas fitted experiment data reasonably well and could be conveniently utilized in dynamic analyses such as seismic ground respond and soil-structure interaction problems. The formulas cover wide variety of soils ranging from sands to highly plastic clays.

4.4 ESTIMATION OF DYNAMIC SOIL PROPERTIES

4.4.1 Estimation of shear wave velocity, v_s , from SPT data

CHAPTER 4 METHODS FOR DETERMINING DYNAMIC PARAMETERS OF SOIL

Recommended equations to estimate shear wave velocity, v_s , are based on standardized SPT blow count (N_{60}^*), depth (Z), Fines Content (FC), geologic age and location of deposit, and Age Scaling Factor (ASF). Equations for estimating shear wave velocity, v_s , are provided in Table 4.1.

Table 4.1 SPT (N_{60}^*) – Shear Wave Velocity, v_s , Equation for Sand
(Andrus et al., 2003)

| Fines Content, FC | Equation for predicting v_s (m/s) | Equation No |
|-------------------|--|-------------|
| < 40% | $v_s = 72.9(N_{60}^*)^{0.224}Z^{0.130}ASF$ | 4.4 |
| 10% to 35% | $v_s = 72.3(N_{60}^*)^{0.228}Z^{0.152}ASF$ | 4.5 |
| <10% | $v_s = 66.7(N_{60}^*)^{0.248}Z^{0.138}ASF$ | 4.6 |

N_{60}^* =blows/0.3m and Z =depth in meters, ASF=Age Scaling Factors.

Recommended age scaling factors (ASF) based on Andrus et al. (2003) are provided in Table 4.2.

Table 4.2 Recommended Age Scaling Factors (ASF) for SPT
(Andrus et al., 2003)

| Geologic Age and Location of Deposit | Fines Content, FC (%) | Age Scaling Factor, ASF | Database Range of Shear Wave Velocity, v_s (m/s) |
|---|-----------------------|-------------------------|--|
| Holocene Coastal Plain | < 40% | 1.00 | 110 – 260 |
| | 10% to 35% | 1.00 | 120 – 240 |
| | < 10% | 1.00 | 110 – 260 |
| Pleistocene Coastal Plain | < 40% | 1.23 | 150 – 270 |
| | 10% to 35% | 1.08 | 160 |
| | < 10% | 1.28 | 150 – 270 |
| Tertiary Coastal Plain Ashley Formation | < 40% | 1.82 | 340 |
| | 10% to 35% | 1.71 | 340 |
| Tertiary Coastal Plain Dry Branch Formation | < 40% | 1.59 | 330 – 350 |
| | 10% to 35% | 1.48 | 330 – 350 |

FC =% passing #200 sieve

The procedures of estimating shear wave velocity, v_s , from SPT data are following:

1. Estimating FC(%) of soil layer at SPT depth

CHAPTER 4 METHODS FOR DETERMINING DYNAMIC PARAMETERS OF SOIL

2. Calculating SPT blow count (N^*_{60}) and Age Scaling Factor (ASF) based on Fine Content (FC) at each depth of SPT (Z)
3. Estimating v_s , from (4.4), (4.5), (4.6) equation with FC(%) and correlation depth of SPT (Z)
4. Drawing relation between v_s and Z

A review of SPT calculated shear wave velocity relationships reveals that few relationships have been developed for clays. This is likely due to SPT blow counts (N) not being the appropriate test for cohesive soils, particularly since soft clays would have SPT blow counts that would be close to zero. This results in the shear wave velocity that also would be close to zero.

4.4.2 Estimation of shear wave velocity, v_s , from CPT data

Recommended equations to estimate shear wave velocity, v_s , for soils are based on CPT tip resistance (q_c), depth (Z), soil behavior type (I_c), geologic age and location of deposit, and Age Scaling Factor (ASF). Equations for estimating shear wave velocity, v_s , of soils provided in Table 4.3.

Table 4.3 CPT (q_c) – Shear Wave Velocity, v_s , Equations for Soils
(Andrus et al., 2003)

| Soil Behavior Type, I_c | Equation for Predicting v_s (m/s) | Equation No |
|---------------------------|--|-------------|
| All value | $v_s = 4.63q_c^{0.342}I_c^{0.688}Z^{0.092}ASF$ | 4.7 |
| < 2.05 | $v_s = 8.27q_c^{0.285}I_c^{0.406}Z^{0.122}ASF$ | 4.8 |
| > 2.6 | $v_s = 0.208q_c^{0.654}I_c^{1.910}Z^{-0.108}ASF$ | 4.9 |

Recommended age scaling factors (ASF) depended on soil behavior type (I_c) and depth (Z) are provided in Table 4.4 (Andrus et al., 2003)

The soil behavior index, I_c depended on the normalized cone resistance, Q, and the normalized friction ratio, F, are computed using the following equation:

$$I_c = [(3.47 - \log Q)^2 + (1.22 + \log F)^2]^{0.5} \tag{4.10}$$

Where:

$$Q = \left[\frac{q_c - \sigma'_v}{P_a} \right] \cdot \left(\frac{P_a}{\sigma'_v} \right)^n \tag{4.11}$$

CHAPTER 4 METHODS FOR DETERMINING DYNAMIC PARAMETERS OF SOIL

$$F = \left[\frac{f_s}{q_c - \sigma'_v} \right] 100\% \tag{4.12}$$

Where:

q_c – CPT Tip Resistance (kPa)

F_s – CPT Skin Resistance (kPa)

P_a – Reference Stress = 100 kPa = 1 atm

σ'_v - Effective Vertical or Overburden Stress (kPa)

n – Exponent ranging from 0.5 to 1.0 depended on computing procedure of soil behavior index.

Table 4.4 Recommended Age Scaling Factors (ASF) for CPT
(Andrus et al., 2003)

| Geologic Age and Location of Deposit | Soil behavior Description | Soil Behavior Type Index, I_c | Age Scaling Factor, ASF | Database Range of Shear Wave Velocity, v_s (m/s) |
|---|-------------------------------------|---|--------------------------------|--|
| Holocene Coastal Plain | All soils | All values | 1.00 | 60 – 260 |
| | Clean sand, silty sand | < 2.05 | 1.00 | 110 – 260 |
| | Clay, silty clayey silt, silty clay | > 2.60 | 1.00 | 60 – 230 |
| Pleistocene Coastal Plain | All soils | All values | 1.23 | 450 – 1000 |
| | Clean sand, silty sand | < 2.05 | 1.34 | 500 – 1000 |
| | Clay, silty clayey silt, silty clay | > 2.60 | 1.16 | 450 – 1000 |
| Tertiary Coastal Plain Ashley Formation | All soils | All values | 2.29 | 230 – 540 |
| Tertiary Coastal Plain Tobacco road Formation | All soils | All values | 1.65 | 310 – 350 |
| | Clay, silty clayey silt, silty clay | > 2.60 | 1.42 | 330 – 350 |
| Tertiary Coastal Plain Dry branch Formation | All soils | All values | 1.38 | 310 – 360 |
| | Clean sand silty sand | < 2.05 | 1.33 | 310 – 360 |

CHAPTER 4 METHODS FOR DETERMINING DYNAMIC PARAMETERS OF SOIL

The procedure for estimating the soil behavior index is following:

1. Calculate soil behavior index, I_c , using equation (5.10) with $n=1.0$ to have $I_c=I_{c1}$
2. If soil behavior index, I_c , is > 2.60 , use computed I_c using $n=1.0$
3. If soil behavior index, I_c , is < 2.60 , recalculate I_c using $n=0.50$
 - a. If the recalculated I_c is < 2.60 , use computed I_c using $n=0.50$
 - b. If the recalculated I_c is > 2.60 , recalculate I_c using $n=0.70$
4. End.

In brief, the estimating procedures of shear wave velocity, v_s , from CPT data are following:

1. Obtain q_c (kPa) and f_s (kPa) at depth, Z , of CPT
2. Calculate σ'_v (kPa) at depth, Z ,
3. Calculate soil behavior index I_c at depth, Z , using equation 4.10
4. Use Table 5.4 to obtain age scaling factor (ASF) from correlated I_c
5. Estimate v_s using 4.7, 4.8, or 4.9 from correlated I_c

4.4.3 Estimation of damping ratio

Damping ratio is a measure of energy dissipation and increases with increase in shear strain amplitude. The damping ratio increases slowly at a low strain level and then increases quickly with increasing strain amplitude. Damping is induced in soil due to the friction between the soil grains, viscous drag between the pore fluid and soil grains, and plastic deformation of the soil grains. The soil grains are very stiff and tend to keep their elasticity at high confining pressure, and thus very little energy dissipates through plastic deformation. In general, the damping ratio of soil is affected by a lot of factors (Ishibashi and Zhang, 1993; Karl, 2005; Zhang et al., 2005) such as effective confining pressure, void ratio, plastic index, stratum age, and loading condition. Therefore accurate estimation of the damping ratio considered all factor is a complex work. In 1993, Ishibashi and Zhang have proposed an equation for estimating the damping ratio of soil based on plastic index, effective confining pressure, and shear strain amplitude. The authors reanalyzed the available experimental data and an attempt is made to establish unified formulas for dynamic shear moduli and damping ratio to cover wide variety of soils ranging from sands to highly plastic clay.

The formula for estimation of damping ratio is expressed as following:

$$h = 0.333 \frac{1+e^{-0.0145 \cdot PI^{1.3}}}{2} \left[0.586 \left(\frac{G}{G_{max}} \right)^2 - 1.547 \left(\frac{G}{G_{max}} \right) + 1 \right] \quad (4.13)$$

where:

$$\left(\frac{G}{G_{max}} \right) = K(\gamma, PI) \bar{\sigma}_0^{m(\gamma, PI) - m_0} \quad (4.14)$$

PI: Index plastic of soil (%)

γ : Medium shear strain amplitude (%)

$\bar{\sigma}_0$: mean effective confining pressure

$$K(\gamma, PI) = 0.5 \left\{ 1 + \tanh \left[\ln \left(\frac{0.000102 + n(PI)}{\gamma} \right)^{0.492} \right] \right\} \quad (4.15)$$

$$m(\gamma, PI) - m_0 = 0.272 \left\{ 1 - \tanh \left[\ln \left(\frac{0.000556}{\gamma} \right)^{0.4} \right] \right\} e^{-0.0145 PI^{1.3}} \quad (4.16)$$

$$n(PI) = \begin{cases} 0.0 & \text{for } PI = 0 \text{ (sandy soil)} \\ 3.37 \times 10^{-6} PI^{1.404} & \text{for } 0 < PI < 15 \text{ (low plastic soils)} \\ 7.0 \times 10^{-7} PI^{1.976} & \text{for } 15 < PI \leq 70 \text{ (medium plastic soils)} \\ 2.7 \times 10^{-5} PI^{1.115} & \text{for } PI > 70 \text{ (high plastic soils)} \end{cases} \quad (4.17)$$

Using the above formulas to calculate the damping ratio for sandy soil and medium plastic soils with PI of 35 % in case of $\bar{\sigma}_0 = 10$ kPa and 400 kPa, respectively, the results are shown in Figure 4.3 and 4.4.

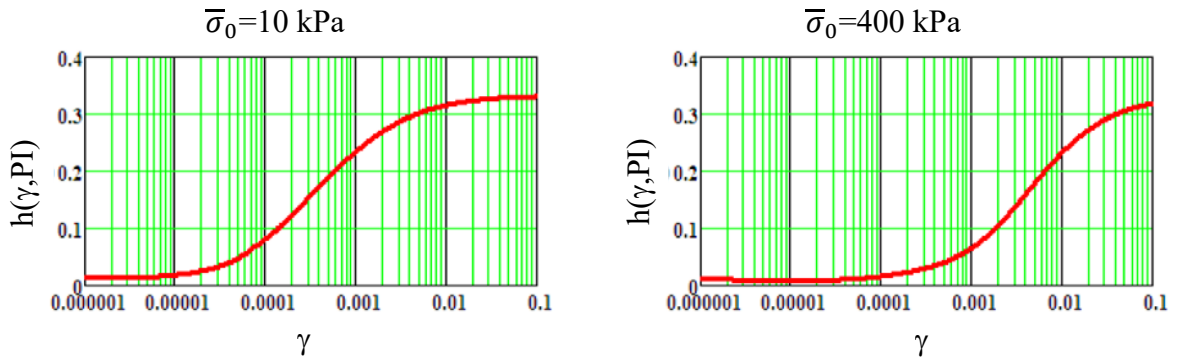
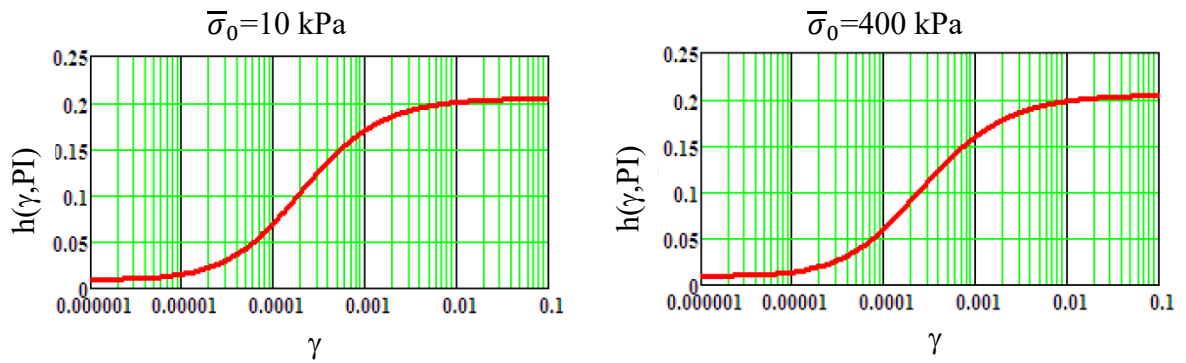


Figure 4.8 $h \sim \gamma$ relation of sandy soils (PI = 0 %)

Figure 4.9 $h\sim\gamma$ relation of plastic soils (PI = 35 %)

4.5 SUMMARY

An analytical procedure for estimation of the soil dynamic parameters in conformity with current condition of Vietnam based on the methods of previous researches in the world has been suggested. The following conclusions were derived based on the calculated results.

The estimation of the soil dynamic parameters based on CPT data with low cost is feasible at current situation in Vietnam.

The methods for estimation of the soil dynamic parameters based on SPT, CPT data bring a feasible research direction for evaluation and establishment of soil dynamic parameters in Vietnam in application for dynamic problems.

REFERENCES

- Das, B. M. (1995): Principles of soil dynamic, PWS-KENT, *publishing company, USA*.
- Kramer, S. L. (1996): Geotechnical Earthquake Engineering, *Prentice Hall, New Jersey*.
- Verruijt, A. (1994, 2008): Soil dynamic, *Delft University of Technology*.
- Karl, L. (2005): Dynamic soil properties out of SCPT and bender element test with emphasis on material damping, *A thesis of doctor of philosophy in Ghent University*.
- Schneider, J. A., Hoyos, L., Mayne, P. W., Macari, E. J., and Rix, G. J. (1999): Field and laboratory measurements of dynamic shear modulus of piedmont residual soils, *Behavioral characteristics of residual soils, GSP 92, ASCE, Reston, VA*, pp.12-25.
- Kavazanjian, E., Matasovib, J. N., Hadi-Hamou, T., and Sabatini, P. J. (1997): Geotechnical Engineering circular No 3 Design guidance geotechnical engineering, *Earthquake engineering for highway, Vol.I design principle*.

CHAPTER 4 METHODS FOR DETERMINING DYNAMIC PARAMETERS OF SOIL

The South Carolina Department of Transportation (SCDOT) (2010): Geotechnical design manual – version 1.1, chapter 12, Geotechnical Earthquake Engineering, Final.

Ishibashi, I., Zhang, X. (1993): Unified dynamic shear moduli and damping ratios of sand and clay, *Japanese Society of soil Mechanics and Foundation Engineering, Soil and Foundations*, Vol.33, No.1, pp.182-191.

Zhang, J., Andrus, R. D., and Juang, C. H. (2005): Normalized shear modulus and material damping ratio relationship, *Journal of geotechnical and geoenvironmental engineering*, ASCE/April 2005.

Till, J. J. Hanebuth, Yoshiki, S., Susumu, T., Quang, L. V., and Quang, T. N. (2005): Sea levels during late marine isotope stage 3 (or older?) reported from the Red River delta (northern Vietnam) and adjacent regions, *Quaternary International*, 145–146 (2006) 119–134.

Trinh, V. B., Dinh, V. T., Nguyen, T. H. Q., Lai, H. P., Bui, H. D. (2003): Estimation of soil and rock elastic parameters for high-rise building design at Caugiay of Hanoi city by seismic survey in boring hole, *Proc. of the 2nd Vietnam National Conf. on problems of building* (in Vietnamese).

Trinh, V. B., Dinh, V. T., Lai, H. P., Tran, A. V. (2011): Influence of earthquake on soil condition in west area of Hanoi, *Earth Science Journal* (in Vietnamese)

Chapter 5

STUDY ON VEHICLE-INDUCED VIBRATION

5.1 INTRODUCTION

Vietnamese government had the plan that Hanoi's transport plan aims to increase the share of public transport from the current low figure of 9 % of trips, to above 60 % by 2030, by which time Hanoi city is slated to have six new metro and three Bus Rapid Transit (BRT) lines. Vietnamese government hopes both traffic and environmental issues can be tackled. It is forecasted that a huge quantity of excavated soil will be discharged from the projects in Hanoi city over the next decade. Therefore, it will become more and more difficult to find reclamation sites for the soil to dump around the city from the environmental point of view. In Japan, LSS is effective backfilling method for using excavated soil in construction work and LSS has been popular as a recycling method for excavated soil. However, LSS indicates a brittle characteristic when the strength increments as increasing an amount of cement stabilizer. In order to improve ductile performance of LSS, a reinforcement method has been created by mixing newspaper as a fiber material into LSS.

LSS was produced by adding and mixing cement stabilizer into liquefied stabilized soil with hand mixer. In the production process, the determination of the density was performed by measuring the mass of slurry filled into a stainless steel mold of 400 cm³ called "AE mortar container". After achieving the desired density, fiber material with amount of 10 kg/m³ was added and mixed by hand mixer. In order to determine fluidity of LSS, the flow test was performed in accordance with JHS A313– Japan Highway Public Corporation Standard. Moreover, the fresh LSS is made to be removed the air inside specimen applying vacuum. However, an investigation on the induction of vehicle-induced building vibration by using LSS has not been performed.

5.2 DEFINITION OF VIBRATION LEVEL

Vibration level is estimated from three parameters as displacement, velocity and acceleration. In Vietnam, vibration velocity is used to estimate the vibration level as an application standard. The abbreviation “VdB” is used for vibration decibels to reduce the potential for confusion with sound decibels (FTA, 2006). Accordingly, maximum vibration level is computed as following (SP, 2004):

$$L = \max(L_i) \leq [L] \text{ [VdB]} \quad (5.1)$$

Where:

$$L_i = 20 \log_{10} \frac{v_i}{v_{ref}} \text{ [VdB]} \quad (5.2)$$

$$v_i = \sqrt{\frac{1}{(t_2 - t_1) f_{SP}} \sum_n v_n^2} \text{ [m/s]} \quad (5.3)$$

$$v_n = \sqrt{v_{xn}^2 + v_{yn}^2} \text{ [m/s]} \quad (5.4)$$

L: Maximum vibration level

L_i : Vibration level with time at time interval of i^{th} one-second

[L]: Criteria for acceptable level of vibration

v_i : Root mean square vibration velocity of measurement point at i^{th} one-second

v_{ref} : Reference vibration velocity, $v_{ref} = 5 \cdot 10^{-8}$ m/s (SP, 2004)

$t_2 - t_1 = 1$ s (FTA, 2006; SP, 2004; Kurbatskii, 2008)

f_{SP} : Number of measured velocity data within one-second period

v_{xn}, v_{yn}, v_n : n^{th} Horizontal, vertical, and total vibration velocity at measurement point

According to Russia standard being used in Vietnam at present, the vibration prediction for building is assessed from the value of velocity at top of foundation (SP, 2004). Therefore, this chapter uses the velocity value at the ground surface to predict the vibration.

National Technical Regulation on Vibration has been promulgated by Natural Resources and Environment in 2010 (QCVN 27, 2010). The regulation gives criteria for acceptable levels of ground-borne vibration from any source such as trains, buses on rough roads, and constructions activities, blasting, pile-driving and operating heavy earth-moving equipment for residence. The maximum permissible level of vibration is assigned

to be 75VdB. The value is also found in reports of Japan. The results of the Japanese study confirm the conclusion that at a vibration velocity level of 75 to 80 VdB, many people will find the vibration annoying (Tokita, 1975).

5.3 ANALYTICAL AND NUMERICAL APPROACHES

5.3.1 Vehicle motion

A single-axle quarter-truck vehicle with 2- degree of freedoms (DOFs) running on a rough road at constant velocity V was reported. The static loads is not considered in this study. Only cyclic loads are determined. Therefore, the equation of motion associate with the body of the vehicle as follows:

$$\begin{bmatrix} m_1 & 0 \\ 0 & m_2 \end{bmatrix} \begin{Bmatrix} \ddot{Z}_1(t) \\ \ddot{Z}_2(t) \end{Bmatrix} + \begin{bmatrix} c_1 & -c_1 \\ -c_1 & c_1 + c_2 \end{bmatrix} \begin{Bmatrix} \dot{Z}_1(t) \\ \dot{Z}_2(t) \end{Bmatrix} + \begin{bmatrix} k_1 & -k_1 \\ -k_1 & k_1 + k_2 \end{bmatrix} \begin{Bmatrix} Z_1(t) \\ Z_2(t) \end{Bmatrix} = \begin{Bmatrix} 0 \\ c_2 \dot{y}(t) + k_2 y(t) \end{Bmatrix} \quad (5.5)$$

where c_1 and k_1 are respectively the damping and stiffness coefficients of the suspension system; m_1 and m_2 are the sprung and unsprung masses, respectively; c_2 and k_2 are the damping, stiffness coefficients of the tire, respectively; \ddot{Z} is the absolute acceleration; \dot{Z} is the absolute velocity; Z is the absolute displacement associated with the vertical vibration of the vehicle body; y is the roughness of road pavement.

After modal analysis, Eq. (5.5) can be written in solution as:

$$\{Z(t)\} = [\varphi_{i,j}] \{Y_j(t)\} = \begin{bmatrix} \varphi_{1,1} & \varphi_{1,2} \\ \varphi_{2,1} & \varphi_{2,2} \end{bmatrix} \begin{Bmatrix} Y_1(t) \\ Y_2(t) \end{Bmatrix} \quad (5.6)$$

where $\varphi_{i,j}$ is the i th component of the j th mode shape and $\varphi_{i,j}$ is the j th modal coordinate of the system.

5.3.2 Road Spectrum

The equation of LaBarre et al.¹⁸⁾ describes the first road spectrum model as follows:

$$S_{yy}(\omega) = \begin{cases} \frac{1}{2\pi V} S(n_0) \left(\frac{\omega}{2\pi V n_0} \right)^{-w_1}, & \omega \leq 2\pi V n_0 \\ \frac{1}{2\pi V} S(n_0) \left(\frac{\omega}{2\pi V n_0} \right)^{-w_2}, & \omega \geq 2\pi V n_0 \end{cases} \quad (5.7)$$

where n_0 , w_1 , w_2 are shape coefficients; ω is circular frequency; $S(n_0)$ is the road roughness coefficient and V is vehicle velocity.

5.3.3 Vehicle loads on pavement

Vehicles running on rough roads can be caused vertical vibrations. Cyclic vehicle load $F(t)$ can be determined as follows:

$$F(t) = -m_1\ddot{Z}_1(t) - m_2\ddot{Z}_2(t) \quad (5.8)$$

In linear system, if the cyclic vehicle load $F(t)$ will be stationary Gaussian random processes with zero, Eq. (A5) is obtained from Eq. (A2) and (A4) as follows:

$$F(t) = -m_1\langle\varphi_{1,1} \ \varphi_{1,2}\rangle \begin{Bmatrix} \ddot{Y}_1(t) \\ \ddot{Y}_2(t) \end{Bmatrix} - m_2\langle\varphi_{2,1} \ \varphi_{2,2}\rangle \begin{Bmatrix} \ddot{Y}_1(t) \\ \ddot{Y}_2(t) \end{Bmatrix} \quad (5.9)$$

The total vehicle load $F(t)$ can be calculated the following equation:

$$F_T(t) = (m_1 + m_2)g + F(t) \quad (5.10)$$

5.3.4 Cyclic vehicle loading spectrum

Closed-form solution for the cyclic load spectrum S_{FF} was proposed by Lin as follows:

$$S_{FF}(\omega) = T_y(\omega)S_{yy}(\omega) \quad (5.11)$$

$$T_y(\omega) = \omega^4(c_2^2 + k_2^2) \sum_{i=1}^2 \sum_{r=1}^2 \sum_{j=1}^2 \sum_{k=1}^2 m_i m_r \frac{\varphi_{i,j} \varphi_{r,k} \varphi_{2,j} \varphi_{2,k}}{M_j M_k} \text{Re}[H_j(\omega)H_k(-\omega)] \quad (5.12)$$

$$\text{Re}[H_j(\omega)H_k(-\omega)] = \frac{(\omega_j^2 - \omega^2)(\omega_k^2 - \omega^2) + (2\xi_j \omega_j \omega)(2\xi_k \omega_k \omega)}{((\omega_j^2 - \omega^2)^2 + (2\xi_j \omega_j \omega)^2)((\omega_k^2 - \omega^2)^2 + (2\xi_k \omega_k \omega)^2)} \quad (5.13)$$

where ξ_j is the j th modal damping ratio of the system and ω_j is the undamped natural frequency of the j th modal.

5.3.5 Generation of a time history of cyclic vehicle loading

During pavement response analysis, the time history of cyclic vehicle load $F(t)$ can be simulated from Eq. 5.11:

$$F(t) = \sum_{i=1}^N \sqrt{S_{FF}(\omega_i) \Delta\omega_i} \sin(\omega_i t + \theta_i) \quad (5.14)$$

where θ_i is a random phase angle uniformly distributed from 0 to 2π ; ω_i is circular frequency; the frequency increment $\Delta\omega_i = \omega_{i+1} - \omega_i$; N is the total number of frequency increments within the frequency interval $(\omega_{min}, \omega_{max})$ in which $S_{FF}(\omega)$ is defined. ω_{min} and ω_{max} are minimum and maximum frequencies, respectively.

5.3.6 Verification

To demonstrate the accuracy application of the cyclic vehicle loads, many researchers simulated a moving load on pavement surface. Hamdy et al. evaluated the cyclic response of asphalt-concrete pavement reinforced with geogrid using cyclic load amplitude of 400 kPa.

Agostinacchio et al. used a Matlab® approach to investigate the vibration induced by surface irregularities in road pavement. The behavior of the cyclic load for the various vehicles travelling at chosen speeds on the different road surfaces profiles was generated in accordance with ISO 8608 Standard²²). The maximum cyclic load produced by a truck is approximately 310 kN.

In addition, Lin J. H simulated cyclic vehicle load on road pavement. The relationship between maximum cyclic vehicle load and the grade of surfaces on roads of various classes is shown in

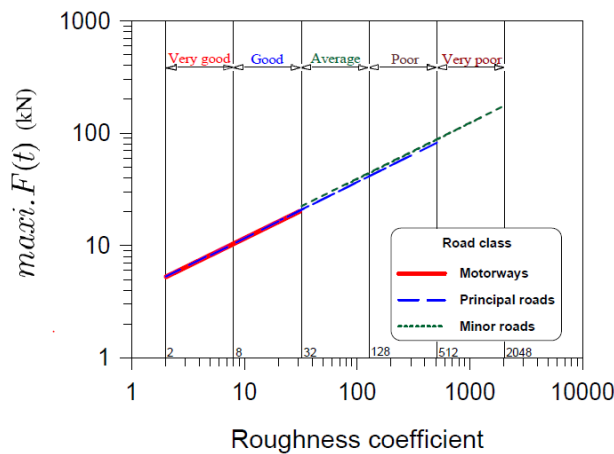


Figure 5.1 Relationship between maximum cyclic vehicle load and the grade of surfaces on roads of various classes

5.4 ANALYSIS PROCEDURE

In order to predict the ground-borne vibration due to moving vehicle on road system in Hanoi city, a 2D finite element model was developed in this study. Plaxis is a program based on finite element method (FEM). The program was originally developed at the University of Delft in Netherland where research in geotechnical design based on FEM in the '70s resulted in a commercial version of the program in 1987 and since 1998 it is available in a Windows version with a user-friendly interface. The program can simulate problems with the most common construction element such as beams and struts. Today, the program is practical for solving most complex geotechnical problems. The program is divided into four sub-programs (Input, Calculation, Output and Curves) (Brinkgreve et al., 2006). From these features, use of Plaxis in geotechnical design works has been becoming widely in Vietnam at present.

However, as using Plaxis in order to solve problems of soil-road interaction under dynamic loading induced by moving train, the program has not sufficiently provided calculation tools as following:

- Dynamic load described in the program is harmonic ones and other cases of load including vehicle-induced dynamic load require the definition by user.

From the above background, this study has proposed an analysis procedure for the ground-borne vibration prediction as shown in Figure 5.2.

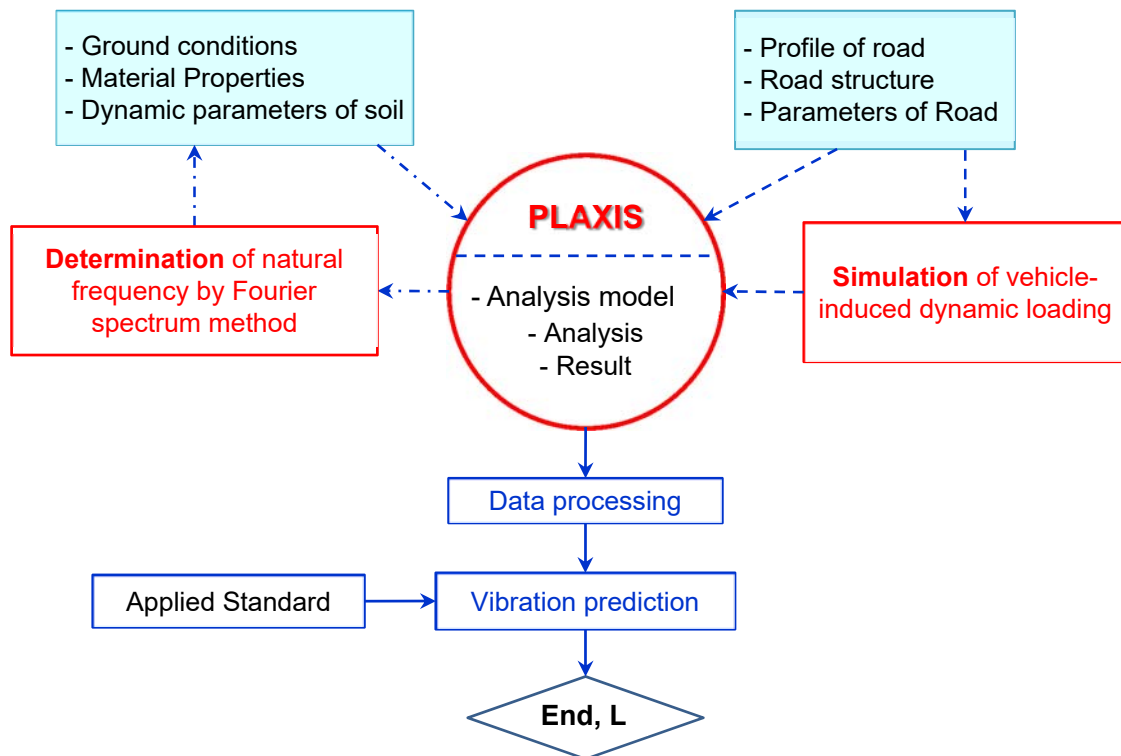


Figure 5.2 Schematic diagram of prediction procedure for train-induced vibration from road

5.4.1 Selection of material model

Generally, medium model is the set of relations describing properties the medium in a process. The model should allow using mathematical language to describe the fundamental behaviors of the medium under loading with high accuracy and reliability. Nowadays, many sophisticated medium models can simulate soil behaviors, which is varied its state during loading. The models with other variables have being improved together with progress of scientific and technology. However, models should be as simple as possible and as accurate as necessary regarding the task they serve. With soil model, it should describe main properties of soil, uniquely defined in term of mathematics and be easy for use of mathematical function. In addition, the model should be practical in current condition, which requires the soil parameters for input data as few as possible.

Recently, based on the results of study on soil kinds in South Asia area by Plaxis and experiment, Ahmad (2010) and Bahatin (2008) have reported that Mohr Coulomb model and Hardening Soil model agree well with experiment results and shows almost not any distinction in analysis with friction soils. Bui (2007) proposed use of modified Cam Clay

model for weak soil layers in Hanoi area. Moreover, the soil parameters for the Mohr Coulomb and modified Cam Clay models can be obtained from data of geologic survey reports in current condition of Vietnam. Therefore, this is the reason why this study use modified Cam-Clay model for weak soil and Mohr-Coulomb for other soil to analyze in Plaxis.

The models and their parameters described in detail can be available found in literature (Fadeev, 1995; Brinkgreve et al., 2006; Kojic, 2005; Helwany, 2007). The parameters of the models for analysis in Plaxis can be classified into two groups, basic parameters and particular ones of each model. The basic parameters can be easily obtained from basic test of soil samples such as unit weigh (ρ), two Rayleigh coefficient (α_R & β_R), friction angle (φ), cohesion (c), and dilatancy angle (ψ). $\psi \approx 0$ is for overconsolidated soil, clay; $\psi \approx \varphi - 30^\circ$ is for sand; $\psi \approx 0$ is for soil kinds with $\varphi \approx 0$ (Brinkgreve, et al., 2006).

Mohr-Coulomb model parameters:

Beside the aforementioned parameters, Mohr-Coulomb model requires more two parameters including Young modulus (E_{eq}), Poisson's ratio (ν) as shown in Figure 6.3, which can be obtained from geologic survey reports or basic test of soil sample. The two parameters can be estimated in Plaxis by means of equation (5.1), (5.2), and (5.3) as providing shear wave velocity (v_s) and compressive wave velocity (v_p).

Modified Cam-Clay model parameters:

Modified Cam Clay model was made based on five particular parameters as shown in Figure 6.4. The parameters including Poisson's ratio (ν_{ur}), Cam-Clay swelling index (κ), Cam-Clay compression index (λ), Tangent of the critical state line (M), initial void ratio (e_{init}) can be obtained from basic test of soil sample. Poisson's ratio ν_{ur} is a real elastic parameter and not a pseudo-elasticity constant as used in the Mohr-Coulomb model. Its value will usually be in range between 0.1 and 0.2 (Brinkgreve, et al., 2006). Compression index and swelling index can be obtained from one-dimensional consolidated compression test as following:

$$\lambda = \frac{c_c}{\ln 10} \text{ and } \kappa = \frac{c_s}{\ln 10} \quad (5.16)$$

CHAPTER 5 STUDY ON VEHICLE-INDUCED VIBRATION

he parameter M should be based on the friction angle and estimated from plastic condition of Mohr-Coulomb as following:

$$M = \frac{6 \cdot \sin\phi}{3 - \sin\phi} \tag{5.17}$$

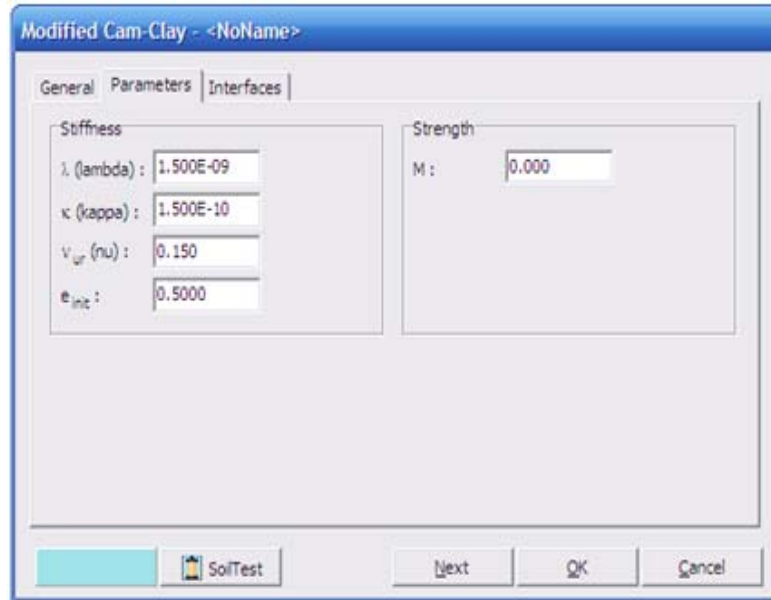


Figure 5.4 Mohr-Coulomb model parameters in Plaxis

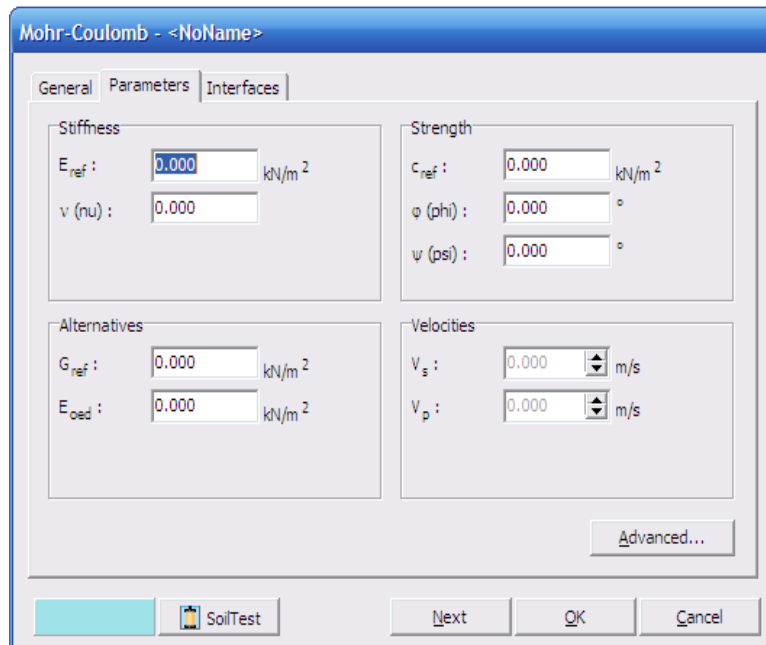


Figure 5.3 Cam-Clay model parameters in Plaxis

5.5 NUMERICAL MODEL AND CONSIDERED PARAMETERS

The road system of Hanoi city as operated will generate ground vibrations which cause undesirable environment and economical impacts such as nuisance of the passenger along the road and deterioration of the alongside existing building structures. On the other hand, the vehicle-induced vibration problem has been not sufficiently mentioned in environmental impact assessment. Therefore, Giai Phong road, Dong Da district in Hanoi city was selected to analyze the train-induced vibration in this study.

5.5.1 Road and ground conditions

Giai Phong road is one of main road in Hanoi city and it is the main connection road from Hanoi to north-south highway of Vietnam. Because, the road was constructed and used. In addition, the purpose of this study is to analyze reduction of vehicle-induced vibration using liquefied stabilized soil. Therefore, two types of soils were used for backfilling process. The geotechnical properties of soil layers in the line are shown in Table 5.1. The soil dynamic parameters have been calculated as shown in Table 4.10 and 4.11 of Chapter 4. The parameters of the road are shown in Table 5.2.

| Material | | Unit | Asphalt concrete | Base (Crushed stone) | Sub-base (Crushed stone) | Sub-grade (Sand) |
|--|----------------|-------------------|---------------------|-------------------------|-----------------------------|---------------------|
| Constitutive model | | | Linear elastic | Mohr-Coulomb | Mohr-Coulomb | Mohr-Coulomb |
| Thickness | | m | 0.1 | 0.3 | 0.4 | 0.4 |
| Young's modulus | | MN/m ² | 2.1x10 ³ | 1.2x10 ² | 49 | 24 |
| Poisson' ratio | | - | 0.45 | 0.35 | 0.3 | 0.3 |
| Dry density | | kN/m ³ | 20 | 20 | 18 | 17 |
| Saturated density | | kN/m ³ | - | 22 | 20 | 18 |
| Cohesion | | kN/m ² | - | 30 | 20 | 0 |
| Friction angle | | Dgree | - | 43 | 40 | 35 |
| Dilatation angle | | Degree | - | 13 | 14 | 5 |
| Coefficient of Hortizontal permeability | k _x | - | - | 1 | 1 | 1 |
| Coefficient of Vertical permeability | k _y | - | - | 1 | 1 | 1 |

Table 5.1 Material properties of road

| Depth (m) | Thickness (m) | Kind | Average N | v | ρ (kN/m ³) | G (MN/m ²) | V _s (m/s) |
|-----------|---------------|------|-----------|------|------------------------|------------------------|----------------------|
| 2.2 | 2.2 | Sand | 9.3 | 0.49 | 17 | 48.921 | 168 |
| 9.5 | 7.3 | Clay | 9.3 | 0.49 | 15 | 67.447 | 210 |
| 14.1 | 4.6 | Clay | 4.5 | 0.49 | 15 | 41.72 | 165 |
| 25.8 | 11.7 | Clay | 9.5 | 0.49 | 15 | 68.656 | 212 |
| 37.8 | 12 | Sand | 40.7 | 0.49 | 19 | 146.735 | 275 |
| 50 | 12.2 | Sand | 98.3 | 0.49 | 20 | 278.103 | 369 |

Table 5.2 Geotechnical properties of soil layers

5.5.2 Finite element model

In this study, a 2D model of road, building, surrounding soil and cyclic loading of vehicles on the road with the use of Plaxis V8.6 finite element software is introduced in order to evaluate vibration propagation due to passing of vehicles to the ground surface.

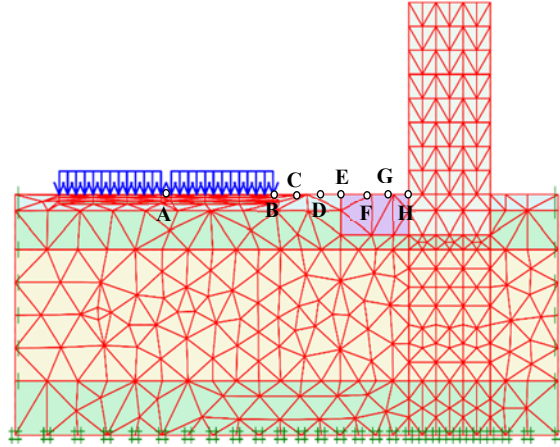


Figure 5.5 Finite element model in Plaxis

5.6 SUMMARY

Within this chapter, an analysis procedure for prediction of vehicle-induced vibration has been performed in conformity with current condition of Vietnam. Two types of backfill soils were selected and analyzed in this study. According to the results of the numerical analysis, the following conclusions are reached in regard to the road induced vibrations in Vietnam.

Based on Bernoulli-Euler beam theory, a model of the dynamic loading on tunnel has been made. Its numerical simulation procedure was accomplished in Mathcad by programming. The numerical result with high reliability can be input data for ground-borne vibration analysis model.

Use of Plaxis a program being popular in Vietnam with application of Fourier spectrum method to estimate natural frequency for dynamic problem of multilayered ground system bring the reliable results

REFERENCES

- Tokita, Y. (1975): Vibration Pollution Problems in Japan, *In Inter-Noise 75, Sendai, Japan*, pp.465-472.
- Fadeev, A. B. (1995): Finite element method in geotechnical engineering, *Education Publishing House* (translated in Vietnamese)

Bathe, K. J. (1982): Finite element procedures in engineering analysis, *Prentice-Hall Inc, Englewood Cliff, New Jersey, USA*.

Zienkiewicz, O. C. and Taylor, R. L. (2000): The finite element method, Vol.1: The basic, Butterworth-Heinemann, *A division of reed education and professional publishing Ltd*.

Zienkiewicz, O. C. and Taylor, R. L. (2000): The finite element method, Vol.2: Solid mechanics, Butterworth-Heinemann, *A division of reed education and professional publishing Ltd*.

Nguyen, T. L. (2005): Study on interaction of nonlinearity dynamic in structure and ground, *PhD. Dissertation, Le Quy Don Technical University of Hanoi* (in Vietnamese).

Nguyen, T. T. (2005): Study on interaction in structure and medium under loading of weapons with consideration of nonlinearity of medium, *PhD. Dissertation, Le Quy Don Technical University of Hanoi* (in Vietnamese).

Carl E. H., David A. T., Lance D. M.: Transit noise and vibration impact assessment, *U.S. Department of Transportation Federal Transit Administration-Office of Planning and Environment 1200 New Jersey Avenue, S.E. Washington, DC 20590, 2006*.

SP 23-105.: Estimation of vibration in design, construction and operation of underground, *Code of practice for design and construction, Russian Metro Standard, 2004*.

Kurbatskii, G. H.: Measurement of vibrations, *Moscow State University of Railway Engineering, 2008*.

QCVN 27:2010/BTNMT.: National Technical Regulation on Vibration, *Ministry of Natural Resources and Environment of Vietnam, 2010* (in Vietnamese).

Tokita, Y.: Vibration Pollution Problems in Japan, *Proceedings Inter-Noise '75, Tohoku university, Sendai 980, Japan, pp.465-472, 1975*.

Duong, H. Q., Kohata, Y., Nguyen Q. D.: Evaluation on Mitigation of Train-induced Vibration as Using LSS for Backfilling Ground of Cut and Cover Tunnel by FEM, *the 50th Japan National Conference on Geotechnical Engineering, pp.2411-2412, 2015*.

Das, B. M.: Principles of soil cyclic, *PWS-KENT, publishing company, USA, 1995*.

TCXDVN.: Design of structure for earthquake resistance, *construction standard of Vietnam, p.1, regulations, earthquake impact with building structure, 2006* (in Vietnamese).

Railway Technical Research Institute: *Explanation for railway structure and design standards, 1999*.

Rao, SS.: The Finite Element Methods in Engineering, *Second Edition*, Pergamon Press, New York, 1989.

Lin J.H.: Simulation of cyclic vehicle load on road pavement, *Vibroengineering PROCEDIA*, Vol. 5, 2015, p.p 503-508, 2015.

LaBarre R. P., Forbes R. T., Andrew S.: The measurement and analysis of road surface roughness. *Motor Industry Research Association*, Report No. 5/1970, Nuneaton, England, 1970.

Lin J. H.: Variations in cyclic vehicle load on road pavement, *International Journal of Pavement Engineering*, Vol. 15, p. 558-563, 2014.

Hamdy F., Ahmed M. H.: 2D plaxis finite element modeling of asphalt-concrete pavement reinforced with geogrid. *Journal of Engineering Sciences*, Vol. 42 No. 6, pp. 1336 – 1348, 2014.

Agostinacchio M., Ciampa D., Olita S.: The vibrations induced by surface irregularities in road pavements – a Matlab® approach, *DOI 10.1007/s12544-013-0127-8*, 2014.

ISO 8608: Mechanical vibration, road surface profiles- Reporting of Measured Data, 2016.

Chapter 6

REDUCTION OF VEHICLE-INDUCED VIBRATION USING LIQUEFIED STABILIZED SOIL

6.1 INTRODUCTION

Vietnamese government had the plan that Hanoi's transport plan aims to increase the share of public transport from the current low figure of 9 % of trips, to above 60 % by 2030, by which time Hanoi city is slated to have six new metro and three Bus Rapid Transit (BRT) lines. Vietnamese government hopes both traffic and environmental issues can be tackled. It is forecasted that a huge quantity of excavated soil will be discharged from the projects in Hanoi city over the next decade. Therefore, it will become more and more difficult to find reclamation sites for the soil to dump around the city from the environmental point of view. In Japan, LSS is effective backfilling method for using excavated soil in construction work and LSS has been popular as a recycling method for excavated soil. However, LSS indicates a brittle characteristic when the strength increments as increasing an amount of cement stabilizer. In order to improve ductile performance of LSS, a reinforcement method has been created by mixing newspaper as a fiber material into LSS.

LSS was produced by adding and mixing cement stabilizer into liquefied stabilized soil with hand mixer. In the production process, the determination of the density was performed by measuring the mass of slurry filled into a stainless steel mold of 400 cm³ called "AE mortar container". After achieving the desired density, fiber material with amount of 10 kg/m³ was added and mixed by hand mixer. In order to determine fluidity of LSS, the flow test was performed in accordance with JHS A313– Japan Highway Public Corporation Standard. Moreover, the fresh LSS is made to be removed the air inside specimen applying vacuum. However, an investigation on the induction of vehicle-induced building vibration by using LSS has not been performed.

CHAPTER 6 REDUCTION OF VEHICLE-INDUCED VIBRATION USING LIQUEFIED TABILIZED SOIL

In this study, the investigation is focused on the effect of using LSS for reduction of nearby building responses based on a parametric study directly in the time domain. Two cases i.e. the use of backfilling soil and LSS for backfill ground of building towards Giai-Phong road, Dong Da district in Hanoi city was evaluated by using the numerical analyses procedure.

6.2 ANALYSIS PROCEDURE

6.2.1 Simulation of cyclic vehicle load

In this paper, the investigation is focused on the effect of using LSS for the reduction of nearby building responses through a parametric study. The cyclic vehicle load on road pavement was directly considered in the mathematical modeling and analysis. Some details are given in Chapter 5. Therefore, as differences from others, the cyclic vehicle load is automatically taken into account and the effect of LSS reinforced with paper is evaluated directly. Responses of the building and backfilling materials are given in terms of accelerations.

In this study, vertical vibrations can be produced during moving vehicles on rough surface of the roads, thereby the transmitting of the inertial force is associated with the vibration through the suspension system and wheels into the pavement. This study was analyzed under 400 kN/m in moving load of vehicles and 10 Hz in frequency when the cyclic load is applied to pavement on the truck with a speed of 60 km/h.

6.2.2 Numerical model and considered parameters

In this study, a reinforced concrete eight-floor building frame with one basement was selected and the model is shown in Figure 6.1.

1- Building, road and ground conditions

The building of 12 m in width and 24 m in height is located to the right hand side of the road. The structure shown in Figure 6.1 is a part of the building that is formed by a series of parallel frames. The height of the floors is 3 m and the basement floor is located at a depth of 4.5 m below ground surface. The frame consists of three bays of 4 m in distance. The distance from left end of building to the right end of the road were assumed to be 15.5 m. The pile foundation is selected to analyze in this study. The excavated area

CHAPTER 6 REDUCTION OF VEHICLE-INDUCED VIBRATION USING LIQUEFIED TABILIZED SOIL

shown as “Backfilling material” in Figure 6.1 was set to 4.5 m in depth equal to the height of basement floor and 10 m in width, which is considered to be reduced a vehicle-induced building vibration from the previous study. In this study, back filling soil as Case 1 and LSS as Case 2 were selected as backfilling materials, and the reducing effect on building on building vibration is discussed. The ground profile of construction area are schematically shown in Figure 6.2. The geotechnical properties of soil layers are shown in Table 6.1. The ground was composed of soft clay and loose sand from the surface to the depth of 30-40 m, and of dense sand or gravel below the depth of 30-40 m.

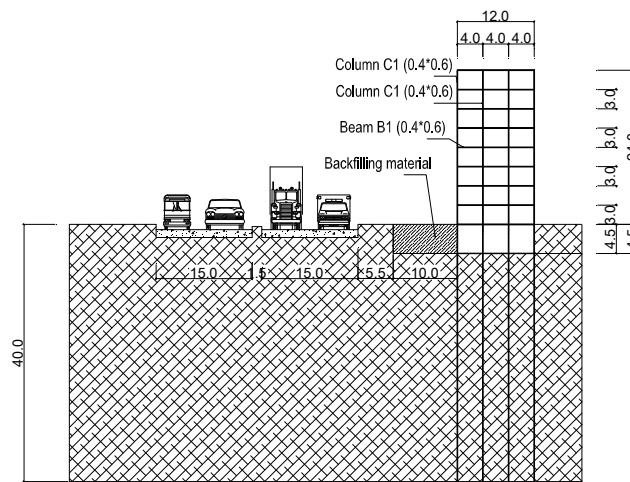


Figure 6.1 Numerical model of the considered soil structure system

| Components | ρ (kN/m ³) | Elastic modulus (MN/m ²) | ν |
|-------------------|-----------------------------|--------------------------------------|-------|
| Piles | 25 | 3500 | 0.15 |
| Basement | 25 | 3500 | 0.15 |
| Columns and beams | 25 | 2500 | 0.2 |

Table 6.1 Parameters of building

| Depth (m) | Thickness (m) | Kind | Average N | ν | ρ (kN/m ³) | G (MN/m ²) | V_s (m/s) |
|-----------|---------------|------|-----------|-------|-----------------------------|------------------------|-------------|
| 2.2 | 2.2 | Sand | 9.3 | 0.49 | 17 | 48.921 | 168 |
| 9.5 | 7.3 | Clay | 9.3 | 0.49 | 15 | 67.447 | 210 |
| 14.1 | 4.6 | Clay | 4.5 | 0.49 | 15 | 41.72 | 165 |
| 25.8 | 11.7 | Clay | 9.5 | 0.49 | 15 | 68.656 | 212 |
| 37.8 | 12 | Sand | 40.7 | 0.49 | 19 | 146.735 | 275 |
| 50 | 12.2 | Sand | 98.3 | 0.49 | 20 | 278.103 | 369 |

Table 6.2 Geotechnical properties of soil layers

CHAPTER 6 REDUCTION OF VEHICLE-INDUCED VIBRATION USING LIQUEFIED TABILIZED SOIL

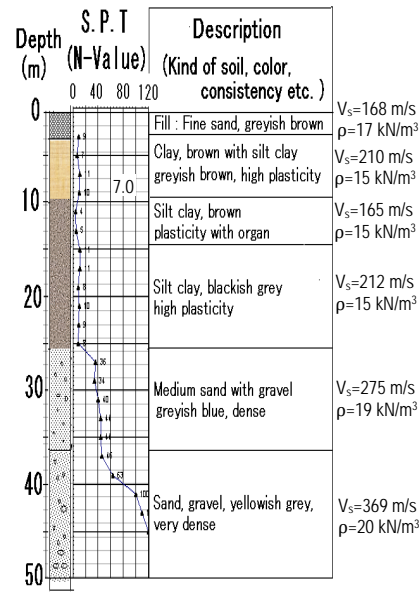


Figure 6.2 Ground profile

Damping ratio of soil layers is assumed to be 4 %, which is in range of 3-8 %, the vibration level of ground is not significantly changed¹³). Also, most soil types in Hanoi area have the damping ratio in range of 3-5 %. Poisson's ratio of all soil layers and the backfilling materials were assumed to be 0.49. The shear elastic wave velocity of ground was calculated from N-value, using the formula of Japanese railway standard. The parameters of building are shown in Table 6.2.

Figure 6.3 shows typical cross section of Giai Phong road where the total thickness of the road embankment is 1.2 m. The thickness of subgrade soil is 0.4 m, sub-base layer is 0.4 m, base layer is 0.3 m and asphalt concrete is 0.1 m, respectively. The total width of the road is 38 m, in which 30 m for traffic including two lanes and 8 m for the sidewalk. This road is one of main road in Hanoi city and it is the main connection road from Hanoi to north-south highway of Vietnam. Material parameters and constitutive model are shown in Table 6.3.

2- Characteristics of backfilling materials

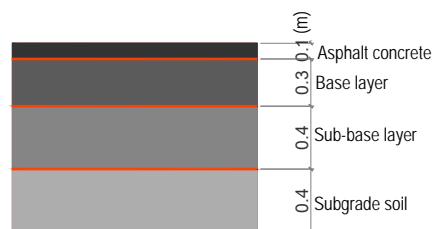


Figure 6.3 Typical cross section of Giai Phong road

CHAPTER 6 REDUCTION OF VEHICLE-INDUCED VIBRATION USING LIQUEFIED TABILIZED SOIL

Table 6.3 Material properties of road

| Material | | Unit | Asphalt concrete | Base (Crushed stone) | Sub-base (Crushed stone) | Sub-grade (Sand) |
|--|----------------|-------------------|---------------------|----------------------|--------------------------|------------------|
| Constitutive model | | | Linear elastic | Mohr-Coulomb | Mohr-Coulomb | Mohr-Coulomb |
| Thickness | | m | 0.1 | 0.3 | 0.4 | 0.4 |
| Young's modulus | | MN/m ² | 2.1x10 ³ | 1.2x10 ² | 49 | 24 |
| Poisson' ratio | | - | 0.45 | 0.35 | 0.3 | 0.3 |
| Dry density | | kN/m ³ | 20 | 20 | 18 | 17 |
| Saturated density | | kN/m ³ | - | 22 | 20 | 18 |
| Cohesion | | kN/m ² | - | 30 | 20 | 0 |
| Friction angle | | Dgree | - | 43 | 40 | 35 |
| Dilatation angle | | Degree | - | 13 | 14 | 5 |
| Coefficient of Horizontal permeability | k _x | - | - | 1 | 1 | 1 |
| Coefficient of Vertical permeability | k _y | - | - | 1 | 1 | 1 |

In this study, the properties of backfilling materials i.e. LSS and backfilling soil used for the analysis model in Plaxis were adopted from the previous research

a- Properties of LSS

The original material was Vinhphuc clay taken from a construction site in Hanoi city. The soil is classified into low liquid limit clay. Geoset 10 made by Taiheiyo Cement Co. was used as cement stabilizer.

Based on results of flow and bleeding tests and unconfined compression tests on samples with curing at 28 days, the content of cement stabilizer was assigned to be 200 kg/m³ and the target slurry density of LSS was 1.350 g/cm³.

The initial Young's modulus of LSS, $E_0 = 58.8 \text{ MN/m}^2$ in case of confining pressure of 49 kPa, unit weight, $\rho = 14.0 \text{ kN/m}^3$ and shear modulus, $G = 197.2 \text{ MN/m}^2$ were set as the basic properties of LSS. The damping ratio of LSS is assumed as 10 %.

b- Properties of backfilling soil

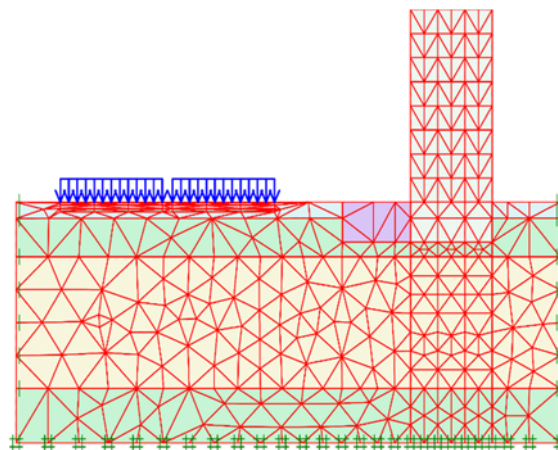


Figure 6.4 Finite element model in Plaxis

CHAPTER 6 REDUCTION OF VEHICLE-INDUCED VIBRATION USING LIQUEFIED TABILIZED SOIL

Table 6.4 Physical properties of backfilling materials

| Backfilling material | V_s (m/s) | ρ (kN/m ³) | h (%) | ν (kN/m ³) |
|-----------------------------|----------------|--------------------------------|------------|-------------------------------|
| Case 1: backfilling soil | 172 | 17 | 4 | 0.49 |
| Case 2: LSS | 370 | 14 | 10 | 0.49 |

Because there are not much investigation results on stiffness of the backfilling soil, the investigation results on backfilling soil (decomposed granite soil, which is “Masado”) in Daikai station, which suffered from the Southern Hyogo prefecture earthquake in 1995, were used as the soil parameters. N value and unit weight, ρ were set at 10 and 17.0 kN/m³, respectively. Shear modulus, $G = 51.531 \text{ MN/m}^2$ was estimated from N value in accordance with Railway Design Standard¹⁵⁾. The damping ratio of this material was assumed as 4 %. The physical properties of two backfilling materials are shown in Table 6.4.

3- Finite element model

The finite element model (FEM) is plotted in Figure 6.4. The FEM is divided by two parts. The first part is a domain including wave source, i.e., road and soil layers. The second part consist of the building frame elements¹⁶⁾.

Eight analyzed points on the ground surface A, B, C, D, E, F, G, H with distance of 0, 15, 17.583, 20.166, 22.749, 25.332, 27.914, 30.5m respectively from origin of coordinate (road center line on the ground surface) are shown in Figure 6.4.

4- Numerical model in Plaxis

In this study, a 2D model of road, building, surrounding soil and cyclic loading of vehicles on the road with the use of Plaxis V8.6 finite element software is introduced in order to evaluate vibration propagation due to passing of vehicles to the ground surface.

In the model, 15-node triangular elements were used infinite element mesh. For determining the optimum size of element in order to get reasonable precise result in a minimized time, four different meshing patterns were analyzed and the result of analysis with very fine and fine meshing were very close to each other, therefore, fine meshing pattern were chosen as Figure 6.4.

The analysis is performed to determine responses of the backfilling area and the building due to applied vehicle loading. Therefore, the building frame is supported to be subjected to static loading of usual dwelling, which are no considered in this analysis.

CHAPTER 6 REDUCTION OF VEHICLE-INDUCED VIBRATION USING LIQUEFIED TABILIZED SOIL

6.3 RESULTS AND DISCUSSION

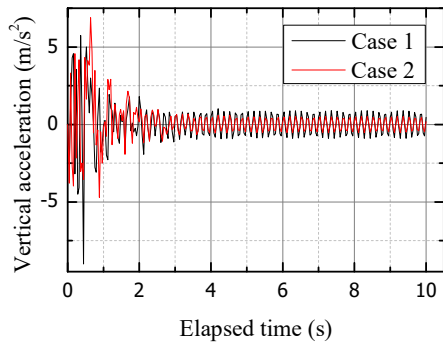


Figure 6.5 Vertical acceleration at point E for load amplitude =400 kN/m, $f = 10$ Hz

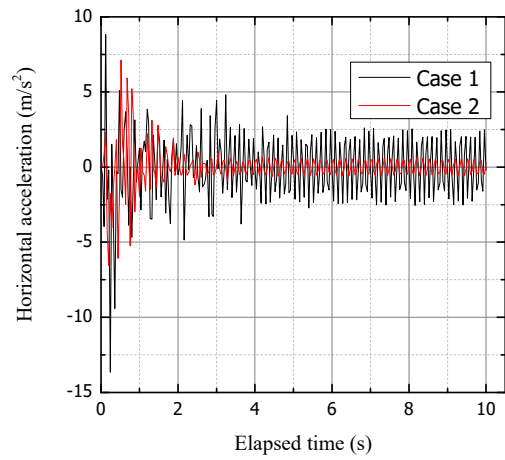


Figure 6.6 Horizontal acceleration at point E for load amplitude =400 kN/m, $f = 10$ Hz

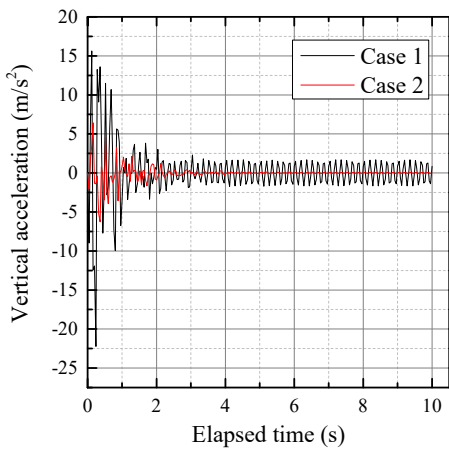


Figure 6.7 Vertical acceleration at point H for load amplitude =400 kN/m, $f = 10$ Hz

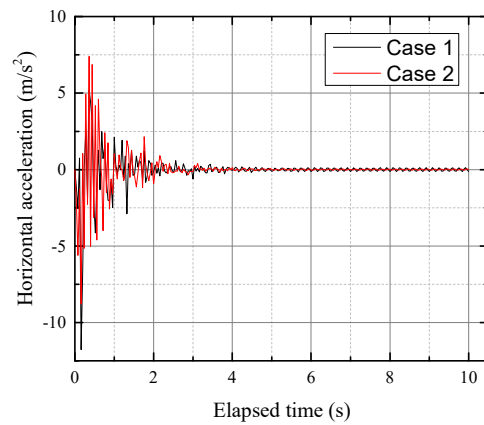


Figure 6.8 Horizontal acceleration at point H for load amplitude =400 kN/m, $f = 10$ Hz

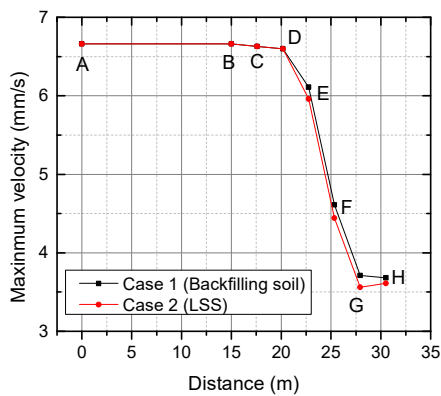


Figure 6.9 Distance and maximum velocity

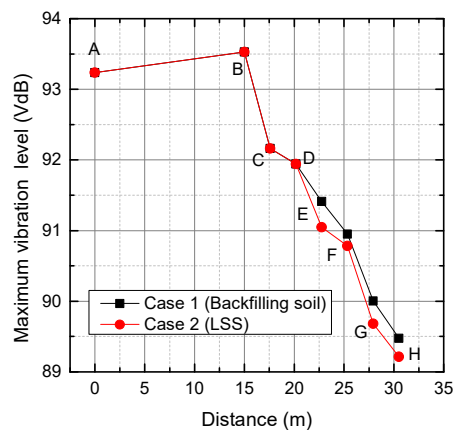


Figure 6.10 Distance and maximum vibration level

CHAPTER 6 REDUCTION OF VEHICLE-INDUCED VIBRATION USING LIQUEFIED TABILIZED SOIL

6.3.1 Vibration acceleration in Case 1 and Case 2

In this study, the effect of LSS for reduction of vibration under cyclic loading of vehicles are evaluated. Therefore, the acceleration is described on points E and H to determine responses of backfilling materials due to cyclic loading. Figure 6.5 shows graph of vertical vibration acceleration at point E for both cases using the backfilling material of backfilling soil (Case 1) and LSS (Case 2), respectively. It can be seen that amplitude of the vertical vibration acceleration at point E in Case 2 is significantly lower than that in Case 1. One of the most important reasons for this difference in the amplitude between Case 1 and Case 2 is the stiffness of which LSS is much larger than backfilling soil. Moreover, it can be seen observed that vertical vibration acceleration in Case 2 is damped more quickly than that in Case 1.

The horizontal vibration time histories at point E for Case 1 and Case 2 are shown in Figure 6.6. The figure indicates a considerable reduction in the acceleration amplitudes that achieve about 50 % for LSS.

In Figure 6.7, the time histories of the vertical acceleration at point H are described. Point H is boundary point between the backfilling area and the building. Analysis of vibration at point H play an important role not only for the backfilling area but also for the building. Therefore, effects of reduction of backfilling materials are considered. In the figure, reduction of the case of backfilling soil is compared with LSS. Although there are only little differences in the vertical vibration accelerations in two cases, the results show the reduction of LSS more useful than backfilling soil.

Figure 6.8 shows the horizontal acceleration time histories at point H. It can be noticed that the acceleration amplitudes in the case of LSS are larger than amplitudes in the case of backfilling soil.

6.3.2 Relationship between distance maximum vibration velocity and level

From eight analyzed points on the ground surface from A to H in Figure 6.4, it can be see that ground conditions at points A~D are the same for Case1 and Case 2. Therefore, the level of vibration and velocity at these points are the same for both cases. In this study, level of vibration and velocity at points E~H are analyzed.

Figure 6.9 shows relationship between distance and maximum vibration velocity with vehicle speed of 60 km/h. Although amplitude of the vibration velocity in two cases is

CHAPTER 6 REDUCTION OF VEHICLE-INDUCED VIBRATION USING LIQUEFIED TABILIZED SOIL

notable difference, amplitude of the vibration velocity in Case 1 is slightly larger than that in Case 2.

The relationship between distance and maximum vibration level is shown in Figure 6.10. It can be seen that the level of vibration rapidly decreases with distance from the center of road for both cases. Moreover, in the backfilling area, at each point, the level of vibration in Case 2 is lower than that in Case 1. According to the figures, the effect of LSS on vibration reduction can be observed apparently.

6.4 CONCLUSIONS

This study was focused on the utilization of backfilling soil and LSS as backfilling material, the reducing effect of ground vibration was discussed. The ground vibration properties were investigated by using the numerical analysis. The model of vehicle body has been improved which is modeled as a system of two degree of freedoms (2-DOFs) with consideration of primary and secondary suspension elements established in previous study. The result of the model in term of the load time history can be input data for numerical model in solution of the road-soil interaction problem and then prediction of vehicle-induced ground vibration. Based on the analysis results, the conclusions were withdrawn as follows:

1) As compared with backfilling soil, LSS indicated significantly better reducing effect of ground vibration induced by cyclic loading of vehicles on road due to its larger stiffness.

2) The analysis results also indicated that the level at the points close to the center of road on the ground surface which is strongest impacted from the vehicle-induced vibration in case of using LSS is lower than that of using backfilling soil.

It is considered that LSS had an effective potential as countermeasure against vehicle-induced vibration on the road. This property was pointed out as a new advantage of LSS.

REFERENCES

- Kuno, G.: Liquefied stabilized soil method-Recycling technology of construction-generated soil and mud, *Gihodo publication*, 1997 (in Japanese).
- Kohata, Y., Fujikawa, T., Ichihara, D., Kanda, M., & Murata, O.: Strength and deformation properties of fibered material mixed in liquefied stabilized soil obtained from uniaxial compression test, *Proc. of the 36th Japan National Conference on*

CHAPTER 6 REDUCTION OF VEHICLE-INDUCED VIBRATION USING LIQUEFIED TABILIZED SOIL

- Geotechnical Engineering*, pp.635-636, 2002 (in Japanese).
- Kohata, Y., & Tsushima, H.: Effect of fibered material mixing in liquefied stabilized soil on the triaxial shear characteristics, *Proc. of the 39th Japan National Conference on Geotechnical Engineering*, pp.721-722, 2004 (in Japanese).
- Kohata, Y.: Mechanical property of liquefied stabilized soil and future issues, *Doboku Gakkai Ronbunshuu*, F, Vol.62, No.4, pp.618-627, 2006 (in Japanese).
- Kohata, Y., Ichikawa, M., Nguyen, C. Gia., & Kato, Y.: Study of damage characteristics of liquefied stabilized soil mixed with fibered material due to triaxial shearing, *Geosynthetics Engineering Journal*, Vol.22, pp.55-62, 2007 (in Japanese).
- Duong, H. Q., Kohata, Y., Omura, S., and Ozaki, K.: Strength and deformation characteristics of liquefied stabilized soil reinforced by fiber material prepared at laboratory and field, *Geosynthetic Engineering Journal*, Vol.29, pp.33-40, 2014.
- Carl E. H., David A. T., Lance D. M.: Transit noise and vibration impact assessment, *U.S. Department of Transportation Federal Transit Administration-Office of Planning and Environment 1200 New Jersey Avenue, S.E. Washington, DC 20590, 2006.*
- SP 23-105.: Estimation of vibration in design, construction and operation of underground, *Code of practice for design and construction*, Russian Metro Standard, 2004.
- Kurbatskii, G. H.: Measurement of vibrations, *Moscow State University of Railway Engineering, 2008.*
- QCVN 27:2010/BTNMT.: National Technical Regulation on Vibration, *Ministry of Natural Resources and Environment of Vietnam, 2010 (in Vietnamese).*
- Tokita, Y.: Vibration Pollution Problems in Japan, *Proceedings Inter-Noise '75, Tohoku university, Sendai 980, Japan*, pp.465-472, 1975.
- Duong, H. Q., Kohata, Y., Nguyen Q. D.: Evaluation on Mitigation of Train-induced Vibration as Using LSS for Backfilling Ground of Cut and Cover Tunnel by FEM, *the 50th Japan National Conference on Geotechnical Engineering*, pp.2411-2412, 2015.
- Das, B. M.: Principles of soil cyclic, *PWS-KENT, publishing company, USA, 1995.*
- TCXDVN.: Design of structure for earthquake resistance, *construction standard of Vietnam*, p.1, regulations, earthquake impact with building structure, 2006 (in Vietnamese).
- Railway Technical Research Institute.: *Explanation for railway structure and design standards*, 1999.

**CHAPTER 6 REDUCTION OF VEHICLE-INDUCED VIBRATION USING
LIQUEFIED TABILIZED SOIL**

- Rao, SS.: The Finite Element Methods in Engineering, *Second Edition*, Pergamon Press, New York, 1989.
- Lin J.H.: Simulation of cyclic vehicle load on road pavement, *Vibroengineering PROCEDIA*, Vol. 5, 2015, p.p 503-508, 2015.
- LaBarre R. P., Forbes R. T., Andrew S.: The measurement and analysis of road surface roughness. *Motor Industry Research Association*, Report No. 5/1970, Nuneaton, England, 1970.
- Lin J. H.: Variations in cyclic vehicle load on road pavement, *International Journal of Pavement Engineering*, Vol. 15, p. 558-563, 2014.
- Hamdy F., Ahmed M. H.: 2D plaxis finite element modeling of asphalt- concrete pavement reinforced with geogrid. *Journal of Engineering Sciences*, Vol. 42 No. 6, pp. 1336 – 1348, 2014.
- Agostinacchio M., Ciampa D., Olita S.: The vibrations induced by surface irregularities in road pavements – a Matlab® approach, *DOI 10.1007/s12544-013-0127-8*, 2014.
- ISO 8608: Mechanical vibration, road surface profiles- Reporting of Measured Data, 2016.

Chapter 7

CONCLUSIONS AND RECOMMENDATIONS

7.1 SUMMARY OF INVESTIGATIONS

The purpose of this study is to promote the use of Liquefied Stabilized Soil (LSS) as a backfilling material for construction projects in Hanoi city. As a central part of this study, experimental and analysis works were developed to investigate more advantages of Liquefied Stabilized Soil (LSS) and LSS mixed with fiber material.

In the experimental works, there are suggestions that LSS can be decreased the slurry density to reduce vertical earth pressure, however, the study on strength and deformation properties of the LSS decreased a slurry density has not been investigated. Therefore, two densities of slurry were made including 1.280 g/cm^3 ($D_{pf} = 100 \%$) and 1.216 g/cm^3 ($D_{pf} = 95 \%$). The triaxial compressive property of LSS decreased slurry density was investigated. The model ground was built with LSS mixed with fiber material amount of 0, 10 kg/m^3 (Pc-0, 10), respectively into four pits in the campus. In parallel, the specimens of the same batch were also molded and cured in the laboratory. The specimens were prepared by trimming LSS retrieved from the model ground (field LSS) and cured laboratory (laboratory LSS) at the same curing time of 28 and 56 days. A series of CUB tests were carried out under the conditions at a constant strain rate of $0.054\%/min$ and the effective confining pressure of 98 kPa. Testing processes had been performed for two time periods in 2016 and 2017, respectively. The experimental results obtained were also compared and analyzed. The influences of slurry density on triaxial compressive properties for LSS and LSS reinforced with fiber material was discussed.

After experimental works, the analysis works were performed, the methods for estimation of soil dynamic parameters, the methods for determination of Vehicle-induced vibration, and analysis model to estimate vehicle-induced vibration as using LSS. In order to determine dynamic parameters of soil, geotechnical approaches were presented. Based on current conditions, the methods to evaluate the dynamic parameters were proposed. In addition, vehicle-induced vibration from the road in Hanoi city was studied. Analytical and numerical approaches were presented to determine cyclic loading caused by vehicles.

After that, a numerical investigation of LSS to be backfilled in order to reduce the building vibrations due to passing vehicles in traffic is discussed. Particularly, finite element (FE) model of a two-dimensional soil-structure system containing the cross-section of a route, the foundation ground, the backfilling LSS and a nearby building including eight floors and one basement is considered. The effects of LSS on the structure response are investigated. Based on the analysis results, the effects of backfilling material on the reduction of vibration caused by passing vehicles in traffic was evaluated.

7.2 SUMMARY OF FINDINGS AND CONCLUSIONS

The relationship between deviator stress $q (= \sigma_1 - \sigma_3)$ and axial strain ε_a has indicated that when the slurry density is slightly decreased from the appropriate slurry density obtained from the standard mix proportion design figure, it is considered that the q_{\max} decreased remarkably. In addition, it is found that the local damage caused by shearing even in the case of low slurry density is reduced by the effect of reinforcement on the fiber material. Moreover, by the addition of the fiber material, the brittle property of LSS cured in the field after the peak is improved. In addition, the deformation properties obtained were also pointed out that the $E_{\tan}/E_0 \sim q/q_{\max}$ relation of both LSS cured in the laboratory and at field shows a relatively similar tendency. It seems that the nonlinearity of $q \sim \varepsilon_a$ relation increase as decreasing slurry density. The experimental results show the influence of slurry density on the degree of damage caused by shear is large and it seems that the degree of damage tends to be reduced by the addition of fiber material. However, it is suggested that the application of LSS mixed with fiber material as a backfilling material to construction sites enables to create a ground with the improved ductile characteristic, although it needs to conduct more study.

At present, The Cone Penetration Test (CPT) is suggested using in Vietnam in order to estimate soil dynamic parameters. Because the estimation of the soil dynamic parameters based on CPT data with low cost is feasible to apply in the practical condition in Vietnam. In addition, modeling procedure of dynamic loading with a single-axle quarter-truck vehicle with 2- degree of freedoms (DOFs) was performed. The numerical result with high reliability can be input data for ground-borne vibration analysis model. On the other hand, the use of Plaxis, a program being popular in Vietnam, has brought reliable results. From Plaxis program, the evaluation on vehicle-induced vibration as using LSS for backfill ground has indicated that as compared with backfilling soil, LSS indicated significantly better-reducing effect of ground vibration induced by cyclic

loading of vehicles on road due to its larger stiffness, and the level at the points close to the center of road on the ground surface which is strongest impacted by the vehicle-induced vibration in case of using LSS is lower than that of using backfilling soil. Therefore, it is considered that LSS had an effective potential as a countermeasure against vehicle-induced vibration on the road. This property was pointed out as a new advantage of LSS.

7.3 RECOMMENDATIONS FOR FUTURE RESEARCH

The experimental works under cyclic loading have not been investigated. Therefore, the triaxial tests under cyclic loading condition simulated as traffic loading need to be performed on specimens retrieved from model ground backfilled by fibered LSS. Then, a rational construction method on practical fieldwork will be proposed.

In order to apply LSS and LSS reinforced with fiber material in Vietnam, the triaxial compressive properties for LSS and LSS reinforced with fiber material need to be determined under longtime curing.

The effect of the temperature on properties of field LSS during curing time should be determined. On the other hand, dynamic parameters of LSS mixed with fiber material should be investigated, and then, reduction of vehicle-induced vibration should be established by the numerical model.